universität wien

DISSERTATION | DOCTORAL THESIS

Titel | Title

Asymptotic PDE models of intermediate complexity for large-scale dynamics of a moist atmosphere

verfasst von | submitted by

Daniel Bäumer BSc MSc

angestrebter akademischer Grad | in partial fulfilment of the requirements for the degree of

Doktor der Naturwissenschaften (Dr.rer.nat.)

Wien | Vienna, 2025

Studienkennzahl lt. Studienblatt | Degree programme code as it appears on the student record sheet:	UA 796 605 405
Dissertationsgebiet lt. Studienblatt | Field of study as it appears on the student record sheet:	Mathematik
Betreut von | Supervisor:	Univ.-Prof. Dr. Norbert Mauser

Erklärung zur Verfassung der Arbeit

Hiermit erkläre ich, dass ich diese Arbeit selbständig verfasst habe, dass ich die verwendeten Quellen und Hilfsmittel vollständig angegeben habe und dass ich die Stellen der Arbeit, die anderen Werken oder dem Internet dem Wortlaut oder dem Sinn nach entnommen sind, auf jeden Fall unter Angabe der Quelle als Entlehnung kenntlich gemacht habe.

Die vorliegende kumulative Dissertation setzt sich aus folgenden vier Fachartikeln zusammen:

1. D. Bäumer, R. Klein und N.J. Mauser: *A general framework for the asymptotic analysis of moist atmospheric flows.* Zur Veröffentlichung angenommen in *Journal of Asymptotic Analysis* (Mai 2025).

2. D. Bäumer, S. Hittmeir und R. Klein: *Scaling approaches to quasigeostrophic theory for moist, precipitating air.* Veröffentlicht in *Journal of the Atmospheric Sciences,* **80,** 1771–1786 (Juli 2023).

3. D. Bäumer und R. Klein: *PQG-DL-Ekman: a triple-deck boundary layer theory for large-scale atmospheric flow with moist process closures.* Eingereicht (April 2025).

4. D. Bäumer: *The diabatic layer equations: well-posedness of a new boundary layer theory for quasi-geostrophic flow.* Manuskript.

In allen angeführten Arbeiten fungierte der Verfasser der Dissertation als Erstautor.

Abstract

In the atmospheric and oceanic sciences, there is a long and rich tradition of utilizing reduced mathematical models in the form of time-dependent partial differential equations, systematically derived from the governing Euler or Navier-Stokes equations by formal asymptotic methods, to further our theoretical understanding of the earth's weather and climate. This thesis makes a contribution to the field "mathematics for meteorology" by unifying two recent developments in the mathematical modeling of geophysical flows: the extension of the classical quasi-geostrophic (QG)-Ekman theory for synoptic-scale atmospheric flows in the middle latitudes by a diabatic layer (DL) of intermediate height due to Klein et al. and the precipitating quasi-geostrophic (PQG) model family of Smith & Stechmann. Two PQG model variants with bulk microphysics closures are derived, one of which turns out to be suited to connect to a moist, precipitating DL. This leads to the first triple-deck boundary layer theory for atmospheric flow with moist process closures, the new PQG-DL-Ekman theory. In a simplified axisymmetric version of this model, explicit solutions in the precipitating DL are found. These solutions permit numerical simulations by well-established methods for the coupled system that illustrate the complex interactions across the various layers. In particular, the simulations show how disturbances initially confined to the DL propagate across the whole troposphere. Furthermore, a first mathematically rigorous investigation of the dry DL equations, which belong to the class of geostrophically and hydrostatically balanced models, is presented.

The thesis contains published and accepted papers, as well as a submitted article and a manuscript.

Zusammenfassung

In den Atmosphären – wie den Ozeanwissenschaften hat die Nutzung von reduzierten mathematischen Modellen in der Gestalt von zeitabhängigen partiellen Differentialgleichungen (systematisch mittels formaler asymptotischer Methoden aus den jeweiligen Euler – oder Navier-Stokes-Grundgleichungen hergeleitet) eine lange und reichhaltige Tradition. Der Zweck solcher Modelle ist es, zu einem besseren theoretischen Verständnis von Wetter – und Klimaphänomenen auf der Erde beizutragen. Die vorliegende Dissertation setzt ebendiese Tradition der mathematischen Modellbildung in der Meteorologie fort, indem sie zwei in jüngerer Zeit entworfene Modelle bzw. Modellfamilien unter einem Dach zusammenführt: Die von Klein et al. entwickelte Erweiterung der klassischen quasi-geostrophischen (QG)-Ekman-Theorie für atmosphärische Strömungen auf der synoptischen Skala in den mittleren Breiten durch eine sogenannte diabatische (Zwischen)schicht (engl.: diabatic layer (DL)), sowie die auf Smith & Stechmann zurückgehende Familie der QG-Gleichungen mit Niederschlag (engl.: precipitating QG (PQG) equations). Zwei PQG-Modellvarianten, inkl. Parametrisierungen wolkenmikrophysikalischer Prozesse, werden hergeleitet; eine derselben lässt die systematische Kopplung an eine feuchte Erweiterung der DL-Gleichungen zu. Auf diesem Weg gelangen wir zur ersten Grenzschichttheorie mit einer asymptotischen Zwischenschicht (engl.: triple-deck boundary layer theory) für atmosphärische Strömungen, die Schließungsterme für Phasenübergänge in feuchter Luft miteinbeziehen: Die neue PQG-DL-Ekman-Theorie. Wir zeigen, dass sich die DL-Gleichungen mit Niederschlag im achsensymmetrischen Fall explizit lösen lassen, und wir verwenden diese Lösungen, um das gekoppelte achsensymmetrische PQG-DL-Ekman-System mit bewährten numerischen Methoden zu studieren. Die resultierenden Simulationen zeigen insbesondere, dass sich im Anfangszustand auf die DL beschränkte dynamische Schwankungen im Laufe der Zeit über die gesamte Troposphäre ausbreiten. Das abschließende Kapitel beinhaltet eine erste mathematisch strenge Analyse der trockenen DL-Gleichungen, die einen Neuzugang in der Familie der Strömungsmodelle in hydrostatischem und geostrophischem Gleichgewicht darstellen.

Diese Dissertation besteht zum Teil aus veröffentlichten bzw. zur Veröffentlichung angenommenen, zum Teil aus eingereichten bzw. als Manuskript vorhandenen Publikationen.

Acknowledgements

As with every project that takes up four years of one's time, there are many people who contributed in a meaningful way to its completion: first, I want to express my thanks to my advisor Norbert J. Mauser, who already supervised my master thesis, helped set me on the scientific path that I am now treading and accompanied and supported me every step of the way.

I am grateful to have Rupert Klein as my main scientific collaborator and as a teacher and mentor in the field of asymptotic modeling in geophysical fluid dynamics. Without his guidance, this thesis could not have come into being.

My co-advisor Sabine Doppler (formerly Hittmeir), who also co-supervised my master thesis, has authored works that in many ways proved foundational for my own; I am grateful for that and for her guiding me through the beginning stages of my doctoral studies.

I thank Edriss Titi and Peter Spichtinger for enriching scientific discussions and for having agreed to referee this thesis.

The Wolfgang Pauli Institute (WPI) in Vienna provided a wonderful work environment. Besides its director N.J. Mauser, I thank the administrative director Stefanie Preuss, and Hans Peter Stimming, who also helped me with implementing my first numerical code. I further thank my colleagues Jakob Möller, Sebastian Schaffer and Jan-Frederik Mennemann for friendly exchanges and advice.

At several workshops in Oberwolfach, Les Houches, and other places, including the WPI, I was fortunate to get to know many leading researchers in the mathematical fluid dynamics community. Here, I specifically want to thank Peter Korn, Leslie Smith and Sam Stechmann for fruitful discussions.

Last, but not least, I want to thank my father for supporting me when I wrote my master thesis and I could not yet sustain myself financially.

This research was funded by the Austrian Science Fund (FWF) 1009 10.55776/F65, 10.55776/I5149, 10.55776/P32788, as well as by the OeAD-WTZ project CZ 1010 09/2023.

I further acknowledge (financial) support by the research platform MMM "Mathematics-Magnetism-Materials" and by the WPI.

Preface

> *"Since the seventeenth century, physical intuition has served as a vital source for mathematical problems and methods. Recent trends have, however, weakened the connection between mathematics and physics; mathematicians, turning away from the roots of mathematics in intuition, have concentrated on refinement and emphasized the postulational side of mathematics, and at times have overlooked the unity of their science with physics and other fields. In many cases, physicists have ceased to appreciate the attitudes of mathematicians. This rift is unquestionably a threat to science as a whole; the broad stream of scientific development may split into smaller and smaller rivulets and dry out. It seems therefore important to direct our efforts toward reuniting divergent trends by clarifying the common features and interconnections of many distinct and diverse scientific facts."*
> (R. Courant, from the preface to "Methods of Mathematical Physics", Vol. 1)

These words by the eminent German mathematician Richard Courant, student, collaborator and friend of David Hilbert, were written almost 90 years ago - yet, from the perspective of someone working at the interface of the mathematical and the physical sciences, they appear more prescient and timely than ever today. This thesis aims to make a contribution in the spirit of Courant's remarks by applying the time-tested methods of dimensional analysis, heuristic scale analysis and singular perturbation theory to the governing partial differential equations of a moist atmosphere, capable of producing warm clouds and rain. In this process, a particular emphasis is placed on highlighting the intimate connection between physically motivated scaling choices on the one hand and the corresponding changes in mathematical structure on the other hand.

The thesis comprises four papers of quite different scope and length, mirroring the various stages of its evolution; in order to clarify their respective significance within the work as a whole, I have compiled a brief "reader's guide" as follows:

1. (D. Bäumer, R. Klein and N.J. Mauser (2025): A general framework for the asymptotic analysis of moist atmospheric flows. *Journal of Asymptotic Analysis,* accepted.)

This article essentially serves as the introductory chapter of the thesis. It focuses on the modeling philosophy behind all subsequent developments, highlighting the unique challenges posed by the occurrence of phase changes in moist air.

2. (D. Bäumer, S. Hittmeir and R. Klein (2023): Scaling approaches to quasi-geostrophic theory for moist, precipitating air. *Journal of the Atmospheric Sciences,* Vol. 80, 1771-1786.)

   In the first part of this paper, chronologically the first of the four, the original precipitating quasi-geostrophic (PQG) equations, due to Smith & Stechmann, are embedded into the modeling framework described in the first chapter. The second part develops a first version of the so-called $\mathrm{PQG}_{\mathrm{DL}}$ equations; these are presented in an updated and refined state in the next chapter, which builds on the foundation established here, but can be read independently.

3. (D. Bäumer and R. Klein (2025): PQG-DL-Ekman: a triple-deck boundary layer theory for large-scale flow with moist process closures. *Submitted.*)

   This work constitutes the core of the thesis. Several potentially interesting model variants are mentioned, but only one is presented in full detail. While the modeling effort takes center stage, the last two sections are devoted to the analytical and also the numerical investigation of the model in an axisymmetric setting.

4. (D. Bäumer (in preparation): The diabatic layer equations: well-posedness of a new boundary layer theory for quasigeostrophic flow.)

   In this final chapter, first steps towards a mathematically rigorous understanding of the PQG-DL-Ekman theory are taken. The findings presented here only apply to the dry DL equations without coupling to the adjacent layers, and they represent work in progress.

Daniel Bäumer
Vienna, May 2025

Contents

1 A general framework for the asymptotic analysis of moist atmospheric flows **1**
1.1 Introduction . . . 1
1.2 Model hierarchies in atmospheric fluid dynamics: a general framework . 2
1.3 Phase changes and their parameterization . . . 14
1.4 Precipitating quasi-geostrophic models . . . 17
1.5 Summary and outlook . . . 22
1.6 References . . . 23

2 Scaling approaches to quasigeostrophic theory for moist, precipitating air **27**
2.1 Introduction . . . 27
2.2 The governing equations . . . 28
2.3 Overview and comparison of resulting model equations . . . 29
2.4 Nondimensionalization and scaling for PQG . . . 31
2.5 Asymptotic expansion and derivation of PQG . . . 32
2.6 Consequences of a different scaling approach: PQG and the diabatic layer 34
2.7 Properties of PQG_{DL}: The omega equation . . . 38
2.8 Conclusions . . . 39
2.9 Appendix A: The moist anelastic buoyancy . . . 39
2.10 Appendix B: Derivation of the Omega equation . . . 41
2.11 References . . . 42

3 PQG-DL-Ekman: a triple-deck boundary layer theory for large-scale atmospheric flow with moist process closures **43**
3.1 Introduction . . . 45
3.2 The governing equations . . . 46
3.3 Overview of resulting model equations . . . 49
3.4 Scaling: non-dimensionalization and choice of a distinguished limit . . . 55
3.5 Asymptotic expansion and derivation of PQG-DL-Ekman . . . 67
3.6 Explicit PDL solutions for axisymmetric flow . . . 93
3.7 Numerical solution of the axisymmetric PQG-DL-Ekman system . . . 96
3.8 Conclusions . . . 108

3.9 References 109

4 The diabatic layer equations: well-posedness of a new boundary layer theory for quasi-geostrophic flow 113
4.1 Introduction 113
4.2 Global well-posedness of the diffusive model 115
4.3 Conclusions and outlook 123
4.4 References 123

CV a

Journal Title
XX(X):1–25

DOI: 10.1177/ToBeAssigned
www.sagepub.com/
SAGE

A general framework for the asymptotic analysis of moist atmospheric flows

Daniel Bäumer[1], Rupert Klein[2], Norbert J. Mauser[1]

Abstract

We deal with asymptotic analysis for the derivation of partial differential equation models for geophysical flows in the earth's atmosphere with moist process closures, and we study their mathematical properties. Starting with the Navier-Stokes equations for dry air, we put the seminal papers of Klein, Majda et al. in a unified context and then discuss the appropriate extension to moist air. In particular, we deal with the scale-independent distinguished limit for the universal parameters of atmospheric motion for moist air, with the Clausius-Clapeyron relation that links saturation vapor pressure and air temperature, and with the mathematical formulation of phase changes associated with cloud formation and rain production. We conclude with a discussion of the *precipitating quasi-geostrophic* (PQG) models introduced by Smith & Stechmann. Our intent is, on the one hand, to convey the problems arising at the modeling stage to mathematicians; on the other hand, we want to present the relevant mathematical methods and results to meteorologists.

Keywords

Mathematical modeling; Geophysical fluid dynamics; Singular perturbations; Moist thermodynamics; Partial differential equations

Introduction

In this paper, we discuss recent developments concerning challenges associated with the derivation and mathematical analysis of reduced models for atmospheric motion with moist process closures. Specifically, we focus on the following topics:

[1]Research platform MMM, c/o Fakultät für Mathematik, Universität Wien, Vienna, Austria
[2]FB für Mathematik und Informatik, Freie Universität Berlin, Berlin, Germany

Corresponding author:
Daniel Bäumer (Research platform MMM, c/o Fakultät für Mathematik, Universität Wien. Oskar-Morgenstern-Platz 1-3, A-1090 Wien)
Email: daniel.baeumer@univie.ac.at

1. The choice of a distinguished limit: as laid out in (Klein, 2010), the rich palette of reduced models used in meteorology can be viewed as an ensemble of scale-specific models that are embedded in *one* scale-independent distinguished limit for the universal parameters of atmospheric motion on our planet. Said distinguished limit, however, does not incorporate the thermodynamic parameters of moist air. This raises the question, crucially important for realistic models, how its systematic extension to that end may be achieved. Here, we base our presentation on the discussion in (Hittmeir and Klein, 2018), which shows that it is a difficult task even just to reconcile formal consistency and physical realism in this endeavor.
2. The Clausius-Clapeyron relation: the consistency issues just mentioned are mainly due to the relationship between saturation vapor pressure and air temperature encoded in the famous Clausius-Clapeyron equation (Bohren and Albrecht, 1998), which was systematically studied for the first time in the context of formal asymptotic analysis by Klein and Majda (2006). We compare and contrast several approaches to resolving this issue. Furthermore, we highlight the significant ways in which the mathematical structure of the reduced moisture equations changes, depending on the chosen approach.
3. The impact of phase changes: one of the most important features of bulk models for cloudy, precipitating air is the presence of closures for the phase transitions associated with cloud formation and rain production. Viewed through a mathematical lens, the first-order discontinuities that occur in these closures provide an interesting challenge already when investigating the full, unapproximated equations of geophysical fluid dynamics (Hittmeir et al., 2017, 2020, 2023; Doppler et al., 2024). In reduced models, the effect of such discontinuities can lead to even more drastic changes in the analytical structure of moist extensions of preexisting models. Here, the precipitating quasi-geostrophic (PQG) model family originally due to Smith and Stechmann (2017) serve as a striking example: the elliptic inversion equation for the pressure perturbation in the potential vorticity formulation of those model equations becomes nonlinear by the inclusion of moisture species, indicating a significant departure from the well-known dry QG dynamics. Once more, we present two contrasting approaches to the moisture parametrization problem, one of which was recently proposed by two of the authors of this article in (Bäumer et al., 2023).

We conclude with an outlook on open questions and areas for future research both on the modeling and the rigorous analysis front.

Model hierarchies in atmospheric fluid dynamics: a general framework

Preliminaries

As it is our primary goal to delineate the physical and mathematical conditions that must be met in order to successfully incorporate moisture into asymptotic models for atmospheric dynamics, we first need to identify the independent physical dimensions of the system's unknowns. In any non-isothermal, compressible fluid, these comprise a velocity field, pressure, density and temperature at a minimum, which means that at least the four independent dimensions length,

time, mass and temperature are involved. For the description of geophysical fluids, these turn out to be sufficient. When investigating a specific geophysical flow phenomenon, one can then conduct a preliminary formal analysis in the following familiar fashion: having identified all of its (dimensional) parameters, derive a representative set of independent dimensionless parameters, translate heuristic notions of "large" and "small" to limit processes and study how the governing equations change in the formal limit(s).

In this work, before discussing scale-specific models, we want to make clear how such a dimensional analysis can be applied in a far more general context: the approach pioneered by and outlined in (Klein, 2010) is to first single out a set of parameters, called *universal characteristics,* that do not depend on the choice of length and timescales appropriate for any particular atmospheric flow. The independent nondimensional parameters that can be derived from said universal characteristics can then be assigned asymptotic scalings to obtain a *scale-independent distinguished limit.* This limit, when chosen properly and supplemented by suitable length - and timescales for some concrete meteorological event, can be used to retrieve already known reduced models, but, more importantly, it clarifies their respective standing within the atmospheric model hierarchy. Establishing a scale-independent distinguished limit thus greatly facilitates

(i) the comparison of different reduced models and
(ii) the study of interactions between such models across multiple scales.

The necessity of distinguished limits: It is well known that asymptotic expansions with respect to multiple small parameters in general yield nonunique limits. A particularly simple, yet illuminating example is provided by the linear oscillator with small mass and damping (Klein, 2010). In technical terms, this is so because the system's differential operator is not Fréchet-differentiable at the origin of the parameter space, rendering the limit dependent on the path toward the origin taken in said space. For this reason, we need to restrict ourselves to *coupled* limit processes dependent on only one generic small parameter ϵ, in other words, a distinguished limit.

Universal characteristics of atmospheric motion

When it comes to the mathematical description of *dry* air flows in the earth's atmosphere, there is general agreement on the equations to be used as a point of departure. These are the compressible Navier-Stokes equations with gravity for a heat-conducting ideal gas in a rotating frame, considered in a thin shell around an (approximately) spherical planet (Pedlosky, 1987; Vallis, 2017). In coordinate-free form, they read

$$\partial_t(\rho\mathbf{v}) + \nabla\cdot(\rho\mathbf{v}\otimes\mathbf{v}) + 2(\mathbf{\Omega}\times\rho\mathbf{v}) + \nabla p = \nabla\cdot\sigma + \rho\nabla\Phi \tag{1a}$$

$$\partial_t\rho + \nabla\cdot(\rho\mathbf{v}) = 0 \tag{1b}$$

$$\partial_t(\rho e) + \nabla\cdot(\rho e\mathbf{v} + p\mathbf{v}) = \nabla\cdot(\sigma\mathbf{v}) - \nabla\cdot\mathbf{j} + \rho\mathbf{v}\cdot\nabla\Phi + \rho Q. \tag{1c}$$

Here, $\mathbf{v}$ denotes the mass-averaged fluid velocity, while p and ρ stand for pressure and density, respectively; $\mathbf{\Omega}$ is the earth rotation vector, Φ the geopotential, incorporating gravitational and centrifugal potential energy, Q is a stand-in for any and all external heat sources, and the following constitutive relations hold:

- The viscous stress tensor of a Newtonian fluid, denoted by σ, reads

$$\sigma = \mu\left(\nabla\mathbf{v} + \nabla\mathbf{v}^{\mathrm{T}}\right) + (\zeta - \frac{2}{3}\mu)(\nabla\cdot\mathbf{v})I. \tag{2}$$

  Here, I is the identity matrix, and μ and ζ denote the viscosity coefficients of the fluid.
- The ideal gas law

$$p = R_d\rho T, \tag{3}$$

  where R_d denotes the gas constant of dry air and T the temperature of the fluid.
- The sum of kinetic and inner energy per unit mass e is given by

$$e = \frac{\mathbf{v}^2}{2} + c_{\mathrm{vd}}T, \tag{4}$$

  with the heat capacity of dry air at constant volume c_{vd}.
- The heat flux density $\mathbf{j}$ obeys Fourier's law and thus reads

$$\mathbf{j} = -\lambda\nabla T, \tag{5}$$

  with the thermal conductivity λ.

In meteorological applications, a number of simplifications typically is assumed from the outset: first of all, the impact of molecular viscosity on meteorological timescales is generally viewed as negligible. Therefore, the terms involving the viscous stress tensor (2) in the momentum and energy equations are typically dropped and replaced by a generic closure term that primarily represents boundary layer friction or turbulence. By the same token, heat conduction proceeds far too slowly to affect the local heat budget in atmospheric motions, and consequently, (5) is either ignored altogether or replaced by a closure for turbulent mixing. It remains to discuss the geopotential Φ and the geometry of planet earth, where quite subtle issues arise: the centrifugal force, while small compared to gravity, *does* make a non-negligible contribution in the plane perpendicular to the earth's gravity vector. As explained, e.g., in chapter 2 of Vallis (2017), naively choosing the latter as the "vertical" direction would then have the undesirable consequence of introducing the centrifugal force as a dominant term in the "horizontal" momentum equations, thus obscuring the balance between horizontal pressure gradient and Coriolis force that is characteristic of large-scale weather systems in the middle latitudes. The customary way out of this dilemma is the following: one introduces an *effective gravity* as the sum of gravitational and centrifugal forces and defines the "vertical" direction accordingly. This yields horizontal surfaces as those of constant geopotential. To be sure, these are not perfect spheres, but due to the fact that the earth is an *oblate spheroid*, i.e., it is flattened at the poles and bulging at the equator, they are very nearly parallel to the actual surface of our planet. Neglecting the (small) deviation from sphericity from that point on is traditional - see Constantin and Johnson (2021) for a detailed investigation that incorporates said deviation in an asymptotic ansatz.

Metric terms in common approximations: When studying models for atmospheric dynamics on length scales significantly smaller than the earth's diameter, one can simplify the equations of motion further by approximating the spherical metric by a *flat* one (at leading order). This

corresponds to a *tangent plane approximation*, which could in principle be justified within the asymptotic scheme. For simplicity of exposition, we will assume it here from the outset, since it is known to be consistent with all models investigated in this article, and the general scaling considerations to follow do not depend on the components of the metric tensor. Bearing all of the above in mind, one can now rewrite the simplified Eqs. (1) in pseudo-cartesian coordinates, in the form

$$D_t \mathbf{u} + 2(\mathbf{\Omega} \times \mathbf{v})_\parallel + \frac{1}{\rho}\nabla_\parallel p = \mathcal{D}_\mathbf{u} \tag{6a}$$

$$D_t w + 2(\mathbf{\Omega} \times \mathbf{v})_\perp + \frac{1}{\rho}\partial_z p = -g + \mathcal{D}_w \tag{6b}$$

$$\partial_t \rho + \nabla \cdot (\rho \mathbf{v}) = 0 \tag{6c}$$

$$c_{\mathrm{pd}} D_t \ln\left(\frac{\theta}{\theta_{\mathrm{ref}}}\right) = \mathcal{D}_\theta + Q. \tag{6d}$$

Here, $\mathbf{v} = (\mathbf{u}, w)^{\mathrm{T}}$, where $\mathbf{u}$ denotes the horizontal velocity field in the tangent plane approximation; we introduced the material derivative D_t, defined as

$$D_t := (\partial_t + \nabla \cdot \mathbf{v}) \tag{7}$$

and rewrote the energy equation in terms of the *potential temperature*

$$\theta = T\left(\frac{p}{p_{\mathrm{ref}}}\right)^{\frac{\gamma-1}{\gamma}} \tag{8}$$

(γ is the isentropic exponent of dry air). This quantity is of central importance, because its logarithm, multiplied by the heat capacity of dry air at constant pressure c_{pd}, yields the *specific entropy* of a dry air parcel (Bohren and Albrecht, 1998). Therefore, (6d) is a transport equation for entropy, and the term Q, accordingly, now represents sources of entropy (we reused the same letter for simplicity, since we will not refer to (1) from here on out). The terms $\mathcal{D}_\star$ on the respective right-hand sides represent closures for turbulent friction, diffusion and mixing, while g represents the acceleration of gravity (which, strictly speaking, incorporates the centrifugal force - see the discussion above).

Atmospheric flows occur on a wide variety of spatial and temporal scales, and the derivation of models of reduced complexity to reveal the characteristics of scale-specific phenomena has long been a cornerstone of theoretical meteorology. Traditionally, such models are derived from the governing equations by a set of assumptions tailored to the problem at hand, followed by careful scale analysis and the identification of dominant terms in the governing equations. This is a standard modeling strategy that has led to many successes, but it has one major drawback: problem-by-problem modeling does not enable the study of *interactions across multiple scales.* Such studies constitute the natural next step when one tries to go beyond single-scale models, and it would therefore be of great interest to establish a framework that allows for the systematic derivation of reduced models by formal asymptotics on *all* viable length and timescales, including, but not limited to, those already recognized by the meteorological community. As already

mentioned, this was achieved in the context of dry air flows by Klein (2010), whose methodology we explain more thoroughly in the following:

Notwithstanding the complexity and unpredictability of the dynamics of our planet's atmosphere, one can identify a number of relevant characteristic quantities that are "universal" in the sense that they set conditions that remain essentially unchanged for *all* atmospheric flows, listed in Table 1.

Earth's radius	$a \sim 6 \times 10^6$ m
Earth's rotation rate	$\Omega \sim 10^{-4}$ s^{-1}
Acceleration of gravity	$g \sim 9.81$ m s^{-2}
Sea-level pressure	$p_{\mathrm{ref}} \sim 10^5$ kg m^{-1} s^{-2}
Water-freezing temperature	$T_{\mathrm{ref}} \sim 273$ K
Tropospheric vertical potential temperature difference	$\Delta\Theta \sim 40$ K
Dry air gas constant	$R_d = 287$ m^2 s^{-2} K^{-1}
Isentropic exponent of dry air	$\gamma = 1.4$

Table 1. Universal characteristics of atmospheric motion

Among these eight parameters, six where already introduced through the governing equations and the constitutive relations. The earth's radius a is necessary to define the spatial domain and consequently also part of the mathematical formulation. Thus, only $\Delta\Theta$ remains as an empirically given quantity - however, if we imagine a setting in which an upper boundary is assumed at the tropopause, this temperature difference could also be derived from the associated boundary condition. We further mention that the equator-to-pole potential temperature difference at fixed altitude is of the same order and could therefore as well be used to define $\Delta\Theta$. Looking ahead to the incorporation of moist quantities, we should also note that the temperature increase that would be incurred if all water vapor in, say, a tropical region condensed out also is of the same order of magnitude. Thus, $\Delta\Theta$ can straightforwardly be derived from the system's parameters if moist processes are included. As far as scaling considerations go, the isentropic exponent of dry air γ is already nondimensional. Since the remaining seven involve the four physical dimensions of length, time, mass and temperature, systematic nondimensionalization yields three independent dimensionless parameters, the choice of which should be guided by meteorological considerations. Here, it is convenient to introduce a number of important derived quantities that are summarized in Table 2.

Sea-level air density	$\rho_{\mathrm{ref}} = p_{\mathrm{ref}}/(R_d T_{\mathrm{ref}}) \sim 1.25$ kg m^{-3}
Density scale height	$h_{\mathrm{sc}} = \gamma p_{\mathrm{ref}}/(g\rho_{\mathrm{ref}}) \sim 11$ km
Speed of sound	$c_{\mathrm{ref}} = \sqrt{\gamma p_{\mathrm{ref}}/\rho_{\mathrm{ref}}} \sim 330$ m s^{-1}
Internal wave speed	$c_{\mathrm{int}} = \sqrt{g h_{\mathrm{sc}} \frac{\Delta\Theta}{T_{\mathrm{ref}}}} \sim 110$ m s^{-1}
Thermal wind velocity	$u_{\mathrm{ref}} = \frac{2}{\pi} \frac{g h_{\mathrm{sc}}}{\Omega a} \frac{\Delta\Theta}{T_{\mathrm{ref}}} \sim 12$ m s^{-1}

Table 2. Quantities derived from universal characteristics

With these in hand, we can write the independent dimensionless parameters chosen by Klein [2010] in the form

$$\begin{aligned}\Pi_1 &= \frac{h_{\mathrm{sc}}}{a} \sim 1.6 \times 10^{-3},\\ \Pi_2 &= \frac{\Delta\Theta}{T_{\mathrm{ref}}} \sim 1.5 \times 10^{-1},\\ \Pi_3 &= \frac{c_{\mathrm{ref}}}{\Omega a} \sim 4.7 \times 10^{-1}.\end{aligned} \tag{9}$$

The parameter Π_1 relates the vertical extent of the troposphere (which is almost exclusively responsible for weather phenomena) to the earth's radius; Π_2 gives an estimate for the relative strength of atmospheric temperature variations, while Π_3 compares a characteristic signal speed to the rotation speed of our planet. Proceeding further, the asymptotic rescaling of these parameters is supposed to serve as the common thread uniting the multitude of reduced models that can be derived from the governing equations. Due to the nonuniqueness of multi-parameter expansions, we cannot treat Π_1, Π_2 and Π_3 as independent parameters when passing to an abstract asymptotic setting, and we therefore need to find a suitable distinguished limit. As for the generic small parameter ϵ, it is traditionally assumed in meteorological studies that it corresponds to a numerical value of $\sim 1/10$, a natural choice for a "scale separation factor" (see Klein (2010) for more background on scale separation). As shown in the cited article, the choice

$$\Pi_1 = c_1\epsilon^3, \quad \Pi_2 = c_2\epsilon, \quad \Pi_3 = c_3\sqrt{\epsilon}, \tag{10}$$

where the prefactors of the form c_i are to be understood as bounded quantities in the limit $\epsilon \to 0$, enables the straightforward derivation of almost all of the classical reduced models utilized by meteorologists, and it thus provides a strong and flexible foundation for future investigations, in particular of the aforementioned interactions across multiple scales.

Distinguished limits for moist air and the Clausius-Clapeyron relation

Now, we want to explore possibilities to extend the distinguished limit described above to include the physical parameters that can be regarded as universal when investigating a mixture of dry air, water vapor and liquid water. In doing so, we do not immediately discuss the difficult issue of the incorporation of cloud microphysics, first highlighting the role of the fundamental *Clausius-Clapeyron relation* (Bohren and Albrecht, 1998) in the study of phase changes; the next section will be devoted to viable parameterizations of processes such as condensation and evaporation in the context of formal asymptotics for the dynamics of a moist atmosphere.

First, we of course need to determine a set of governing equations that is suited to serve as a common point of departure for the derivation of a wide variety of moist flow phenomena. Here, we opt for the state-of-the-art system used in (Hittmeir and Klein, 2018; Bäumer et al., 2023; Bäumer and Klein, 2025), which incorporates fairly detailed moist thermodynamics and bulk microphysics closures for transitions between the various moisture species in the spirit of Kessler

(1995):

$$D_t\mathbf{u} + 2(\mathbf{\Omega}\times\mathbf{v})_{\parallel} + \frac{1}{\rho}\nabla_{\parallel}p = \frac{\rho_d}{\rho}q_r V_r \partial_z \mathbf{u} + \mathcal{D}_{\mathbf{u}}, \tag{11a}$$

$$D_t w + 2(\mathbf{\Omega}\times\mathbf{v})_{\perp} + \frac{1}{\rho}\partial_z p = -g + \frac{\rho_d}{\rho}q_r V_r \partial_z w + \mathcal{D}_w, \tag{11b}$$

$$D_t\rho_d + \rho_d(\nabla\cdot\mathbf{v}) = 0, \tag{11c}$$

$$\begin{aligned} CD_t \ln\left(\frac{\theta}{\theta_{\mathrm{ref}}}\right) + \Sigma D_t \ln\left(\frac{p}{p_{\mathrm{ref}}}\right) \\ + \frac{L(T)}{T} D_t q_v = c_l V_r q_r \left(\partial_z \ln\left(\frac{\theta}{\theta_{\mathrm{ref}}}\right) + \frac{R_d}{c_{\mathrm{pd}}}\partial_z \ln\left(\frac{p}{p_{\mathrm{ref}}}\right)\right) \\ + Q + \mathcal{D}_\theta, \end{aligned} \tag{11d}$$

$$D_t q_v = S_{\mathrm{ev}} - S_{\mathrm{cd}} + \mathcal{D}_v, \tag{11e}$$

$$D_t q_c = S_{\mathrm{cd}} - S_{\mathrm{cr}} - S_{\mathrm{ac}} + \mathcal{D}_c, \tag{11f}$$

$$D_t q_r - \frac{1}{\rho_d}\partial_z(\rho_d V_r q_r) = S_{\mathrm{cr}} + S_{\mathrm{ac}} - S_{\mathrm{ev}} + \mathcal{D}_r, \tag{11g}$$

with the supplementary relations

$$\rho = \rho_d(1 + q_v + q_c + q_r), \tag{12a}$$

$$p = R_d\rho_d T(1 + \frac{q_v}{R_d/R_v}), \tag{12b}$$

$$T = \theta\left(\frac{p}{p_{\mathrm{ref}}}\right)^{\frac{R_d}{c_{\mathrm{pd}}}} \equiv \theta\pi, \tag{12c}$$

$$\mathbf{v} = \mathbf{u} + w\mathbf{k}, \tag{12d}$$

$$S_{\mathrm{ev}} = C_{\mathrm{ev}}\frac{p}{\rho}(q_{\mathrm{vs}} - q_v)^+ q_r, \tag{12e}$$

$$S_{\mathrm{cd}} = C_{\mathrm{cn}}(q_v - q_{\mathrm{vs}})^+ q_{\mathrm{cn}} + C_{\mathrm{cd}}(q_v - q_{\mathrm{vs}})q_c, \tag{12f}$$

$$S_{\mathrm{ac}} = C_{\mathrm{ac}}(q_c - q_{\mathrm{ac}})^+, \tag{12g}$$

$$S_{\mathrm{cr}} = C_{\mathrm{cr}} q_c q_r, \tag{12h}$$

$$C = c_{\mathrm{pd}} + c_{\mathrm{pv}} q_v + c_l(q_c + q_r), \tag{12i}$$

$$\Sigma = (\frac{c_{\mathrm{pv}}}{c_{\mathrm{pd}}}R_d - R_v)q_v + \frac{c_l}{c_{\mathrm{pd}}}R_d(q_c + q_r), \tag{12j}$$

$$L(T) = L_{\mathrm{ref}} - (c_l - c_{\mathrm{pv}})(T - T_{\mathrm{ref}}) \equiv L_{\mathrm{ref}}\phi(T). \tag{12k}$$

This system extends (6) by three transport equations for the moist constituents q_v, q_c and q_r, denoting the mixing ratios of water vapor, cloud water and rain, respectively. As before, terms of the form $\mathcal{D}_\star$ denote generic closures for turbulent mixing and diffusion, while the terminal rainfall velocity V_r appears as a new parameter. There is no universally valid scaling for this quantity, for reasons explained in the next section, and that is why we do not include it in Table

3 below. Notice further that the effect of moisture on total density is accounted for by Eq. (12a), where ρ_d stands for the density of dry air. As far as the pressure is concerned, we assume ideal gas behavior for *both* dry air and water vapor, implying in particular the relation

$$e = R_v \rho_v T = R_v \rho_d q_v T \tag{13}$$

for the vapor pressure $e = p - p_d$. Eq. (12b) then results from adding the two ideal gas laws. Finally, the terms S_{ev}, S_{cd}, S_{ac} and S_{cr} denote closures for the microphysical processes evaporation, condensation, autoconversion of cloud droplets into raindrops, and collection of cloud water by falling rain, respectively. We defer a thorough discussion of this closure scheme and its integration into the asymptotic framework to the next section, only pointing out their dependence on the saturation mixing ratio of water vapor q_{vs}, which to leading order is determined by CC and therefore itself a function of temperature (see the discussion below).

Having thus set the stage, our point of departure is Clausius-Clapeyron (CC) in the form valid for an ideal gas (a very good approximation for atmospheric water vapor), which reads

$$\frac{d \ln e_s}{dT} = \frac{L(T)}{R_v T^2}. \tag{14}$$

Here, $e_s = e_s(T)$ stands for the (nondimensional) saturation vapor pressure over a flat surface of liquid water at temperature T, while R_v is the specific gas constant of water vapor, and $L(T)$ the enthalpy (latent heat) of vaporization, which also varies with temperature. For the latter, it is generally considered a valid approximation to assume a linear relationship, which reads

$$L(T) = L_{\mathrm{ref}} - (c_l - c_{\mathrm{pv}})(T - T_{\mathrm{ref}}). \tag{15}$$

In this approximation, the specific heat capacities of water vapor at constant pressure and of liquid water are denoted by c_{pv} and c_l, respectively, assumed constant. We should mention that the dependence of c_l on temperature can be significant, but over the range of temperatures that we encounter in the lowest ~ 15 km of the atmosphere, the corresponding variations can be neglected.

Remark 1. *We do not include ice and mixed-phase clouds in our considerations. While these are clearly of great importance for a comprehensive understanding of moisture in the atmosphere, to the best of the authors' knowledge, the only systematic asymptotic analysis of atmospheric dynamics with explicit closures for the ice phase to date has been conducted by Dolaptchiev et al. (2023), who studied interactions between gravity wave dynamics and cirrus clouds, building on the application of asymptotic methods to the homogeneous nucleation process by Baumgartner and Spichtinger (2019). No fully general framework that treats both liquid and solid hydrometeors, coupled to the compressible flow equations, has been developed as of yet.*

Next, going back to the already established distinguished limit (10), we need to make one important adjustment: in Table 1, the isentropic exponent of dry air γ was introduced, a dimensionless quantity. This parameter can be written in terms of R_d and the specific heat capacity of dry air at constant pressure, c_{pd}. In the following, we replace γ by c_{pd} and reconsider the asymptotic rescaling of the ratio $R_d/c_{\mathrm{pd}} = (\gamma - 1)/\gamma$, which under the standard assumption

$\gamma = O(1)$ would also be a bounded quantity in the limit process $\epsilon \to 0$. The reason for this change will become apparent momentarily. - We thus consider the parameters listed in Table 3 below, with the scalings in (10) still in place, and try to find a distinguished limit that enables us to represent moist processes in the earth's atmosphere in a physically and mathematically sound way.

Dry air gas constant	$R_d = 287$ J/kg/K
Heat capacity of dry air at constant pressure	$c_{\mathrm{pd}} = 1005$ J/kg/K
Water vapor gas constant	$R_v = 462$ J/kg/K
Heat capacity of water vapor at constant pressure	$c_{\mathrm{pv}} = 1850$ J/kg/K
Heat capacity of liquid water	$c_l = 4218$ J/kg/K
Enthalpy of vaporization at $T = T_{\mathrm{ref}}$	$L_{\mathrm{ref}} \approx 2.5 \times 10^6$ J/kg

Table 3. Fundamental thermodynamic parameters for a cloudy, ice-free atmosphere

Now, before we proceed to discuss the derivation of an extended distinguished limit, let us state the three principles that shall guide us in this endeavor:

1. Our aim is to contribute to the theoretical understanding of real-world phenomena. Therefore, we will only take scalings into consideration that lead to physically reasonable relations.
2. As we now have twelve physical parameters and three nondimensional parameters have been assigned asymptotic rescalings already, the fundamental rules of dimensional analysis dictate that only five further scalings can be chosen freely.
3. Recall that, in the sense of a heuristic correspondence, we assumed $\epsilon \sim 1/10$. As far as possible, we will assign scalings that reflect the numerical values of our thermodynamic parameters accordingly.

As a first step, let us take a closer look at the thermodynamic evolution equation (11d). Notwithstanding the great variation in cloud types and precipitation intensities across spatial and temporal scales, one statement holds true for *all* atmospheric flow phenomena that are substantially influenced by moist processes: latent heating, i.e. temperature changes connected to phase changes of atmospheric water, is present in the leading-order equation for spatiotemporal thermodynamic perturbations. This translates to

$$C\left(D_t\tilde{\theta} + \tilde{w}\frac{d\bar{\theta}}{dz}\right) \sim \frac{L(\bar{T})}{\bar{T}}\left(D_t\tilde{q}_v + \tilde{w}\frac{d\bar{q}_{\mathrm{vs}}}{dz}\right) \tag{16}$$

in a generic formal asymptotic ansatz, where $\bar{f} = \bar{f}(z)$ is a given vertical background profile and $\tilde{f}$ denotes perturbations with unrestricted dependence on $(t, \mathbf{x}, z)$ about a vertical background state. Depending on the cloud and / or precipitation type under consideration, one of the terms on either side may of course drop out of the leading-order balance. We thus see that the scaling of the nondimensional parameter

$$\frac{L_{\mathrm{ref}}}{c_{\mathrm{pd}}T_{\mathrm{ref}}} \approx 9.1 \tag{17}$$

plays a crucial role in determining the relative strength of moist thermodynamic perturbations. Here, the only sensible choice in accordance with guideline 3 is to assign the scaling

$$\frac{L_{\mathrm{ref}}}{c_{\mathrm{pd}}T_{\mathrm{ref}}} = L\epsilon^{-1}, \tag{18}$$

which we shall treat as a given from now on. Next, going back to CC in differential form (14), notice that the ansatz (15) with constant heat capacities lets us integrate it exactly, leading to

$$e_s(T) = e_{s\,\mathrm{ref}} \left(\frac{T_{\mathrm{ref}}}{T}\right)^{\frac{c_l - c_{\mathrm{pv}}}{R_v}} \exp\left\{\left(\frac{L_{\mathrm{ref}}}{R_v T_{\mathrm{ref}}} + \frac{c_l - c_{\mathrm{pv}}}{R_v}\right)\frac{T - T_{\mathrm{ref}}}{T}\right\}. \tag{19}$$

Since, by the ideal gas laws summarized in (12b), e_s is related to the saturation mixing ratio q_{vs} by the formula

$$q_{\mathrm{vs}} = \frac{R_d}{R_v}\frac{e_s}{p - e_s}, \tag{20}$$

fixing the asymptotic magnitude of e_s relative to the dry air pressure $p - e_s$ and determining a suitable scaling for R_d/R_v will also fix the asymptotic magnitude of q_{vs}, which in turn provides an upper bound for the local water vapor mixing ratio q_v. This holds true because supersaturation attained in the real atmosphere is invariably quite small. Let us also bear in mind the following:

(i) The saturation vapor pressure at $T = T_{\mathrm{ref}}$ is very small compared to the total atmospheric pressure close to the surface.
(ii) At leading order, temperature decreases with height in the troposphere.
(iii) The exponential term makes the dominant contribution in (19) when temperatures decrease, since $x^\alpha = e^{\alpha \ln x} \leq e^{\alpha(x-1)} \quad \forall x > 0$, and hence

$$e_s(T) \leq \exp\left\{\frac{L_{\mathrm{ref}}}{R_v T_{\mathrm{ref}}}\frac{T - T_{\mathrm{ref}}}{T}\right\} \tag{21}$$

for all T.

In determining an asymptotic representation of CC, describing the rapid decrease of available moisture at greater atmospheric altitudes, we thus need to look to the asymptotic expansion of the term

$$\frac{L_{\mathrm{ref}}}{R_v T_{\mathrm{ref}}}\frac{T - T_{\mathrm{ref}}}{T}. \tag{22}$$

It is now straightforward to see why the standard dry air limit $R_d/c_{\mathrm{pd}} = O(1)$ is troublesome when applied to CC: the resulting thermodynamic background state includes a linearly decreasing absolute temperature at leading order, implying

$$\frac{T - T_{\mathrm{ref}}}{T} = O(1). \tag{23}$$

Moreover, we have

$$\frac{L_{\mathrm{ref}}}{R_v T_{\mathrm{ref}}} = \frac{R_v}{c_{\mathrm{pd}}}\frac{L_{\mathrm{ref}}}{c_{\mathrm{pd}} T_{\mathrm{ref}}} > \frac{L_{\mathrm{ref}}}{c_{\mathrm{pd}} T_{\mathrm{ref}}}, \tag{24}$$

so this factor should by all rights be asymptotically *large.* Adopting the standard limit now yields

$$e_s(T) \sim \exp\left(\frac{L_{\mathrm{ref}}}{R_v T_{\mathrm{ref}}}\frac{T-T_{\mathrm{ref}}}{T}\right) \sim \exp\left(-\frac{1}{\epsilon}\right), \tag{25}$$

for temperatures $T < T_{\mathrm{ref}}$. The saturation vapor pressure consequently vanishes *to all orders* above said temperature threshold, with translates to the statement that any nonzero amount of moisture at such temperatures (which are characteristic of middle to high tropospheric levels) *immediately crosses the saturation threshold.* This is clearly unphysical because a significant amount of water vapor is present even in the driest regions of the real troposphere.

Remark 2. *The chosen reference temperature $T_{ref} = 273.15$ K is significantly lower than average surface temperatures in the tropics and most of the middle latitudes. Therefore, one should also be interested in the asymptotic behavior of CC for $T > T_{ref}$. Here, the situation is even more dire: the exponent* (24) *(which can be seen to determine the leading-order behavior also in this case) blows up, and the formal limit does not even exist in the first place.*

Going back to the drawing board, let us recall that the *potential* temperature can generally be taken constant at leading order, since its tropospheric variation is of the order $\sim 30 - 40$ K. Due to the relationship

$$T = \theta\left(\frac{p}{p_{\mathrm{ref}}}\right)^{\frac{R_d}{c_{\mathrm{pd}}}}, \tag{26}$$

absolute temperature will be constant at leading order if and only if $R_d/c_{\mathrm{pd}} = o(1)$ in the adopted distinguished limit (pressure always exhibits $O(1)$ variations). To achieve a finite saturation vapor pressure in the limit $\epsilon \to 0$, one can thus propose the scaling

$$\frac{R_d}{c_{\mathrm{pd}}} = \epsilon\Gamma, \tag{27}$$

known as the *Newtonian limit,* borrowed from combustion theory (Parkins et al., 2000). This is the choice made by Klein and Majda (2006), later also adopted by Hittmeir and Klein (2018), as well as Bäumer and Klein (2025). With the Newtonian limit in place, the exponent of the dominant term in (19) reads

$$\epsilon^{-2}\frac{R_d}{R_v}\frac{L}{\Gamma}\frac{T-T_{\mathrm{ref}}}{T} \sim O(\epsilon^{-1})\frac{R_d}{R_v}. \tag{28}$$

Thus, in order to achieve $O(1)$ variations of the saturation vapor pressure throughout the free troposphere in the formal limit, we must also assume

$$\frac{R_d}{R_v} = \epsilon E, \tag{29}$$

with $E = O(1)$ in the limit $\epsilon \to 0$. This scaling is still somewhat awkward when looking at the numerical value

$$\frac{R_d}{R_v} \approx 0.62, \tag{30}$$

but it is forced if we respect guidelines 1 and 2 *and* try to do the least amount of violence to guideline 3. Having established (18), (27) and (29), only asymptotic scalings for the ratios of the various heat capacities remain to complete the description of the distinguished limit for a moist atmosphere. Here, we need to take a closer look at the coefficient (12j) in the thermodynamic equation. In scaled form, the term

$$\frac{c_{\mathrm{pv}}}{c_{\mathrm{pd}}}\frac{R_d}{c_{\mathrm{pd}}} - \frac{R_v}{c_{\mathrm{pd}}} \approx 0.067 \tag{31}$$

only adjusts toward a positive value if we assume $c_{\mathrm{pv}}/c_{\mathrm{pd}} = O(\epsilon^{-1})$, which corresponds to a Newtonian limit for water vapor. On the other hand, the heat capacity of liquid water is significantly larger than that of water vapor, and hence we choose

$$\frac{c_l}{c_{\mathrm{pd}}} = \epsilon^{-1} k_l, \quad \frac{c_{\mathrm{pv}}}{c_{\mathrm{pd}}} = \epsilon^{-1} k_v. \tag{32}$$

The empiricist's alternative: Hittmeir and Klein (2018), who first derived the above distinguished limit in the context of the dynamics of convective cloud towers, also considered an alternative approach that sacrifices formal consistency for more accurate representation of the actual numerical values. To be specific, they proposed a limit that deviates from the formally consistent one *only* in the scalings of R_d/R_v and $c_{\mathrm{pv}}/c_{\mathrm{pd}}$, both of which were considered $O(1)$ when occurring in isolation; in CC, nevertheless, the ratio $L_{\mathrm{ref}}/(R_v T_{\mathrm{ref}})$ was scaled as an $O(\epsilon^{-1})$ quantity, which leads to an obvious contradiction when writing it as a product (as in (24)). Similarly, the term (31) was ad hoc assigned an asymptotic magnitude of $O(\epsilon)$, implying another formal inconsistency. Even so, the reduced models coming out of such an ansatz might have merit - in the words of the authors of the cited article:

> "The second regime, in contrast, has been defined purely on the basis of the actual magnitudes of the dimensionless parameters. Numbers between 0.4 and 3.0 are considered of order unity, while smaller or larger values are associated with asymptotic rescalings in terms of ϵ. This provides a scaling that better matches with the actual numbers than the first regime, but it is not strictly consistent with similarity theory. Although this is at odds with the usual procedures, it may actually open up an interesting route of investigation. The thermodynamics of moist air may just be asymptotically compatible with a family of equation systems that features the same functional forms in the constitutive equations as those of moist air, but whose set of determining parameters is less constrained. The results of Sect. 4.2, in which we compare asymptotic and error-controlled numerical approximations to the moist adiabatic distribution, corroborate this point of view."

Beyond Hittmeir and Klein (2018), said limit was also adopted in the derivation of the large-scale model of Bäumer and Klein (2025), mainly because it preserves the traditional form of the hydrostatic balance relation. The jury is still out on the question whether one of the two distinguished limits described here can generally be considered "better" than the other. Adopting the terminology of the two cited articles, we refer to the formally consistent regime as $\alpha = 0$, while the value-based alternative is indicated by $\alpha = 1$, see Table 4 for an overview.

	Value	Regime $\alpha = 1$	Regime $\alpha = 0$
Nondimensional parameters			
$\frac{R_d}{c_{\mathrm{pd}}}$	0.29	$\epsilon\Gamma$	$\epsilon\Gamma$
$\frac{c_{\mathrm{pv}}}{c_{\mathrm{pd}}}$	1.8	k_v	$\epsilon^{-1}k_v$
$\frac{R_v}{c_{\mathrm{pd}}}$	0.46	$1/A$	$1/A$
$\frac{c_l}{c_{\mathrm{pd}}}$	4.2	$\epsilon^{-1}k_l$	$\epsilon^{-1}k_l$
$\frac{L_{\mathrm{ref}}}{c_{\mathrm{pd}}T_{\mathrm{ref}}}$	9.1	$\epsilon^{-1}L$	$\epsilon^{-1}L$
Derived nondimensional parameters			
$\frac{R_d}{R_v}$	0.62	E	ϵE
$\frac{c_{\mathrm{pv}}}{c_{\mathrm{pd}}}\frac{R_d}{c_{\mathrm{pd}}} - \frac{R_v}{c_{\mathrm{pd}}}$	0.067	$\epsilon\kappa_v$	κ_v

Table 4. Two viable moist extensions of the distinguished limit for dry air

Scaling the moist constituents: Mixing ratios are dimensionless quantities, and in the case of atmospheric water, they are invariably small. Even in the tropical troposphere, the biggest atmospheric moisture reservoir, the mixing ratio of water vapor at saturation does not exceed a couple percent. Therefore, the scaling

$$q_{\mathrm{vs}} = O(\epsilon^2) \tag{33}$$

suggests itself. Recalling (20), this implies that we scale the saturation vapor pressure as

$$\frac{e_{s_{\mathrm{ref}}}}{p_{\mathrm{ref}}} = O(\epsilon^{1+\alpha}), \tag{34}$$

with $\alpha \in \{0, 1\}$ referring to the two regimes summarized in Table 4. Again, the formally consistent regime $\alpha = 0$ can be seen to systematically *overestimate* moist contributions relative to the numerical values. As already mentioned, supersaturation in the earth's atmosphere rarely exceeds even 1% (Houze, 2014), which implies that (33) also sets the maximum magnitude of the water vapor mixing ratio q_v. Turning to the mass fractions of liquid water, it is not hard to see that no universally valid scaling can be expected: while the available supply of water vapor sets an obvious upper limit also for the magnitudes of q_c and q_r, the phenomenologically "correct" scaling depends on the cloud type and therefore the scale under consideration. To be more specific, convective cloud towers as discussed, e.g., by Hittmeir and Klein (2018) produce much more intense rain than the stratiform clouds characteristic of midlatitude cyclones. Even typical terminal fall velocities vary significantly between the two phenomena, since convective updrafts produce much bigger raindrops. This is why the scalings of both the rain mixing ratio q_r *and* the terminal velocity V_r differ between the cited study and the large-scale models of, e.g., Smith and Stechmann (2017) or Bäumer and Klein (2025).

Phase changes and their parameterization

Choosing an appropriate closure scheme

The representation of phase changes of water on the macroscopic level of atmospheric motions poses one of the biggest challenges for both the theoretical and the numerical modeler:

condensation kernels on which cloud droplets start to form have diameters on the order of *microns.* As more and more liquid water diffuses onto a droplet, it may grow to precipitable size, gain a non-negligible fall speed, and then continue to accelerate downward until a balance between gravity and the drag force exerted on it by the surrounding air is reached. The droplet - now a raindrop - then attains its terminal velocity. This velocity depends on the drop's size, which in turn is a function of its interactions with other drops and droplets; crucially, it strongly increases with the intensity of local updrafts. Finally, as the raindrop gets closer to the ground, it may either fall unimpeded or (partially) evaporate in dry boundary layer air.

This sketch of the life cycle of one individual drop makes the complexity of the subject matter apparent: there is no clear-cut distinction between non-precipitating and precipitating water drops, fall speeds of the latter vary significantly, and they strongly depend on environmental conditions. Then, of course, there are the intricacies of the two-stage process of nucleation and condensation, which happen on very small spatial and temporal scales. In the hydrodynamic setting, we therefore need to assume quite drastic simplifications from the outset. In particular, in the context of asymptotic model hierarchies, it is prudent to keep the complexity of the chosen closure scheme to a manageable minimum. This is why the governing equations (11) include transport equations for only three moist constituents. Even though, as already remarked, the subdivision of liquid water into cloud water and rain is somewhat arbitrary, this simple bulk model is sufficient to capture the essentials of moist dynamics on all meteorological scales (without the ice phase). Phase changes in such a model are traditionally parameterized in a form originally devised by Kessler (1995); for the reader's convenience, we restate the closure scheme employed here below. It goes back to Klein and Majda (2006), and has further been utilized in the asymptotic modeling studies of Hittmeir and Klein (2018), Bäumer et al. (2023) and Bäumer and Klein (2025):

$$S_{\mathrm{ev}} = C_{\mathrm{ev}} \frac{p}{\rho} (q_{\mathrm{vs}} - q_v)^+ q_r, \tag{35a}$$

$$S_{\mathrm{cd}} = C_{\mathrm{cn}} (q_v - q_{\mathrm{vs}})^+ q_{\mathrm{cn}} + C_{\mathrm{cd}} (q_v - q_{\mathrm{vs}}) q_c, \tag{35b}$$

$$S_{\mathrm{ac}} = C_{\mathrm{ac}} (q_c - q_{\mathrm{ac}})^+, \tag{35c}$$

$$S_{\mathrm{cr}} = C_{\mathrm{cr}} q_c q_r. \tag{35d}$$

In the above relations, terms of the form $C_\star$ denote rate constants of the associated processes. The first term from the left in (35b) constitutes a closure for *heterogeneous nucleation*, the initial formation of a droplet around a condensation nucleus; here, q_{cn} represents the local density of cloud condensation kernels. In (35c), q_{ac} denotes an "activation threshold" for the conversion of cloud water into rain, as introduced by Kessler (1995). We remark that the loss of smoothness at the phase interface makes the analytical treatment of the moisture equations (11e)-(11g) challenging, whether they are passively transported by a given velocity field or coupled to the full governing equations. See Hittmeir et al. (2017, 2020, 2023) for global well-posedness results regarding the hydrostatic primitive equations and Doppler et al. (2024) for a local result concerning the full compressible system (11). All of the cited works utilize standard closures for turbulent diffusion and mixing for access to parabolic regularity.

Remark 3. *We emphasize that* (35) *was chosen pragmatically as the simplest qualitatively accurate bulk scheme, where all phase transitions are functions of the respective mixing ratios or their excess beyond a certain threshold only. More realistic bulk microphysics closures involve fractional powers of the liquid water mixing ratios, which are quite awkward to use in a formal asymptotic framework. For the reader interested in more accurate parameterizations, the overview in Chapter 3 of Houze (2014) is a good starting point. We further mention the double-moment scheme of Seifert and Beheng (2001) as an example of a parameterization that balances moderate complexity with a systematic treatment of autoconversion, accretion and self-collection.*

Asymptotic treatment of phase changes

At first sight, it might seem straightforward to find proper scalings for the conversion terms (35) on the respective right-hand sides of the moisture equations (11e)-(11g): having determined the appropriate asymptotic magnitudes of the various mixing ratios and the scaled value of the average terminal rainfall velocity V_r for a given time - and length scale, one estimates the scaled conversion rates relative to the reference time and can thus determine their respective asymptotic strengths. The problem with this naive approach is that the rate constants on the respective right-hand sides of (35), essentially representing "best fits" for long-time averages, will in general depend on the type of cloud and precipitation under consideration. Specifically, since the bulk modeling approach does not differentiate between drops and droplets of different sizes, we cannot expect all of the characteristic differences between convective and stratiform precipitation to be captured by the mixing ratios of cloud water and rain alone. Therefore, we certainly should not assume *one* particular choice of the constants $C_\star$ to be valid across all meteorological scales, and instead critically re-evaluate the respective strengths of all microphysical processes for each scale-specific model. Awareness of this is of particular importance when looking ahead to multiscale models that will systematically explore interactions between moist processes from the convective to the synoptic scale. Now, going back to already established single-scale models, we can discern two principally different approaches to the modeling of phase transitions in asymptotic studies:

1. *Continuous re-parameterization:* This modeling strategy, pursued by, e.g., Bäumer et al. (2023) and Bäumer and Klein (2025), assumes that the averaged effects of the various microphysical processes on the given meteorological scale can be parametrized by continuous functions of the same type as the original closures in (35). As laid out above, this does *not* amount to a scaling assumption on the original rate constants, since those might themselves be scale-dependent.
2. *Fast microphysics:* This ansatz builds on the straightforward observation that microphysical processes are resolved on accordingly small scales, and can therefore be considered immediate on the much larger meteorological timescales. Most asymptotic studies dealing with a moist atmosphere that the authors are aware of treat the condensation term in this manner, with some extending it to all phase transitions, see, e.g., Smith and Stechmann (2017).

As shown below, the transition from the first approach to the second can be achieved - at least for the condensation term - by a straightforward rescaling of the appropriate rate constants.

We devote the last section to a detailed comparison of the respective outcomes, choosing the precipitating quasi-geostrophic (PQG) model family as a representative example.

Let us consider the following situation: we are in the process of constructing a reduced single-scale model by a generic regular asymptotic expansion, and the scaling is already fully in place. However, we want to obtain a fast microphysics limit for the condensation term *as a byproduct* of the formal derivation. In this context, the *fast condensation limit* refers to the following alternative:

$$\begin{cases} q_v = q_{\mathrm{vs}}, & q_c = q_t - q_{\mathrm{vs}} - q_r & \text{in saturated air} \\ q_v < q_{\mathrm{vs}}, & q_c = 0 & \text{in undersaturated air,} \end{cases} \tag{36}$$

with the total water content $q_t = q_v + q_c + q_r$. This alternative reduces the number of prognostic variables by one, since q_c can be calculated explicitly from q_t and q_r at any given time (and q_{vs}, which in general is a function of temperature and therefore also part of the system's output):

$$q_c = \max\left(q_t - q_{\mathrm{vs}} - q_r, 0\right). \tag{37}$$

Similarly, one gets

$$q_v = \min\left(q_{\mathrm{vs}}, q_t - q_r\right). \tag{38}$$

On a formal level, this alternative can be recovered systematically simply by rescaling the respective nucleation and condensation rates appropriately: instead of assuming continuous reparameterization, we recognize both C_{cn} and C_{cd} as asymptotically fast with respect to the chosen timescale and make the ansatz

$$C_{\mathrm{cn}} t_{\mathrm{ref}} \sim C_{\mathrm{cd}} t_{\mathrm{ref}} \sim \epsilon^{-n}, \tag{39}$$

for some sufficiently large n. In the scaled moisture equations, this yields the leading-order balance

$$\begin{aligned} S_{\mathrm{cd}}^{(0)} =& C_{\mathrm{cn}}(q_v^{(1)} - q_{\mathrm{vs}}^{(1)})^+ q_{\mathrm{cn}}^{(0)} \\ &+ C_{\mathrm{cd}}(q_v^{(1)} - q_{\mathrm{vs}}^{(1)}) q_c^{(0)} = 0, \end{aligned} \tag{40}$$

which, since $q_c^{(0)}$ and $q_{\mathrm{cn}}^{(0)}$ cannot be negative, immediately leads to (36).

Precipitating quasi-geostrophic models

Fundamentals

The classical quasi-geostrophic (QG) theory is of central importance in the mathematical analysis of both atmospheric and oceanic fluid dynamics (Pedlosky, 1987; Vallis, 2017). In particular, it captures the essential dynamics of the midlatitude atmosphere with its alternating cyclonic-anticyclonic structure, and its standard formulation highlights the importance of *potential vorticity,* a fundamental quantity in all of meteorology (Ertel, 1942; Hoskins et al., 1985). In the following, we will use the notation

$$D_t^{\parallel} := \partial_t + \mathbf{u} \cdot \nabla_{\parallel} \tag{41}$$

for the material derivative with respect to the horizontal velocity field. To set the stage for the rest of this section, let us very briefly recap the equations and their main properties: starting with the governing equations (6) for dry air, systematic scale analysis - which can be performed in the Klein (2010) framework - and asymptotic expansion lead to

$$f\mathbf{u} = \nabla_{\parallel}^{\perp}\tilde{\phi} \tag{42}$$

as the leading-order horizontal momentum balance, where f is the Coriolis parameter at the reference latitude and $\phi = \tilde{p}/\bar{\rho}$ denotes the pressure perturbation scaled by the background density. This relation is known as *geostrophic balance.* The vertical momentum equation yields

$$\partial_z\tilde{\phi} = g\frac{\tilde{\theta}}{\theta_{\mathrm{ref}}}, \tag{43}$$

which is known as *hydrostatic balance.* The first-order contribution to horizontal momentum, combined with the mass continuity equation, can be written in the form

$$D_t^{\parallel}\left[\zeta + \beta y\right] = \frac{f}{\bar{\rho}}\partial_z(\bar{\rho}\tilde{w}), \tag{44}$$

where $\zeta = v_x - u_y$ denotes the vertical component of the vorticity, β the variation of the Coriolis force with latitude, and $\tilde{w}$ the small geostrophic vertical velocity. Finally, the thermodynamic Eq. (6d) reads

$$D_t^{\parallel}\tilde{\theta} + \tilde{w}\frac{d\bar{\theta}}{dz} = Q \tag{45}$$

at leading order. Here, $d\bar{\theta}/dz > 0$ is assumed throughout, which translates to the atmosphere being *stably stratified* in the large-scale mean.

Having collected (42)-(45), one can achieve a significant simplification of this system by eliminating the vertical velocity: adding the vorticity Eq. (44) and the vertical derivative of a suitable multiple of (45) naturally leads to

$$D_t^{\parallel}\mathrm{PV} = \frac{f}{\bar{\rho}}\partial_z\left(\frac{\bar{\rho}Q}{d\bar{\theta}/dz}\right), \tag{46}$$

the evolution equation for the *QG potential vorticity* (PV), defined as

$$\mathrm{PV} := \zeta + \beta y + \frac{f}{\bar{\rho}}\partial_z\left(\frac{\bar{\rho}\tilde{\theta}}{d\bar{\theta}/dz}\right). \tag{47}$$

Substituting the geostrophic and hydrostatic balances (42) and (43), we get

$$\frac{1}{f}\Delta_{\parallel}\tilde{\phi} + \frac{f}{\bar{\rho}}\partial_z\left(\frac{\bar{\rho}\partial_z\tilde{\phi}}{N^2}\right) = \mathrm{PV} - \beta y, \tag{48}$$

where N denotes the background buoyancy frequency,

$$N := \sqrt{g\frac{d\bar{\theta}/dz}{\theta_{\text{ref}}}}. \tag{49}$$

Due to the assumption of stable stratification stated above, N is real-valued and (48) constitutes a linear elliptic equation for $\tilde{\phi}$ when PV is given. The process of retrieving the pressure from (48) is known as *potential vorticity inversion.* Thus, the evolution of the QG system is governed exclusively be the PV transport Eq. (47), an *active scalar equation.*

There is a rich mathematical literature on the QG equations. Global well-posedness of the full system is addressed, e.g., by Bourgeois and Beale (1994), while Novack and Vasseur (2018, 2020) cover its extension to a boundary layer theory. We would be remiss not to mention that the 2D *surface QG* (SQG) equation, derived from a simplified version of the original system with PV $\equiv 0$, has captured the attention of mathematicians ever since Constantin et al. (1994) alerted the mathematical fluid dynamics community to its intriguing parallels to the 3D Euler equations.

Moist extension and the structural effect of fast microphysics

The passage from continuous phase transitions to switches as in the "fast condensation limit" (36) can fundamentally alter the analytical structure of the resulting reduced model. The *precipitating QG* (PQG) model family, going back to Smith and Stechmann (2017), here serves as an ideal example, since variants of the PQG equations both with fast phase changes and with full Kessler-style closures have already been derived and investigated. We begin with the PQG model recently derived by Bäumer and Klein (2025), which preserves the original form of the bulk microphysics closures (35). In their "raw" form, the equations of this model in dimensional form read

$$f\mathbf{k}\times\mathbf{u} = -\nabla_{\parallel}\tilde{\phi} \tag{50a}$$

$$\partial_z\tilde{\phi} = g\frac{\tilde{\theta}}{\theta_{\text{ref}}} \tag{50b}$$

$$D_t^{\parallel}\left[\zeta+\beta y\right] = \frac{f}{\bar{\rho}}\partial_z(\bar{\rho}\tilde{w}) \tag{50c}$$

$$D_t^{\parallel}\tilde{\theta}_e + \tilde{w}\frac{d\bar{\theta}_e}{dz} = 0 \tag{50d}$$

$$D_t^{\parallel}\tilde{q}_v + \tilde{w}\frac{d\bar{q}_{\text{vs}}}{dz} = S_{\text{ev}} - S_{\text{cd}} \tag{50e}$$

$$D_t^{\parallel}q_c = S_{\text{cd}} - S_{\text{ac}} - S_{\text{cr}} \tag{50f}$$

$$-\frac{1}{\bar{\rho}}\partial_z(\bar{\rho}V_r q_r) = S_{\text{ac}} + S_{\text{cr}} - S_{\text{ev}}, \tag{50g}$$

where $\theta_e = \theta + \frac{L_{\text{ref}}}{c_{\text{pd}}}q_v$ is the (linearized) equivalent potential temperature, $\tilde{q}_{\text{vs}}$ is a linear function of potential temperature $\tilde{\theta}$, by asymptotic expansion of CC, and the leading-order phase changes

read

$$S_{\mathrm{ev}} = \bar{C}_{\mathrm{ev}} \left(\tilde{q}_{\mathrm{vs}} - \tilde{q}_v\right)^+ q_r \tag{51a}$$
$$S_{\mathrm{cd}} = \bar{C}_{\mathrm{cn}} \left(\tilde{q}_v - \tilde{q}_{\mathrm{vs}}\right)^+ q_{\mathrm{cn}} + \bar{C}_{\mathrm{cd}} \left(\tilde{q}_v - \tilde{q}_{\mathrm{vs}}\right) q_c \tag{51b}$$
$$S_{\mathrm{ac}} = \bar{C}_{\mathrm{ac}} \left(q_c - q_{\mathrm{ac}}\right)^+ \tag{51c}$$
$$S_{\mathrm{cr}} = \bar{C}_{\mathrm{cr}} q_c q_r. \tag{51d}$$

The derivation of a PV equation here proceeds in essentially the same fashion as for the classical dry air model. Due to the presence of a moist background, however, we further need to introduce a new moisture variable to fully eliminate the vertical velocity. We refer to Bäumer and Klein (2025) for a detailed derivation, only stating the result:

$$D_t^{\parallel} \mathrm{PV}_e = - \frac{f}{d\bar{\theta}_e/dz} \partial_z \mathbf{u} \cdot \nabla_{\parallel} \left(\frac{L_{\mathrm{ref}}}{c_{\mathrm{pd}}} \tilde{q}_v \right) \tag{52a}$$
$$D_t^{\parallel} \tilde{M} = B(z) \left[S_{\mathrm{ev}} - S_{\mathrm{cd}} \right] \tag{52b}$$
$$D_t^{\parallel} q_c = S_{\mathrm{cd}} - S_{\mathrm{ac}} - S_{\mathrm{cr}} \tag{52c}$$
$$-\frac{1}{\bar{\rho}} \partial_z \left(\bar{\rho} V_r q_r \right) = S_{\mathrm{ac}} + S_{\mathrm{cr}} - S_{\mathrm{ev}} \tag{52d}$$
$$\begin{aligned} \frac{1}{f} \Delta_{\parallel} \tilde{\phi} + \frac{f}{\bar{\rho}} \partial_z \left(\frac{\bar{\rho}}{d\bar{\theta}_e/dz} \frac{B(z)}{L_{\mathrm{ref}}/c_{\mathrm{pd}} + B(z)} \partial_z \tilde{\phi} \right) =& \mathrm{PV}_e - \beta y \\ & - \frac{f}{\bar{\rho}} \partial_z \left(\frac{\bar{\rho}}{d\bar{\theta}_e/dz} \frac{L_{\mathrm{ref}}/c_{\mathrm{pd}}}{L_{\mathrm{ref}}/c_{\mathrm{pd}} + B(z)} \tilde{M} \right) \end{aligned} \tag{52e}$$
$$f \mathbf{k} \times \mathbf{u} = - \nabla_{\parallel} \tilde{\phi} \tag{52f}$$
$$\partial_z \tilde{\phi} = g \frac{\tilde{\theta}}{\theta_{\mathrm{ref}}}, \tag{52g}$$

where PV_e is the QG potential vorticity based on linearized equivalent potential temperature $\theta_e = \theta + \frac{L_{\mathrm{ref}}}{c_{\mathrm{pd}}} q_v$, the moisture variable $\tilde{M}$ is a linear combination of $\tilde{\theta}_e$ and $\tilde{q}_v$ and the following additional relations hold:

$$B(z) = -\frac{d\bar{\theta}_e/dz}{d\bar{q}_{\mathrm{vs}}/dz} \tag{53a}$$
$$\tilde{q}_v = \frac{1}{L_{\mathrm{ref}}/c_{\mathrm{pd}} + B(z)} \left(\tilde{M} - \tilde{\theta} \right). \tag{53b}$$

Notice that the PV_e inversion equation here is still linear when all prognostic variables are given.

PQG$_{DL}$ in the fast condensation limit

Let us now go back to the reduced moisture and thermodynamic equations in their preliminary form to examine the effect of fast condensation: we have

$$D_t^{\parallel}\tilde{q}_v + \tilde{w}\frac{d\bar{q}_{\rm vs}}{dz} = S_{\rm ev} - S_{\rm cd}^{(n)} \tag{54a}$$

$$D_t^{\parallel}q_c = S_{\rm cd}^{(n)} - S_{\rm ac} - S_{\rm cr} \tag{54b}$$

$$-\frac{1}{\bar{\rho}}\partial_z(V_r\bar{\rho}q_r) = S_{\rm ac} + S_{\rm cr} - S_{\rm ev} \tag{54c}$$

$$D_t^{\parallel}\tilde{\theta}_e + \tilde{w}\frac{d\bar{\theta}_e}{dz} = 0, \tag{54d}$$

which necessitates elimination of the higher-order term $S_{\rm cd}^{(n)}$. This leads to the introduction of the auxiliary variable $\tilde{q}_{\rm vc} = \tilde{q}_v + q_c$ and the reduced system

$$D_t^{\parallel}\tilde{q}_{\rm vc} + \tilde{w}\frac{d\bar{q}_{\rm vs}}{dz} = \frac{1}{\bar{\rho}}\partial_z(V_r\bar{\rho}q_r) \tag{55a}$$

$$-\frac{1}{\bar{\rho}}\partial_z(V_r\bar{\rho}q_r) = S_{\rm ac} + S_{\rm cr} - S_{\rm ev} \tag{55b}$$

$$D_t^{\parallel}\tilde{\theta}_e + \tilde{w}\frac{d\bar{\theta}_e}{dz} = 0. \tag{55c}$$

Eliminating the vertical velocity and deriving the PV$_e$ equation as before then yields

$$D_t^{\parallel}\tilde{M} = \frac{B(z)}{\bar{\rho}}\partial_z(V_r\bar{\rho}q_r) \tag{56a}$$

$$-\frac{1}{\bar{\rho}}\partial_z(V_r\bar{\rho}q_r) = S_{\rm ac} + S_{\rm cr} - S_{\rm ev} \tag{56b}$$

$$D_t^{\parallel}{\rm PV}_e = -\frac{f}{d\bar{\theta}_e/dz}\partial_z\mathbf{u}\cdot\nabla_{\parallel}\left(\frac{L_{\rm ref}}{c_{\rm pd}}\tilde{q}_v\right), \tag{56c}$$

where we can write

$$\tilde{q}_v = \min\left(\tilde{q}_{\rm vs}, \frac{1}{L_{\rm ref}/c_{\rm pd} + B(z)}(\tilde{M} - \tilde{\theta})\right) \tag{57}$$

($\tilde{M}$ is now defined in terms of $\tilde{\theta}_e$ and $q_{\rm vc}$). Determining the local saturation status therefore requires knowledge of $\tilde{\theta}$, which is clearly part of the *output* of the PV$_e$ inversion equation. In said equation,

$$\frac{1}{f}\Delta_{\parallel}\tilde{\phi} + \frac{f}{\bar{\rho}}\partial_z\left(\frac{\bar{\rho}\tilde{\theta}_e}{d\bar{\theta}_e/dz}\right) = {\rm PV}_e - \beta y, \tag{58}$$

we similarly can only write

$$\tilde{\theta}_e = \min\left(\tilde{\theta} + \frac{L_{\rm ref}}{c_{\rm pd}}\tilde{q}_{\rm vs}, \frac{B(z)}{L_{\rm ref}/c_{\rm pd} + B(z)}\tilde{\theta} + \frac{L_{\rm ref}/c_{\rm pd}}{L_{\rm ref}/c_{\rm pd} + B(z)}\tilde{M}\right). \tag{59}$$

Therefore, the functional form of the inversion equation is only known on either side of the phase interface, which in turn depends on the solution of the equation. We thus get an a priori only *piecewise* elliptic equation that involves a free boundary problem; this makes the analytical and numerical study of PQG models with fast microphysics very challenging. A first step toward the rigorous validation of such models was taken by Remond-Tiedrez et al. (2024), who proved the well-posedness of the nonlinear PV inversion equation of Smith and Stechmann (2017) in a weak formulation. To summarize: we have obtained the system

$$D_t^{\parallel}\mathrm{PV}_e = -\frac{f}{d\bar{\theta}_e/dz}\partial_z\mathbf{u}\cdot\nabla_{\parallel}\left(\frac{L_{\mathrm{ref}}}{c_{\mathrm{pd}}}\tilde{q}_v\right) \tag{60a}$$

$$D_t^{\parallel}\tilde{M} = \frac{B(z)}{\bar{\rho}}\partial_z(V_r\bar{\rho}q_r) \tag{60b}$$

$$-\frac{1}{\bar{\rho}}\partial_z\left(\bar{\rho}V_r q_r\right) = S_{\mathrm{ac}} + S_{\mathrm{cr}} - S_{\mathrm{ev}} \tag{60c}$$

$$\frac{1}{f}\Delta_{\parallel}\tilde{\phi} + \frac{f}{\bar{\rho}}\partial_z\left(\frac{\bar{\rho}\tilde{\theta}_e}{d\bar{\theta}_e/dz}\right) = \mathrm{PV}_e - \beta y \tag{60d}$$

$$f\mathbf{k}\times\mathbf{u} = -\nabla_{\parallel}\tilde{\phi} \tag{60e}$$

$$\partial_z\tilde{\phi} = g\frac{\tilde{\theta}}{\theta_{\mathrm{ref}}}, \tag{60f}$$

with the auxiliary relations (57) and (59), as the fast condensation equivalent of (52).

Summary and outlook

We discussed recent steps towards a general framework for the asymptotic modeling of moist atmospheric flows, omitting the ice phase for the time being. In particular, we showed in detail that the incorporation of the fundamental Clausius-Clapeyron relation makes it difficult to obtain a distinguished limit that is both formally consistent and faithful to the numerical magnitudes of the thermodynamic parameters of moist air. We argued, as Hittmeir and Klein (2018) did, that two different regimes could be considered viable, summarized in Table 4. Furthermore, we laid out two contrasting approaches to the modeling of phase changes and highlighted the profound structural changes arising from a transition to fast microphysics in the family of precipitating quasi-geostrophic models.

As far as directions for future research are concerned, we can only offer a personal selection, since the field has a whole is still in its infancy: on the modeling side, the systematic study of interactions between small-scale moist convection and large-scale cloud regions stands out as a problem of great theoretical and practical relevance. The connection of reduced models for moist atmospheric dynamics to the planetary boundary layer constitutes another important challenge. Here, Bäumer and Klein (2025) achieved significant progress by merging the recent triple-deck boundary layer theory of Klein et al. (2022) with the PQG model family (the equations for the bulk flow are stated in (52)). Of course, much still needs to be learned about the properties of previously derived models. - Again highlighting developments in the PQG context, numerical

convergence studies as in (Zhang et al., 2022) are a promising avenue of investigation, as is the derivation of families of physically meaningful explicit solutions, achieved by Wetzel et al. (2019) for discontinuous fronts. Regarding the rigorous analysis of models based on the Navier-Stokes or Euler equations with moist process closures as in (11), most research to date has been concerned with the well-posedness of the full system with viscosity and closures for turbulent diffusion and mixing. No results for the inviscid system seem to be available. Looking to reduced models, very few investigations have been conducted: besides the aforementioned work of Remond-Tiedrez et al. (2024), the only rigorous results that the authors are aware of have been obtained by Majda and Souganidis (2010) and Li and Titi (2016) in the context of the early Frierson et al. (2004) model for a moist tropical atmosphere. Remarkably, Li and Titi (2016) went beyond well-posedness and proved convergence to the so-called relaxation limit, which in our terminology corresponds to the transition to a fast microphysics scheme. It would be interesting to see whether results in the same spirit can be obtained for more comprehensive bulk models as in (35). We should also note that one of the authors of the present article (Bäumer, in preparation) has obtained first results on the dry version of the triple-deck boundary layer theory developed by Klein et al. (2022). Last, but certainly not least, the question under which conditions and in which sense solutions of the unapproximated Eqs. (11) converge to solutions of the reduced moist flow model under consideration is completely open - it remains to be seen whether a general framework in analogy to the classical theory of singular limits (Klainerman and Majda, 1981; Schochet, 1994) can be developed.

References

Bäumer D (in preparation) The diabatic layer equations: well-posedness of a new boundary layer theory for quasigeostrophic flow.

Bäumer D, Hittmeir S and Klein R (2023) Scaling approaches to quasigeostrophic theory for moist, precipitating air. *J. Atmos. Sci.* 80: 1771–1786. DOI:10.1175/JAS-D-22-0225.1.

Baumgartner M and Spichtinger P (2019) Homogeneous nucleation from an asymptotic point of view. *Theoretical and computational fluid dynamics* 33(1): 83–106.

Bohren CF and Albrecht B (1998) *Atmospheric thermodynamics*. Oxford Univ. Press.

Bourgeois A and Beale J (1994) Validity of the quasi-geostrophic model for large-scale flow in the atmosphere and ocean. *SIAM journal on mathematical analysis* 25(4): 1023–1068.

Bäumer D and Klein R (2025) PQG-DL-Ekman: a triple-deck boundary layer theory for large-scale atmospheric flow with moist process closures. URL `https://arxiv.org/abs/2504.20191`.

Constantin A and Johnson R (2021) On the modelling of large-scale atmospheric flow. *Journal of Differential Equations* 285: 751–798. DOI:https://doi.org/10.1016/j.jde.2021.03.019.

Constantin P, Majda A and Tabak E (1994) Formation of strong fronts in the 2-d quasi-geostrophic thermal active scalar. *Nonlinearity* 7(6): 1495–1533.

Dolaptchiev SI, Spichtinger P, Baumgartner M and Achatz U (2023) Interactions between gravity waves and cirrus clouds: Asymptotic modeling of wave-induced ice nucleation. *Journal of the Atmospheric Sciences* 80(12): 2861 – 2879. DOI:10.1175/JAS-D-22-0234.1.

Doppler S, Klein R, Liu X and Titi E (2024) Local well-posedness of a system coupling compressible atmospheric dynamics and a micro-physics model of moisture in air. URL `https://arxiv.org/abs/2408.15749`.

Ertel H (1942) Ein neuer hydrodynamischer Wirbelsatz. *Meteorologische Zeitschrift* : 277–281.

Frierson DM, Majda AJ and Pauluis OM (2004) Large scale dynamics of precipitation fronts in the tropical atmosphere: A novel relaxation limit. *Communications in mathematical sciences* 2(4): 591–626.

Hittmeir S and Klein R (2018) Asymptotics for moist deep convection I: refined scalings and self-sustaining updrafts. *Theor. Comput. Fluid Dyn.* 32: 137–164. DOI:10.1007/s00162-017-0443-z.

Hittmeir S, Klein R, Li J and Titi E (2017) Global well-posedness for passively transported nonlinear moisture dynamics with phase changes. *Nonlinearity* 30: 3676–3718. DOI: 10.1088/1361-6544/aa82f1.

Hittmeir S, Klein R, Li J and Titi E (2020) Global well-posedness for the primitive equations coupled to nonlinear moisture dynamics with phase changes. *Nonlinearity* 33: 3206–3236. DOI:10.1088/1361-6544/ab834f.

Hittmeir S, Klein R, Li J and Titi E (2023) Global well-posedness for the thermodynamically refined passively transported nonlinear moisture dynamics with phase changes. *Journal of nonlinear science* 33. DOI:10.1007/s00332-023-09915-z.

Hoskins B, McIntyre M and Robertson A (1985) On the use and significance of isentropic potential vorticity maps. *Quarterly Journal of the Royal Meteorological Society* 111: 877–946. DOI:10.1002/qj.49711147002.

Houze R (2014) *Cloud Dynamics*. 2nd edition. Elsevier Science.

Kessler E (1995) On the continuity and distribution of water substance in atmospheric circulations. *Atmos. Res.* 38: 109–145. DOI:10.1016/0169-8095(94)00090-Z.

Klainerman S and Majda A (1981) Singular limits of quasilinear hyperbolic systems with large parameters and the incompressible limit of compressible fluids. *Communications on Pure and Applied Mathematics* 34(4): 481–524. DOI:10.1002/cpa.3160340405.

Klein R (2010) Scale-dependent models for atmospheric flows. *Annu. Rev. Fluid Mech.* 42: 249–274. DOI:10.1146/annurev-fluid-121108-145537.

Klein R and Majda A (2006) Systematic multiscale models for deep convection on mesoscales. *Theor. Comput. Fluid Dyn.* 20: 525–551. DOI:10.1007/s00162-006-0027-9.

Klein R, Schielicke L, Pfahl S and Khouider B (2022) QG-DL-Ekman: Dynamics of a diabatic layer in the quasi-geostrophic framework. *J. Atmos. Sci.* 79: 887–905. DOI:10.1175/JAS-D-21-0110.1.

Li J and Titi ES (2016) A tropical atmosphere model with moisture: global well-posedness and relaxation limit. *Nonlinearity* 29(9): 2674. DOI:10.1088/0951-7715/29/9/2674.

Majda A and Souganidis P (2010) Existence and uniqueness of weak solutions for precipitation fronts: A novel hyperbolic free boundary problem in several space variables. *Communications on Pure and Applied Mathematics* 63(10): 1351–1361. DOI:10.1002/cpa.20337.

Novack MD and Vasseur AF (2018) Global in time classical solutions to the 3D quasi-geostrophic system for large initial data. *Communications in mathematical physics* 358(1): 237–267.

Novack MD and Vasseur AF (2020) Classical solutions for the 3D quasi-geostrophic system on a bounded domain. *Physica. D* 404: 132362.

Parkins CJ, Blythe PA and Crighton DG (2000) Hot spot ignition: the Newtonian limit. *Proc. Roy. Soc. Physical and Engineering Science* 456: 2857–2882.

Pedlosky J (1987) *Geophysical Fluid Dynamics*. 2nd edition. Springer-Verlag.

Remond-Tiedrez A, Smith LM and Stechmann SN (2024) A nonlinear elliptic pde from atmospheric science: Well-posedness and regularity at cloud edge. *Journal of mathematical fluid mechanics* 26(2).

Schochet S (1994) Fast singular limits of hyperbolic pdes. *Journal of Differential Equations* 114(2): 476–512.

Seifert A and Beheng KD (2001) A double-moment parameterization for simulating autoconversion, accretion and selfcollection. *Atmospheric research* 59: 265–281.

Smith L and Stechmann S (2017) Precipitating quasigeostrophic equations and potential vorticity inversion with phase changes. *J. Atmos. Sci.* 74: 3285–3303. DOI:10.1175/JAS-D-17-0023.1.

Vallis G (2017) *Atmospheric and Oceanic Fluid Dynamics*. 2nd edition. Cambridge University Press.

Wetzel AN, Smith LM and Stechmann SN (2019) Discontinuous fronts as exact solutions to precipitating quasi-geostrophic equations. *SIAM journal on applied mathematics* 79(4): 1341–1366.

Zhang Y, Smith LM and Stechmann SN (2022) Convergence to precipitating quasi-geostrophic equations with phase changes: asymptotics and numerical assessment. *Philosophical transactions of the Royal Society of London. Series A: Mathematical, physical, and engineering sciences* 380(2226): 20210030–20210030.

Scaling Approaches to Quasigeostrophic Theory for Moist, Precipitating Air

DANIEL BÄUMER,[a] SABINE HITTMEIR,[a] AND RUPERT KLEIN[b]

[a] *Fakultät für Mathematik, Universität Wien, Vienna, Austria*
[b] *FB Mathematik und Informatik, Freie Universität Berlin, Berlin, Germany*

(Manuscript received 12 October 2022, in final form 25 February 2023, accepted 3 April 2023)

ABSTRACT: Quasigeostrophic (QG) theory is of fundamental importance in the study of large-scale atmospheric flows. In recent years, there has been growing interest in extending the classical QG plus Ekman friction layer model (QG–Ekman) to systematically include additional physical processes known to significantly contribute to real-life weather phenomena. This paper lays the foundation for combining two of these developments, namely, Smith and Stechmann's family of *precipitating quasigeostrophic* (PQG) models on the one hand, and the extension of QG–Ekman for dry air by a strongly *diabatic layer* (DL) of intermediate height (QG–DL–Ekman) on the other hand. To this end, Smith and Stechmann's PQG equations for soundproof motions are first corroborated within a general asymptotic modeling framework starting from a full compressible flow model. The derivations show that the PQG model family is naturally embedded in the asymptotic hierarchy of scale-dependent atmospheric flow models introduced by one of the present authors. Particular emphasis is then placed on an asymptotic scaling regime for PQG that accounts for a generic Kessler-type bulk microphysics closure and is compatible with QG–DL–Ekman theory. The detailed derivation of a moist QG–DL–Ekman model is deferred to a future publication.

KEYWORDS: Atmosphere; Boundary layer; Diabatic heating; Moisture/moisture budget; Quasigeostrophic models

1. Introduction

Ever since its inception, the mathematical model provided by quasigeostrophic (QG) theory has proven highly successful as a streamlined setting for the explanation of major features of large-scale atmospheric flow in the midlatitudes. Its textbook derivation by scale analysis and asymptotic expansion, as found, e.g., in Pedlosky (1987), is a beautiful example of the interplay between theoretical meteorology and applied mathematics.

This well-established model, however, does not describe the contributions of moisture to the large-scale flow in an explicit fashion: only balance equations for dry air are prescribed, and the only way to integrate the vitally important effect of latent heat on the energy budget without extending the model itself is its parameterization as a heat source in the temperature equation. This approach has been pursued, e.g., by De Vries et al. (2010), who also provide a discussion of different parameterization schemes.

As far as actual extensions of the dry QG model are concerned, they still tend to treat moisture as a supplement; the model proposed by Lapeyre and Held (2004) is emblematic of this approach, in which the authors take QG for dry air as the starting point and then formulate an equation for the mixing ratio of water vapor based on certain ad hoc assumptions. Steps toward a more systematic embedding of moisture into QG theory were made by Monteiro and Sukhatme (2016). These authors *did* include moisture in their scaling and asymptotic analysis, but their derivation took place within the confines of a one-layer shallow-water model.

Seeking a more generally valid extension of QG theory that supplies balance equations for water vapor and precipitation and explicitly models the impact of moisture on the energy budget therefore poses an interesting challenge. Moreover, the mathematical derivation of such a model should proceed along the same lines as that of the classical theory. To this date, to the best of the authors' knowledge, only one model has been proposed that meets these criteria: the *precipitating quasigeostrophic* (PQG) equations of Smith and Stechmann (2017). To clarify their key ideas, the authors first provided a detailed derivation starting from a somewhat simplified cloud-resolving model, the *fast autoconversion and rain evaporation* (FARE) system of Hernandez-Duenas et al. (2013). That model adopts the Boussinesq equations for the dynamics, linearized thermodynamic relations, and the limit of fast conversion of cloud into rainwater. The authors point out, however, that the PQG equations form an entire model family parameterized by the asymptotic scalings assumed for the adopted flow models, e.g., Boussinesq or anelastic, the thermodynamic equations of state, and the bulk microphysics closure (see sections 6 and 9 of their paper).

Common to the QG and PQG models is the assumption of a strong background stratification of the (equivalent) potential temperature which, true to the well-known QG scalings, is equivalent to a small (moist) internal wave Froude number. In this context, let us quote from Smith and Stechmann (2017): "locally in some regions, such as in the vicinity of fronts, assumptions of strong moist stratification and/or classical QG scaling may not hold." Flow regimes of this kind are addressed explicitly by Klein et al. (2022) through their QG–diabatic layer (DL)–Ekman triple-deck boundary layer theory. Within its additional DL of intermediate height of ~3 km, the potential temperature is not restricted to small deviations from a given background stratification but can freely evolve, even toward

Corresponding author: Daniel Bäumer, daniel.baeumer@univie.ac.at

DOI: 10.1175/JAS-D-22-0225.1

neutral stratification, instead. This way, systematically stronger diabatic effects are allowed for in the DL than those accounted for in the classical (P)QG models. The QG–DL–Ekman theory has thus far been derived only for dry air flows, though, and within our current ongoing work we aim to extend it to include moist processes.

The present paper is our first step in this direction and it provides two main contributions: In sections 4 and 5 we illuminate the relationship between the PQG equations in their anelastic form (based on the FARE model for moist processes) on the one hand, and the system for moist compressible flow with the generic Kessler-type bulk microphysics closure of Hittmeir and Klein (2018) on the other hand. To this end, we proceed by systematically deriving the former from the latter utilizing asymptotic techniques. This will also demonstrate how the PQG model family can be embedded naturally in the rich hierarchy of known scale-dependent atmospheric models as discussed in Klein (2010).

This paper's second main contribution is a self-contained derivation of a *particular version* of PQG-type equations that is set up for the subsequent inclusion in a moist QG–DL–Ekman triple-deck theory. The underlying scalings combine features of several of the aforementioned versions of PQG, which is why we place particular emphasis on the justification of and the reasoning behind our scaling choices. In section 6, this leads indeed to a PQG model that is tailor-made to be coupled with the diabatic layer of Klein et al. (2022). We will further explore its implications in future publications. To provide some first insight into the model's characteristics, we discuss in section 7 its related "omega equation," which often serves to diagnose upward vertical velocities in weather forecast model output.

Finally, appendix A sketches a derivation of the moist anelastic system of Hernandez-Duenas et al. (2013). There, we also point to the key differences between an asymptotic analysis that starts from a fully compressible system and one that is based on the anelastic approximation. This, in particular, serves to explain the occurrence of additional background terms in our derivation of the buoyancy in section 5.

2. The governing equations

Our point of departure is a system that not only accurately describes compressible flow, but also includes fairly detailed moist thermodynamics [see Cotton et al. (2011) for a broad discussion of possible modeling approaches]. This model formulation goes back to Hittmeir and Klein (2018), and it includes established bulk microphysics closures as proposed and investigated in Kessler (1995), Grabowski and Smolarkiewicz (1996), and Klein and Majda (2006):

$$D_t\mathbf{u} + 2(\mathbf{\Omega}\times\mathbf{v})_\parallel + \frac{1}{\rho}\boldsymbol{\nabla}_\parallel p = 0, \tag{1a}$$

$$D_t w + 2(\mathbf{\Omega}\times\mathbf{v})_\perp + \frac{1}{\rho}\partial_z p = -g, \tag{1b}$$

$$D_t\rho_d + \rho_d(\boldsymbol{\nabla}\cdot\mathbf{v}) = 0, \tag{1c}$$

$$CD_t\ln\theta + \Sigma D_t\ln p + \frac{L(T)}{T}D_t q_v = c_l V_r q_r\left(\partial_z\ln\theta + \frac{R_d}{c_{\mathrm{pd}}}\partial_z\ln p\right), \tag{1d}$$

$$D_t q_v = S_{\mathrm{ev}} - S_{\mathrm{cd}}, \tag{1e}$$

$$D_t q_c = S_{\mathrm{cd}} - S_{\mathrm{cr}} - S_{\mathrm{ac}}, \tag{1f}$$

$$D_t q_r - \frac{1}{\rho_d}\partial_z(\rho_d V_r q_r) = S_{\mathrm{cr}} + S_{\mathrm{ac}} - S_{\mathrm{ev}}, \tag{1g}$$

with the additional relations

$$\rho = \rho_d(1 + q_v + q_c + q_r), \tag{2a}$$

$$p = R_d\rho_d T\left(1 + \frac{q_v}{\frac{R_d}{R_v}}\right), \tag{2b}$$

$$\theta = T\left(\frac{p_{\mathrm{ref}}}{p}\right)^{(\gamma-1)/\gamma}, \tag{2c}$$

$$\mathbf{v} = \mathbf{u} + w\mathbf{k}, \tag{2d}$$

$$S_{\mathrm{ev}} = C_{\mathrm{ev}}\frac{p}{\rho}(q_{\mathrm{vs}} - q_v)^+ q_r, \tag{2e}$$

$$S_{\mathrm{cd}} = C_{\mathrm{cn}}(q_v - q_{\mathrm{vs}})^+ q_{\mathrm{cn}} + C_{\mathrm{cd}}(q_v - q_{\mathrm{vs}})q_c, \tag{2f}$$

$$S_{\mathrm{ac}} = C_{\mathrm{ac}}(q_c - q_{\mathrm{ac}})^+, \tag{2g}$$

$$S_{\mathrm{cr}} = C_{\mathrm{cr}}q_c q_r, \tag{2h}$$

$$C = c_{\mathrm{pd}} + c_{\mathrm{pv}}q_v + c_l(q_c + q_r), \tag{2i}$$

$$\Sigma = \left(\frac{c_{\mathrm{pv}}}{c_{\mathrm{pd}}}R_d - R_v\right)q_v + \frac{c_l}{c_{\mathrm{pd}}}R_d(q_c + q_r), \tag{2j}$$

$$L(T) = L_{\mathrm{ref}} + (c_{\mathrm{pv}} - c_l)(T - T_{\mathrm{ref}}) \equiv L_{\mathrm{ref}}\phi(T). \tag{2k}$$

In the above equations, $[\mathbf{u} = (u, v, 0), w, \rho, \rho_d, T, \theta, p, q_v, q_c, q_r, q_{\mathrm{vs}}]$ denote horizontal and vertical velocity, density, dry air density, temperature, potential temperature, pressure, and the mixing ratios of water vapor, cloud water, and rain, as well as the saturation mixing ratio, respectively; g is the gravitational acceleration, $\mathbf{\Omega}$ the Earth rotation vector, and the subscripts $\parallel$ and $\perp$ indicate horizontal and vertical components, respectively. We denote the positive part of a function f by f^+. As usual, c_{pd} and c_{pv} denote the specific heat capacities at constant pressure of dry air and water vapor, while c_l is the heat capacity of liquid water, here assumed constant for simplicity, and V_r is the terminal rainfall velocity; R_d and R_v are the gas constants for dry air and water vapor, $\gamma = c_{\mathrm{pd}}/(c_{\mathrm{pd}} - R_d)$ is the isentropic exponent of dry air, $\mathbf{k}$ the vertical unit vector, $p_{\mathrm{ref}} = 10^5$ Pa the reference pressure, and the material derivative is given by

$$D_t = \partial_t + \mathbf{v}\cdot\boldsymbol{\nabla} = \partial_t + \mathbf{u}\cdot\boldsymbol{\nabla}_\parallel + w\partial_z. \tag{3}$$

In line with usual assumptions (Cotton et al. 2011), the dry air mass obeys the continuity equation, (1c). Note that the density appearing in the momentum equations, (1a) and (1b), is the full density from (2a) and not the dry air density. Therefore, the effect of moisture on (total) density is properly accounted for. Individual contributions from the moist constituents are the following: in the thermodynamic equation, (1d), C denotes the "total moist heat capacity," specified in (2i); Σ, defined in (2j), collects moist contributions related to the work done by pressure forces, and $L(T)$ is the latent heat of vaporization, which can be written as a linear function of temperature under the assumption of constant c_l. The reference values for latent heat and temperature are $L_{\text{ref}} = 2.5 \times 10^6$ J kg^{-1} K^{-1} and $T_{\text{ref}} = 273.15$ K, respectively. Finally, the right-hand side represents temperature changes caused by precipitation. In the transport equations for the respective mixing ratios, (1e)–(1g), terms of the form $S_\bigstar$ denote the usual Kessler-type closures for the microphysical processes of condensation (cd), evaporation (ev), autoconversion (ac), and collection (cr), respectively. In (2e)–(2h), $C_\bigstar$ denote rate constants of the respective processes, while q_{cn} represents the density of condensation kernels and q_{ac} denotes an activation threshold for the autoconversion of cloud droplets into raindrops.

We do not explicitly consider cold clouds that would necessitate parameterization of the ice phase. While a comprehensive treatment of cloud formation and precipitation on synoptic scales in the midlatitudes *should* include bulk microphysics closures for the ice phase (Houze 2014), we reserve this endeavor for future work.

3. Overview and comparison of resulting model equations

For reference, we now briefly summarize and compare the results of the derivations in sections 4 and 5 (for Smith and Stechmann's anelastic/FARE PQG model) and section 6 (for the new model) in dimensional form. For brevity, we will refer to the former just as PQG and to the latter as PQG$_{\text{DL}}$ from here on out.

Our notation here is as follows: for any model variable f with a leading-order vertical background profile, we denote it by $\overline{f} = \overline{f}(z)$, while $\tilde{f} = \tilde{f}(t, \mathbf{x}, z)$ stands for the corresponding perturbation. We will always assume $\tilde{f} \ll \overline{f}$. Furthermore, we write

$$D_t^g = \partial_t + \mathbf{u} \cdot \boldsymbol{\nabla}_\parallel \tag{4}$$

for the material derivative with respect to the geostrophic horizontal velocity $\mathbf{u}$.

a. The PQG model

The following are equivalent to Eqs. (65) and (66) in Smith and Stechmann (2017), if a β-plane approximation is adopted:

Diagnostic relations: These are the usual geostrophic and hydrostatic balances,

$$f\mathbf{k} \times \mathbf{u} = -\boldsymbol{\nabla}_\parallel \phi, \tag{5a}$$

$$g\frac{\tilde{\theta}}{\theta_{\text{ref}}} = \partial_z \phi, \tag{5b}$$

where $\phi = \tilde{p}/\overline{\rho}$ is the pressure perturbation scaled by the background density and f the reference value of the Coriolis parameter.

Transport equations: As in classical dry air theory, we obtain prognostic equations for the geostrophic vertical vorticity ζ and for potential temperature; in PQG, we get an additional prognostic equation for total moisture q_T:

$$D_l^g[\zeta + \beta y] = \frac{f}{\overline{\rho}}\partial_z(\overline{\rho}\tilde{w}), \tag{6a}$$

$$D_l^g \tilde{\theta}_e + \tilde{w}\frac{d\overline{\theta}_e}{dz} = 0, \tag{6b}$$

$$D_l^g \tilde{q}_T + \tilde{w}\frac{d\overline{q}_T}{dz} - \frac{1}{\overline{\rho}}\partial_z(\overline{\rho}V_r\tilde{q}_r) = 0, \tag{6c}$$

where β denotes the latitudinal variation of the Coriolis parameter, $\zeta = \partial_x v - -\partial_y u$ the vertical vorticity and $\tilde{w}$ the small geostrophic vertical velocity; θ_e denotes the (linearized) equivalent potential temperature, given by

$$\theta_e = \theta + \frac{L_{\text{ref}}}{c_{\text{pd}}} q_v. \tag{7}$$

Owing to the simplified phase changes in the FARE setting (Hernandez-Duenas et al. 2013), $\tilde{q}_r$ and $\tilde{q}_v$ can be written in terms of q_T, so that only one equation for moisture is needed (see the next section for details).

As laid out by Smith and Stechmann (2017), the vertical velocity can be eliminated from this system to yield a potential vorticity formulation. Here we only state the results of this calculation and refer the reader to the cited article for more information. Thus, the potential vorticity Q based on equivalent potential temperature in PQG reads

$$Q = \zeta + \beta y + \frac{f}{\overline{\rho}}\partial_z\left(\frac{\overline{\rho}\tilde{\theta}_e}{d\overline{\theta}_e/dz}\right). \tag{8}$$

This quantity can be rewritten in terms of the pressure perturbation ϕ and the moisture-related variable

$$M = \tilde{q}_T + G_M\tilde{\theta}_e, \quad \text{where} \quad G_M = -\frac{d\overline{q}_T/dz}{d\overline{\theta}_e/dz}. \tag{9}$$

For given M and Q, the result is a second-order diagnostic reconstruction equation for the pressure perturbation ϕ:

$$\Delta_\parallel \phi + f\beta y + \frac{f^2}{\overline{\rho}}\partial_z\left[\frac{\overline{\rho}}{d\overline{\theta}_e/dz} H_u \frac{1}{D_M}\left(\frac{\theta_{\text{ref}}}{g}\partial_z\phi + \frac{L_{\text{ref}}}{c_{\text{pd}}}M\right)\right] + \frac{f^2}{\overline{\rho}}\partial_z\left[\frac{\overline{\rho}}{d\overline{\theta}_e/dz} H_s\left(\frac{\theta_{\text{ref}}}{g}\partial_z\phi + \frac{L_{\text{ref}}}{c_{\text{pd}}}q_{\text{vs}}\right)\right] = fQ\,, \tag{10}$$

where $D_M := 1 + L_{\text{ref}}G_M/c_{\text{pd}}$ and H_u, H_s are Heaviside switching functions for the unsaturated and saturated state, respectively. For later comparison with the PQG$_{\text{DL}}$ model, and following Wetzel et al. (2019), we rewrite (10) as

$$\Delta_\parallel \phi + \frac{1}{\overline{\rho}}\partial_z\left(\frac{\overline{\rho} f^2}{N^2}\partial_z \phi\right) = f(Q - \beta y) - \frac{f^2}{\overline{\rho}}\partial_z\left[\overline{\rho} g L^*\left(H_u \frac{M}{N_u^2} + H_s \frac{q_{vs}}{N_s^2}\right)\right], \quad (11)$$

where

$$N^2 = H_u N_u^2 + H_s N_s^2 \quad \text{and} \quad L^* = \frac{L_{ref}}{c_{pd}\theta_{ref}}. \quad (12)$$

Here N is the local buoyancy frequency, while $N_u = \sqrt{(g/\theta_{ref})d\overline{\theta}/dz}$ and $N_s = \sqrt{(g/\theta_{ref})d\overline{\theta}_e/dz}$ are the buoyancy frequencies in undersaturated and saturated air, respectively.

As Smith and Stechmann point out, the elliptic operator on the left of (11) has nonconstant coefficients owing to the switch in the Brunt–Väisälä frequency defined in (12). Moreover, the switching functions depend on q_T and therefore implicitly on $\partial\phi/\partial z$ through the hydrostatic balance in (5b) together with the definitions of M in (9) and θ_e in (7). As a consequence, the elliptic PDE, (11), is nonlinear, and its right-hand side involves a surface δ distribution along the phase boundary because the vertical derivative is applied to a discontinuous function. As discussed by Wetzel et al. (2019), the numerical solution of the PV–M-inversion problem is, for these reasons, much more involved than it is for the classical QG model.

The transport equation for the PQG potential vorticity reads

$$D_t^g Q = -\frac{f}{d\overline{\theta}_e/dz}\partial_z \mathbf{u}\cdot\boldsymbol{\nabla}_\parallel \tilde{\theta}_e. \quad (13)$$

Remark: Smith and Stechmann chose Q and M as given quantities for potential vorticity inversion, because q_T does not constitute a balanced quantity in the sense that its evolution equation depends on the vertical velocity (Wetzel et al. 2019).

b. The PQG$_{DL}$ model

Compared to PQG, this model has a fundamentally different aim: as already stated in the introduction, it is meant to connect to the diabatic layer of Klein et al. (2022), which necessitates various changes in the scaling of the moist constituents. In particular, the mixing ratios here do *not* decompose into a vertical background and corresponding perturbations. The quantities q_j ($j = v, c, r$) therefore simply denote the respective leading-order contributions from moist constituents. Moreover, PQG$_{DL}$ incorporates more detailed cloud microphysics, keeping the original number of moisture species in the asymptotic regime.

Diagnostic relations: The geostrophic and hydrostatic balances take the same form as above, see (5a) and (5b). However, the scaling of the terminal rainfall velocity V_r now produces an additional diagnostic relation for q_r, which is determined from

$$\partial_z q_r = -\frac{\overline{\rho}}{V_r}[S_{ag,m} + S_{cr} - S_{ev}]. \quad (14)$$

Here, $S_{ag,m}$ represents an ad hoc parameterization of the generation of raindrops through aggregation and melting, see section 6 for details.

Transport equations: Since PQG$_{DL}$ does not assume fast autoconversion, the cloud water evolution equation is retained in the leading-order equations, increasing the number of prognostic equations by one relative to PQG,

$$D_t^g[\zeta + \beta y] = \frac{f}{\overline{\rho}}\partial_z(\overline{\rho}\tilde{w}), \quad (15a)$$

$$D_t^g \tilde{\theta}_e + \tilde{w}\frac{d\overline{\theta}}{dz} = c_l V_r q_r \frac{R_d}{c_{pd}}\partial_z \ln\overline{p}, \quad (15b)$$

$$D_t^g q_v = S_{ev} - S_{cd}, \quad (15c)$$

$$D_t^g q_c = S_{cd} - S_{ag,m} - S_{cr}. \quad (15d)$$

We observe that rain now influences the system's dynamics in two ways: it moistens dry air by evaporating, while producing a cooling effect in the thermodynamic equation even in saturated air. This constitutes the main departure from PQG, which we will illustrate by means of a diagnostic relation for the vertical velocity later on. Moreover, due to the fact that the moisture constituents do not feature a background stratification and that above heights of 3 km their mixing ratios are roughly by an order of magnitude smaller than assumed for PQG, the background potential temperature stratification and that of the equivalent potential temperature are identical in the PQG$_{DL}$ regime, i.e., $\overline{\theta}_e \equiv \overline{\theta}$.

Potential vorticity in the PQG$_{DL}$ regime can be defined exactly as in (8). The absence of a background distribution of moisture, however, removes the vertical velocity from all moist transport equations. Therefore, instead of (11), in this scenario the diagnostic equation for the pressure perturbation reads

$$\Delta_\parallel \phi + \frac{1}{\overline{\rho}}\partial_z\left(\frac{\overline{\rho} f^2}{N^2}\partial_z \phi\right) = f(Q - \beta y) - \frac{f^2}{\overline{\rho}}\partial_z\left(\frac{\overline{\rho} L^*}{N^2} q_v\right), \quad (16)$$

where now

$$N^2 = \frac{g}{\theta_{ref}}\frac{d\overline{\theta}}{dz}, \quad (17)$$

while Q and q_v can be chosen as given quantities to initiate potential vorticity inversion. In addition, q_c will be needed to determine q_r from (14) and complete the diagnostic determination of all model variables. Finally, the evolution equation for potential vorticity also takes a different form, due to the nonzero right-hand side in (15b):

$$D_t^g Q = -\frac{f}{d\overline{\theta}/dz}\partial_z \mathbf{u}\cdot\boldsymbol{\nabla}_\parallel \tilde{\theta}_e + \frac{f}{\overline{\rho}}\left[\frac{\overline{\rho} c_l V_r q_r \frac{R_d}{c_{pd}}\partial_z \ln\overline{p}}{d\overline{\theta}/dz}\right]. \quad (18)$$

In contrast to the PV inversion equation for PQG in (11), its PQG$_{DL}$ version in (16) is linear for given Q and q_v, and it features smooth coefficients in the linear operator. Moreover, q_v is generally continuous—though not continuously differentiable—so that

the right-hand side in (16) involves merely discontinuities at phase boundaries instead of surface Dirac distributions as in PQG. We conclude that numerical PV inversion in $\mathrm{PQG_{DL}}$ is much less of a challenge than it is in PQG. In the envisioned PQG–DL–Ekman triple deck model, much stronger effects of moist processes will be included, but confined to the intermediate DL.

4. Nondimensionalization and scaling for PQG

Let us first recap the generic and space–time-scale independent distinguished limit for the traditional dry air model from Klein (2010): Coupling the usual dimensionless parameters to one small parameter ϵ with a physical magnitude of ~1/10, we choose the following scaling for the Mach, external Froude, and Rossby numbers:

$$M = \frac{u_{\mathrm{ref}}}{\sqrt{p_{\mathrm{ref}}/\rho_{\mathrm{ref}}}} = \epsilon^{3/2} = \frac{u_{\mathrm{ref}}}{\sqrt{g h_{\mathrm{sc}}}} = \mathrm{Fr}_{\mathrm{ext}},$$

$$\mathrm{Ro} = \frac{u_{\mathrm{ref}}}{2\boldsymbol{\Omega} l_{\mathrm{ref}}} = O(\epsilon), \tag{19}$$

where the horizontal reference velocity is $u_{\mathrm{ref}} \approx 10\ \mathrm{m\ s^{-1}}$, the pressure scale height $h_{\mathrm{sc}} \approx 10$ km, and l_{ref} is on the order of a synoptic length scale, such that

$$\frac{h_{\mathrm{sc}}}{l_{\mathrm{ref}}} = \epsilon^2. \tag{20}$$

Notice that the *internal* Froude number $\mathrm{Fr}_{\mathrm{int}} = u_{\mathrm{ref}}/N h_{\mathrm{sc}}$, with N denoting the buoyancy frequency, is on the same order of magnitude as Ro, in accordance with classical QG scaling. The buoyancy frequency in this context will depend on the moisture content, see the appendix of Smith and Stechmann (2017).

We work with the standard β-plane approximation, within which the Coriolis parameter is a linear function of latitudinal distance y:

$$\boldsymbol{\Omega} = (f_0 + \beta y)\mathbf{k}. \tag{21}$$

As in the textbook derivation of classical QG (Pedlosky 1987), the β effect is $O(\epsilon)$ compared to f_0.

Regarding moisture, we start by incorporating the simplifications of the FARE model. As described by Hernandez-Duenas et al. (2013), fast autoconversion and rain evaporation imply that the cloud phase can be omitted altogether, since cloud droplets grow to critical size quasi instantaneously in this regime, *and* since rain can be recovered from the total water content $q_T = q_v + q_r$ by comparison with the saturation mixing ratio q_{vs}. We can now combine all moisture balances into one by adding the corresponding equations and obtain

$$D_l q_T - \frac{1}{\rho_d}\partial_z(\rho_d V_r q_r) = 0, \tag{22}$$

where

$$q_r = (q_T - q_{\mathrm{vs}})^+. \tag{23}$$

The average water vapor content in the midlatitude troposphere does not exceed a few percent and we assume

$$q_{\mathrm{vs}} = O(\epsilon^2), \tag{24}$$

which imposes the same upper bound on the magnitudes of q_v and q_r. Following Smith and Stechmann (2017), we assume $q_{\mathrm{vs}} = q_{\mathrm{vs}}(z)$ to be a given function of altitude. We take the terminal velocity V_r to be constant and, in accordance with Smith and Stechmann (2017), comparable to the vertical reference velocity $w_{\mathrm{ref}} = \epsilon^2 u_{\mathrm{ref}}$. This scaling is related to the horizontal reference velocity through the horizontal-to-vertical aspect ratio [the vertical velocity scaling directly follows the classical derivation of the QG model, e.g., in Pedlosky (1987)]. Thus, we let

$$\frac{V_r}{w_{\mathrm{ref}}} =: V_T = O(1). \tag{25}$$

These scaling choices were all explicit in Smith and Stechmann's derivation. For the remaining nondimensional parameters, which govern the thermodynamics of moist air, we present a self-contained justification, based on the following guidelines (which we will more comprehensively refer to in the derivation of our new model in section 6):

1) The "dry air limit" that we obtain by letting moisture $q_T \to 0$ in our model equations must agree with the dry QG system.
2) The leading-order balances resulting from our choice of the distinguished limit should encapsulate physically meaningful and—at least qualitatively—accurate relations.
3) Finally, we aim for a scaling that is formally consistent and assigns realistic values to our system parameters.

Following Hittmeir and Klein (2018), we proceed with the following general scaling ansatz,

$$\frac{L_{\mathrm{ref}}}{c_{\mathrm{pd}} T_{\mathrm{ref}}} = \frac{L}{\epsilon^a}, \quad \frac{R_d}{c_{\mathrm{pd}}} = \epsilon^b \Gamma, \quad \frac{R_v}{c_{\mathrm{pv}}} = \epsilon^{b_v}\Gamma_v,$$

$$\frac{c_l}{c_{\mathrm{pd}}} = \frac{k_l}{\epsilon^{b_l}}, \quad \frac{R_d}{R_v} = \epsilon^c E, \tag{26}$$

where all parameters on the right-hand sides are $O(1)$ as $\epsilon \to 0$. Thus, L, Γ, etc., are *defined* by the above relations, dependent on nonnegative numbers a, b, … that are to be determined in accordance with the principles stated above.

Staying true to guideline 3 and comparing with the physical reference values

$$\frac{L_{\mathrm{ref}}}{c_{\mathrm{pd}} T_{\mathrm{ref}}} \approx 9.1 \quad \text{and} \quad \frac{R_d}{R_v} \approx 0.62 \tag{27}$$

(cf. Hittmeir and Klein 2018), we are compelled to choose $a = 1$ and $c = 0$. The choice for b_l is not as obvious, but with the reference value

$$\frac{c_l}{c_{\mathrm{pd}}} \approx 4.2 \tag{28}$$

and $\epsilon \sim 1/10$, $b_l = 1$ gives the best fit. Moving on to b, we have

$$\frac{R_d}{c_{\mathrm{pd}}} \approx 0.29, \tag{29}$$

which is quite ambiguous, as far as heuristic matching is concerned, and both $b = 0$ and $b = 1$ are reasonable choices. A closer look at the temperature equation

$$CD_t \ln\theta + \Sigma D_t \ln p + \frac{L(T)}{T} D_t q_v = c_l V_r q_r \left(\partial_z \ln\theta + \frac{R_d}{c_{\mathrm{pd}}} \partial_z \ln p \right), \tag{30}$$

however, reveals that—given our scaling up to this point—$b = 0$ would raise the rainfall term $c_l V_r q_r (R_d/c_{\mathrm{pd}}) \partial_z \ln p$ on the right-hand side to a leading-order effect. Yet, no term that depends on q_r occurs in the temperature evolution equation of PQG and this is accommodated here by letting $b = 1$. This amounts to the so-called *Newtonian limit* for dry air (Parkins et al. 2000) [see also the discussion of anelastic models and Eq. (2.18) in Bannon (1995)]. Finally, b_v does not play a part in the leading-order dynamics, and since the derived quantity

$$k_v := \frac{c_{\mathrm{pv}}}{c_{\mathrm{pd}}} \approx 1.8 \sim O(1), \tag{31}$$

we choose $b_v = 1$ purely for consistency.

With these scalings in place, the dimensionless equations now read

$$D_t \mathbf{u} + \frac{1}{\epsilon} f \mathbf{k} \times \mathbf{u} + \frac{1}{\epsilon^3} \frac{1}{\rho} \boldsymbol{\nabla}_{\parallel} p = 0, \tag{32a}$$

$$D_t w + \frac{1}{\epsilon^5} \frac{1}{\rho} \partial_z p = -\frac{1}{\epsilon^5}, \tag{32b}$$

$$\partial_t \rho_d + \boldsymbol{\nabla}_{\parallel} \cdot (\rho_d \mathbf{u}) + \partial_z (\rho_d w) = 0, \tag{32c}$$

$$C_\epsilon D_t \ln\theta + \epsilon^3 \Sigma_\epsilon D_t \ln p + \epsilon \frac{L \phi_\epsilon}{T} D_t q_v = \epsilon^2 k_l V_T q_r (\partial_z \ln\theta + \epsilon \Gamma \partial_z \ln p), \tag{32d}$$

$$D_t q_T - \frac{1}{\rho_d} \partial_z (\rho_d V_T q_r) = 0, \tag{32e}$$

where

$$\rho = \rho_d [1 + \epsilon^2 (q_v + q_r)], \tag{33a}$$

$$p = \rho_d T \left(1 + \epsilon^2 \frac{q_v}{E} \right), \tag{33b}$$

$$T = \theta p^{\epsilon\Gamma} \equiv \theta \pi, \tag{33c}$$

$$C_\epsilon = 1 + \epsilon \left(\epsilon k_v q_v + k_l (q_r) \right), \tag{33d}$$

$$\Sigma_\epsilon = \Gamma k_l (q_r) + \epsilon \kappa_v q_v, \tag{33e}$$

$$\kappa_v = \left(\frac{c_{\mathrm{pv}}}{c_{\mathrm{pd}}} \Gamma - \frac{1}{E} \Gamma \right), \tag{33f}$$

$$\phi_\epsilon = 1 - \frac{k_l - \epsilon k_v}{L} (T - 1), \tag{33g}$$

$$q_r = (q_T - q_{\mathrm{vs}})^+. \tag{33h}$$

5. Asymptotic expansion and derivation of PQG

In this section, we derive the anelastic version of PQG given by Eqs. (65) and (66) in Smith and Stechmann (2017). As in QG theory for dry air, we presume an expansion for density, pressure, and temperature that admits purely vertical profiles up to $O(\epsilon)$, and the latter are indicated by *single* subscripts. Instead, when the background distribution of some variable at some given asymptotic order is constant, then this is indicated by a *double* subscript. Superscripts in brackets denote perturbation variables with generic dependence on (t, x, y, z). Thus, the expansions, including the velocity components, for the PQG regime read

$$p = p_0 + \epsilon p_1 + \epsilon^2 p^{(2)} + o(\epsilon^2), \tag{34a}$$

$$\rho = \rho_0 + \epsilon \rho_1 + \epsilon^2 \rho^{(2)} + o(\epsilon^2), \tag{34b}$$

$$\theta = \theta_{00} + \epsilon \theta_1 + \epsilon^2 \theta^{(2)} + o(\epsilon^2), \tag{34c}$$

$$T = T_{00} + \epsilon T_1 + \epsilon^2 T^{(2)} + o(\epsilon^2), \tag{34d}$$

$$\mathbf{u} = \mathbf{u}^{(0)} + \epsilon \mathbf{u}^{(1)} + o(\epsilon), \tag{34e}$$

$$w = w^{(0)} + \epsilon w^{(1)} + o(\epsilon). \tag{34f}$$

The constant leading-order terms in the expansions of both θ and T are a consequence of the Newtonian limit (see Klein and Majda 2006; Hittmeir and Klein 2018).

One important feature of Smith and Stechmann's PQG model is that it assumes a vertical background profile for water vapor while rain is comparatively weak and on the order of a perturbation of the total water content only. The expansions of the respective mixing ratios then read

$$q_v = \epsilon^2 q_{v0} + \epsilon^3 q_v^{(1)} + o(\epsilon^3), \tag{35a}$$

$$q_r = \epsilon^3 q_r^{(1)} + o(\epsilon^3), \tag{35b}$$

implying *small horizontal and temporal variations* of the total water content. Informally speaking, this condition will be met as long as the air in our model atmosphere does not dry out too much. In their PQG model, Smith and Stechmann consider a regime in which the moisture perturbation variables determine the local saturation status. To realize this within the asymptotic framework based on an expansion of the saturation water vapor profile via

$$q_{vs} = \epsilon^2 q_{vs0} + \epsilon^3 q_{vs1} + \cdots, \tag{36}$$

we must assume an atmosphere close to saturation, so that

$$q_{v0} = q_{T0} = q_{vs0}\,. \tag{37}$$

Then, saturation is reached wherever

$$q_T^{(1)} \geq q_{vs1}\,. \tag{38}$$

The analysis of the leading-order momentum and mass balances now proceeds along the same lines as for dry air with the following results:

Mass balance: By the usual reasoning, anticipating (41), we conclude that

$$w^{(0)} = 0 \tag{39}$$

from the balance at leading order, while the *anelastic constraint*

$$\rho_0 \nabla_\parallel \cdot \mathbf{u}^{(1)} + \partial_z[\rho_0 w^{(1)}] = 0 \tag{40}$$

holds for the first-order perturbations. This contrasts with derivations using the Boussinesq approximation, where $(\mathbf{u}^{(1)}, w^{(1)})$ would obey an incompressibility constraint.

Horizontal momentum balance: At leading order, we obtain geostrophic balance:

$$f_0 \mathbf{k} \times \mathbf{u}^{(0)} + \frac{1}{\rho_0}\nabla_\parallel p = 0\,, \tag{41}$$

while the first-order perturbation reads

$$D_t^{(0)}\mathbf{u}^{(0)} + \beta y \mathbf{k} \times \mathbf{u}^{(0)} + f_0 \mathbf{k} \times \mathbf{u}^{(1)} + \frac{1}{\rho_0}\nabla_\parallel p^{(3)} - \frac{\rho_1}{\rho_0^2}\nabla_\parallel p^{(2)} = 0 \tag{42}$$

with

$$D_t^{(0)} = \partial_t + \mathbf{u}^{(0)} \cdot \nabla_\parallel \tag{43}$$

since $w^{(0)} \equiv 0$. Taking the vertical component of the curl yields

$$D_t^{(0)}[\zeta^{(0)} + \beta y] + f_0 \nabla_\parallel \cdot \mathbf{u}^{(1)} = 0, \tag{44}$$

which is the equation for transport of vorticity in the quasi-geostrophic regime.

Vertical momentum balance: The leading-order equation accepts the explicit solutions

$$T_{00}\rho_0(z) = p_0(z) = p_0(0)e^{-z/T_{00}}, \tag{45}$$

where we have used the ideal gas law to obtain $\rho_0 = p_0/T_{00}$, and the leading-order vertical momentum equation to derive the hydrostatic balance relation, $\partial_z p_0 = -\rho_0 = -(1/T_{00})p_0$. At first order we obtain

$$\partial_z p_1 = -\rho_1, \tag{46}$$

which, by application of the ideal gas law, further implies

$$\frac{T_1}{T_{00}} = \partial_z\left(\frac{p_1}{\rho_0}\right). \tag{47}$$

For the second-order perturbations, we get the analogous result

$$\partial_z p^{(2)} = -\rho^{(2)}, \tag{48}$$

which we will analyze in more detail shortly.

In summary, we have derived (41) as the nondimensional form of (5a), while the substitution of (40) into (44) yields (6a).

Moisture balances: Here, we only need to consider one balance equation for the total water content,

$$D_t q_T - \frac{1}{\rho_d}\partial_z(\rho_d V_T q_r) = 0\,. \tag{49}$$

With the expansion scheme summarized in (35)–(38), the leading-order balance from (49) gives

$$D_t^{(0)} q_T^{(1)} + w^{(1)}\frac{dq_{T0}}{dz} - \frac{1}{\rho_0}\partial_z\left(\rho_0 V_T q_r^{(1)}\right) = 0. \tag{50}$$

This is the nondimensional equivalent of Eq. (6c).

Temperature transport: The leading-order balance of (32d) reads

$$D_t^{(0)}\theta^{(2)} + LD_t^{(0)}q_v^{(1)} + w^{(1)}\frac{d\theta_1}{dz} + Lw^{(1)}\frac{dq_{v0}}{dz} = 0. \tag{51}$$

Utilizing the (linearized) equivalent potential temperature, as defined in (7), we can rewrite the above as

$$D_t^{(0)}\theta_e^{(2)} + w^{(1)}\frac{d\theta_{e1}}{dz} = 0, \tag{52}$$

which is equivalent to Eq. (6b) in nondimensional form.

Buoyancy: We now take a closer look at Eq. (48). By the ideal gas law, (33b), we get

$$p^{(2)} = \rho_0 T^{(2)} + \rho_1 T_1 + \rho^{(2)} T_{00} + \rho_0 T_{00}\left(\frac{1}{E} - 1\right)q_{v0}, \tag{53}$$

which implies

$$\begin{aligned}\partial_z\left(\frac{p^{(2)}}{\rho_0}\right) &= \frac{\partial_z p^{(2)} + \frac{1}{T_{00}}p^{(2)}}{\rho_0} \\ &= \frac{1}{T_{00}}\frac{1}{\rho_0}\Big[-T_{00}\rho^{(2)} + \rho_0 T^{(2)} + \rho_1 T_1 \\ &\quad + \rho^{(2)}T_{00} + \rho_0 T_{00}\left(\frac{1}{E} - 1\right)q_{v0}\Big] \\ &= \frac{T^{(2)}}{T_{00}} + \frac{\rho_1}{\rho_0}T_1 + \left(\frac{1}{E} - 1\right)q_{v0}.\end{aligned} \tag{54}$$

With the help of (33c), we can further rewrite (54) in the form

$$\partial_z\left(\frac{p^{(2)}}{\rho_0}\right) = \frac{\theta^{(2)}}{\theta_{00}} + \pi_1\theta_1 + \pi_2 + \frac{\rho_1}{\rho_0}T_1 + \left(\frac{1}{E} - 1\right)q_{v0}. \quad (55)$$

Now, the *leading-order* buoyancy, as defined in Smith and Stechmann (2017), reduces to exactly the leading-order (dry) potential temperature perturbation, that is, $\theta^{(2)}/\theta_{00}$. Our result here shows quite a few extra terms—all background profiles, however, which means that we can recover the exact form of the anelastic PQG equations at leading order by shifting them over to the left-hand side and then identifying the appropriate definition of the pressure perturbation: setting

$$\phi := \frac{p^{(2)}}{\rho_0} - \int_0^z \left[\pi_1\theta_1 + \pi_2 + \frac{\rho_1}{\rho_0}T_1 + \left(\frac{1}{E} - 1\right)q_{v0}\right]d\zeta, \quad (56)$$

we recover (5b) in nondimensional form. Since all extra terms are functions of z only, geostrophic balance remains unaffected and our derivation from the compressible equations with refined moist thermodynamics can be viewed as complete, at least at leading order.

Still, the question remains: Where does the initial discrepancy in the form of the moist buoyancy stem from? Essentially, this is caused by what we could call the higher "asymptotic resolution" of our expansion ansatz, where the background stratification of pressure, density, and temperature is composed of *two terms of different order* each instead of one. Appendix A explains this in more detail by describing a sample derivation of the moist anelastic buoyancy.

6. Consequences of a different scaling approach: PQG and the diabatic layer

In section 2, we laid out the guiding principles for our choice of a distinguished limit and applied them to the thermodynamic parameters of moist air. Some of our scaling choices, however, are only valid under quite specific conditions. Motivated by the recent introduction of the novel intermediary *diabatic layer* in Klein et al. (2022), we therefore propose a different distinguished limit that is better suited to connect with this adjacent boundary layer. We then sketch the resulting model, which we will develop in more detail in an upcoming paper.

a. The framework

First, let us clarify the scope and limitations of our model, which are summarized in the following points:

1) As stated above, our QG model is meant to be incorporated into a triple-deck boundary layer theory, coupled to the diabatic layer, as well as to the Ekman layer. In particular, this has the consequence that *our scaling assumptions have to hold strictly at altitudes ≥ 3 km only, letting certain model variables attain asymptotically larger or smaller values in the lower layers.*
2) On the length and time scales of QG theory, we cannot capture convective processes explicitly, since they require much higher vertical velocities and a drastically different aspect ratio. Therefore, the primary form of precipitation that we consider here is *stratiform rain*, which is generated from nimbostratus, frequently with cold seeder cells aloft—cf. chapter 6 of Houze (2014).
3) We are interested in scenarios with a very thick cloud cover. Therefore, we take the *highest observed liquid water contents* in stratiform clouds as a baseline for our scaling; we discuss the consequences for our scaling in detail further down.
4) Since we have not incorporated the ice phase and the associated phase changes as of yet, we stick with the simplified subdivision of water into vapor, cloud droplets, and rain. However, most stratiform rain actually originates from snow and other ice particles that, while falling from the upper troposphere through the cloud, increase in size and eventually melt. As laid out in Houze (2014) it is this two-stage process of aggregation and melting that dominates in stratiform rain, *not* accretion, which is the driving force in convective rain. For the time being, we will therefore—inaccurately—treat liquid cloud water and cloud ice as one substance, assume that all solid hydrometeors eventually turn into rain, and parameterize aggregation and melting in the same manner as autoconversion. All this, of course, is subject to future refinement.

Keeping the above in mind, let us discuss our scaling choices in depth:

b. Terminal rainfall velocity

The terminal velocity V_r of raindrops is strongly dependent on their diameter. In the context of a bulk parameterization and large-scale dynamics, however, the subtleties of the size spectrum cannot be captured. Thus, we opt for the most straightforward approach and assign a constant value to V_r, to be understood as an average over the size distribution of raindrops. Further, it is only the relative magnitude $V_r/w_{\mathrm{ref}} = V_T$ that matters for scaling purposes. Next, we therefore consider typical sedimentation velocities in stratiform rain.

Large raindrops can approach fall speeds up to 10 m s^{-1}, while the average value is considerably lower and also depends on the form of precipitation under consideration (see Khvorostyanov and Curry 2014, chapter 12). In convective rain, where also hailstones with much higher fall velocities can occur, the choice $V_T \sim \epsilon^{-2}$ would certainly be appropriate. Stratiform rain, generally speaking, is gentler and does not produce comparably large hydrometeors, leading us to choose

$$V_T \sim \epsilon^{-1} \quad (57)$$

for the present regime, which corresponds to velocities comparable to ~1 m s^{-1}.

c. The saturation mixing ratio

Sample calculations, using approximate solutions to the Clausius–Clapeyron equation as shown in Fig. 1, show that

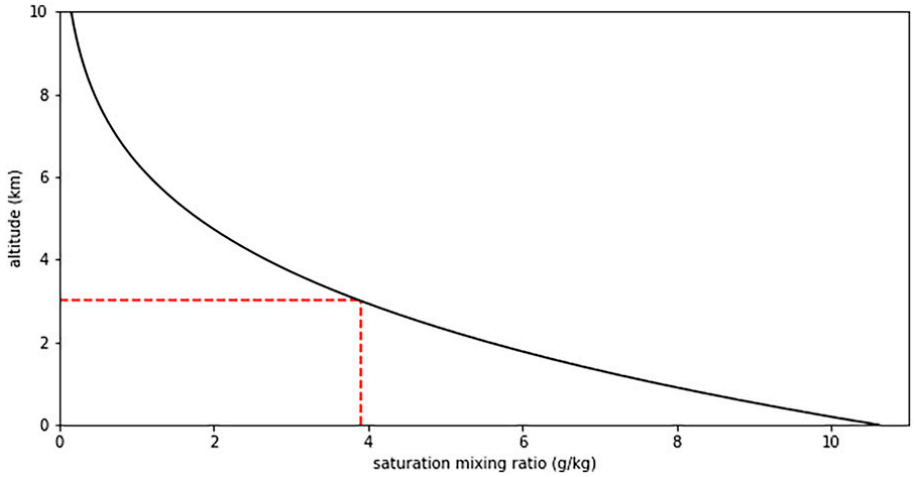

FIG. 1. Saturation mixing ratio in the midlatitude troposphere. At 3 km, the top of the diabatic layer, q_{vs} is already <4 g kg^{-1}, dropping well below 1 g kg^{-1} toward the tropopause.

the saturation mixing ratio q_{vs} is $\ll 10$ g kg^{-1} in the bulk of the midlatitude troposphere [see also sample values in Weischet and Endlicher (2018)]. We therefore stipulate

$$q_{vs} \sim \epsilon^3, \tag{58}$$

keeping in mind that by asymptotic matching, this still allows the saturation mixing ratio to increase up to $O(\epsilon^2)$ through the diabatic and Ekman layers below. The scaling then agrees very well with the observed magnitudes.

d. Moisture components

Water vapor: Supersaturation levels cannot significantly exceed q_{vs} in magnitude, so that the following scaling for the water vapor content,

$$q_v \sim \epsilon^3, \tag{59}$$

suggests itself.

Cloud water: Typically, the cloud water mixing ratio q_c will be smaller than q_v by an order of magnitude, especially in thinner midlevel clouds, as evidenced by observational data, e.g., in Fleishauer et al. (2002). Yet, datasets, e.g., from Zhao and Lei (2014, p. 96) or Zhang et al. (2020) show that the liquid water content in a nimbostratus cloud frequently approaches 0.5 g m^{-3} at altitudes 3–4 km, corresponding to $q_c \sim 0.6$–0.7 g kg^{-1}. With our stated aim to describe an atmosphere with a consistently thick cloud cover, also keeping in mind that we implicitly include cloud ice, this justifies the scaling

$$q_c \sim \epsilon^3 . \tag{60}$$

By letting $q_c^{(0)} \to 0$, we can also discuss "almost cloud-free" regions later on, once we have derived our model equations.

Rain: Regarding the rain mixing ratio q_r, we simply make the assumption that the total amount of precipitation that eventually reaches the ground is on the same order of magnitude as the total cloud water content. Assuming a water vapor (saturation) mixing ratio $O(\epsilon^2)$ near the ground, this implies q_r should be one order of magnitude smaller than q_v. Since nimbostratus clouds extend downward to rather low levels and rain accumulates as it falls through the various cloud layers, we further expect q_r to increase downward asymptotically in the same manner as q_{vs} and q_v, indicating that it should be as low as

$$q_r \sim \epsilon^4 \tag{61}$$

in the free troposphere (3–12 km above ground level). Notice that convective processes are filtered out on QG scales, whence exceptionally heavy rain is not covered by our model in absence of parameterizations of the related processes.

e. Phase changes

Here, we briefly assess which source terms in the Kessler-type parameterization play a role in the leading-order dynamics. Our guiding principle will be that all microphysical processes which are considered dominant should be represented at leading order in our bulk model as well. This principle is also grounded in the heuristic rule of asymptotic analysis that significant limits should retain a maximal number of terms, known as the *principle of least degeneracy* (Kevorkian and Cole 1996). In the following, we will argue on purely qualitative grounds and implicitly assume that the respective rate constants scale accordingly; for example, the condensation rate needs to fulfill $C_{cd}t_{ref} = O(\epsilon^{-3})$ for (62) to hold.

Condensation: First, let us recall that nimbostratus is primarily generated by gentle updrafts, continually lifting air parcels just above their condensation level. With the QG vertical velocity $w^{(1)}$ being very small, the leading-order equation for q_c will only deal with *horizontal* transport, which might lead one to conclude that condensation does not constitute a leading-order effect in our regime. It should be accounted for, however, that the formation of nimbostratus is significantly fueled by convective cells on the sides of, above or

even embedded in the cloud itself (Houze 2014, section 6.4). These processes are external to our model in the sense that they arise from vertical velocities that exceed $w^{(1)}$ by several orders of magnitude. Even though we do not intend to model convection as such, as we have repeatedly emphasized, we argue that the impact of these local events *on the development of the stratiform cloud* suffices to raise condensation to a leading-order effect and therefore opt for the ansatz

$$S_{\mathrm{cd}} \sim \epsilon^3 \tag{62}$$

for the (nondimensionalized) condensation term—which might be supplemented by a parameterization of the aforementioned convective updrafts.

Autoconversion, aggregation, and melting: Autoconversion of cloud water by coalescence that causes droplets to cross a size threshold is a very slow process. As already stated above, aggregation and subsequent melting of solid ice particles is the *dominant microphysical mechanism* in stratiform precipitation (Houze 2014, p. 144). Hence, we replace S_{ac} by a source term $S_{\mathrm{ag},m}$ that parameterizes this mechanism in a manner to be specified later on. Due to our assumption on the maximum cloud water and rain mixing ratios, the scaling

$$S_{\mathrm{ag},m} \sim \epsilon^3 \tag{63}$$

is justified.

Evaporation: In undersaturated regions, rain evaporates very quickly on QG time scales. In a fully developed nimbostratus cloud, though, it is continually resupplied through melting snow and ice, as described above. The evaporation term should therefore balance $S_{\mathrm{ag},m}$ in the equation for q_r, leading to the asymptotic rescaling

$$S_{\mathrm{ev}} \sim \epsilon^3. \tag{64}$$

Accretion: Here, we refer again to Houze (2014, p. 144): while accretion is considered to be the primary growth mechanism in convective clouds, it is of minor importance in nimbostratus. Aiming to account for the presence of convective cells, which might play a significant role in clouds that extend into the diabatic layer, we tentatively include the corresponding source term as well and assume

$$S_{\mathrm{cr}} \sim \epsilon^3. \tag{65}$$

Remark: The scaling choices in (62)–(65) are physically sensible and necessary to let $\mathrm{PQG_{DL}}$ stand on its own. We do not, however, exclude the possibility that connection to the diabatic layer might permit the consideration of different distinguished limits in future work.

f. Thermodynamic parameters

As far as the scalings of the latent heat and various heat capacities are concerned, we stick with the distinguished limit derived in section 3, with one exception:

Since we do not aim to conserve equivalent potential temperature in our variant of PQG, thus allowing precipitation to alter its evolution, the ratio

$$\frac{R_d}{c_{\mathrm{pd}}} = \Gamma \tag{66}$$

does not require the "Newtonian limit" anymore; we thus assume

$$\Gamma = O(1) \tag{67}$$

from here on out, which yields the standard leading-order solutions for the pressure and density in the troposphere.

g. Asymptotic expansion and derivation

The governing equations, rescaled for the $\mathrm{PQG_{DL}}$ regime as described above, now read as

$$D_t\mathbf{u} + \frac{1}{\epsilon} f\mathbf{k}\times\mathbf{u} + \frac{1}{\epsilon^3}\frac{1}{\rho}\boldsymbol{\nabla}_{\parallel} p = 0, \tag{68a}$$

$$D_t w + \frac{1}{\epsilon^5}\frac{1}{\rho}\partial_z p = -\frac{1}{\epsilon^5}, \tag{68b}$$

$$\partial_t \rho_d + \boldsymbol{\nabla}_{\parallel}\cdot(\rho_d\mathbf{u}) + \partial_z(\rho_d w) = 0, \tag{68c}$$

$$C_\epsilon D_t \ln\theta + \epsilon^3\Sigma_\epsilon D_t \ln p + \epsilon^2\frac{L\phi_\epsilon}{T} D_t q_v = \epsilon^2 k_l V_T q_r(\partial_z \ln\theta + \Gamma\partial_z \ln p), \tag{68d}$$

$$D_t q_v = S_{\mathrm{ev}} - S_{\mathrm{cd}}, \tag{68e}$$

$$D_t q_c = S_{\mathrm{cd}} - S_{\mathrm{ag},m} - S_{\mathrm{cr}}, \tag{68f}$$

$$\epsilon D_t q_r - \frac{1}{\rho_d}\partial_z(\rho_d V_T q_r) = S_{\mathrm{ag},m} + S_{\mathrm{cr}} - S_{\mathrm{ev}}, \tag{68g}$$

where

$$\rho = \rho_d\Big(1 + \epsilon^3(q_v + q_c + \epsilon q_r)\Big), \tag{69a}$$

$$p = \rho_d T\Big(1 + \epsilon^3\frac{q_v}{E}\Big), \tag{69b}$$

$$T = \theta p^{\Gamma} \equiv \theta\pi, \tag{69c}$$

$$S_{\mathrm{ev}} = C_{\mathrm{ev}}\frac{p}{\rho}(q_{\mathrm{vs}} - q_v)^+ q_r, \tag{69d}$$

$$S_{\mathrm{cd}} = C_{\mathrm{cn}}(q_v - q_{\mathrm{vs}})^+ q_{\mathrm{cn}} + C_{\mathrm{cd}}(q_v - q_{\mathrm{vs}})q_c, \tag{69e}$$

$$S_{\mathrm{cr}} = C_{\mathrm{cr}} q_c q_r, \tag{69f}$$

$$C_\epsilon = 1 + \epsilon^3\Big(k_v q_v + k_l(q_c + q_r)\Big), \tag{69g}$$

$$\Sigma_\epsilon = \Gamma k_l(q_c + q_r) + \epsilon\kappa_v q_v, \tag{69h}$$

$$\phi_\epsilon = 1 - \frac{k_l - \epsilon k_v}{L}(T - 1). \tag{69i}$$

The newly introduced source term $S_{\mathrm{ag},m}$ could be parameterized in analogy with S_{ac}, e.g., as

$$S_{\mathrm{ag},m} = C_{\mathrm{ag},m}(q_c - q_{\mathrm{ag},m})^+, \tag{70}$$

where $q_{\mathrm{ag},m}$ now denotes an activation threshold for the conversion of melting snow into raindrops. Naturally, this is subject to refinement once the ice phase is introduced.

The scaling assumptions outlined earlier in this section imply changes in the asymptotic expansions relative to those for the PQG regime in (34) and (35). Since we do not invoke the Newtonian limit anymore [see (67)], the leading-order temperature is no longer constant, so that

$$T = T_0 + \epsilon T_1 + \epsilon^2 T^{(2)} + o(\epsilon^2). \tag{71}$$

(Recall that T_{00} denoted a constant in the PQG expansions, whereas here T_0 is a z-dependent background distribution.) In contrast, the moisture variables expand as

$$\begin{aligned} q_v &= \epsilon^3 q_v^{(0)} + o(\epsilon^3), \\ q_c &= \epsilon^3 q_c^{(0)} + o(\epsilon^3), \\ q_r &= \epsilon^4 q_r^{(1)} + o(\epsilon^4). \end{aligned} \tag{72}$$

That is, their absolute magnitude is reduced by one order in ϵ relative to the PQG regime [see (35)], and they do not feature time independent, vertically stratified background states.

With these expansions, the leading-order equations for mass and horizontal momentum remain unchanged relative to those found in the PQG regime. Note, however, that from the second-order vertical momentum balance in (48), we may now infer

$$\partial_z\left(\frac{p^{(2)}}{p_0}\right) = \frac{1}{T_0}\left[T^{(2)} + \frac{\rho_1}{\rho_0}T_1\right], \tag{73}$$

which involves the leading-order temperature stratification $T_0(z)$. This equation can be rewritten in terms of the potential temperature perturbation to yield the hydrostatic balance, (5b), with a pressure perturbation ϕ defined in the same manner as in section 4.

Let us also recall that by taking the horizontal gradient and utilizing geostrophic balance, we obtain for the potential temperature perturbation $\theta^{(2)}$:

$$\frac{\partial \mathbf{u}^{(0)}}{\partial z} \cdot \boldsymbol{\nabla}_\parallel \theta^{(2)} = 0, \tag{74}$$

which can be viewed as a consequence of the thermal wind relation.

The explicit solutions for the leading-order pressure and density now read

$$p_0 = (1 - \Gamma z)^{1/\Gamma} \tag{75}$$

and

$$\rho_0 = (1 - \Gamma z)^{(1-\Gamma)/\Gamma}, \tag{76}$$

respectively, while the leading-order temperature profile drops off linearly with height:

$$T_0 = 1 - \Gamma z. \tag{77}$$

Moisture at leading order: The leading-order equation for water vapor is one for quasi-horizontal transport, since $w^{(0)} = 0$:

$$D_t^{(0)} q_v^{(0)} = S_{\mathrm{ev}}^{(0)} - S_{\mathrm{cd}}^{(0)}. \tag{78}$$

In the same fashion, we arrive at the equation

$$D_t^{(0)} q_c^{(0)} = S_{\mathrm{cd}}^{(0)} - S_{\mathrm{ag},m}^{(0)} - S_{\mathrm{cr}}^{(0)} \tag{79}$$

for the cloud water content—which is again transported only quasi horizontally. Cloud formation via condensation is expected to arise through local updrafts in small-scale convective cells, so that this effect is included on the present synoptic scales through an effective parameterization as part of the condensation source term $S_{\mathrm{cd}}^{(0)}$.

For rain, the vertical fallout term dominates:

$$\partial_z(\rho_0 q_r^{(0)}) = -\frac{\rho_0}{V_T}[S_{\mathrm{ag,m}}^{(0)} + S_{\mathrm{cr}}^{(0)} - S_{\mathrm{ev}}^{(0)}], \tag{80}$$

while the leading-order potential temperature balance—recalling (7)—reads

$$D_t^{(0)}\theta_e^{(2)} + w^{(1)}\frac{d\theta_1}{dz} = -k_l V_T q_r^{(0)}\Gamma(1 - \Gamma z)^{-1}. \tag{81}$$

Here we have used that, owing to the systematically lower moisture content compared to the PQG regime, the equivalent potential temperature equals the dry potential temperature to leading and first order. Coupled with the first-order mass balance, (40), and the vorticity transport equation, (44), this allows us to derive an equation for the QG potential vorticity based on the equivalent potential temperature perturbation $Q = \zeta^{(0)} + \beta y + (f_0/\rho_0)\partial_z(\rho_0\theta_e^{(2)}/(d\theta_1/dz))$:

$$D_t^{(0)} Q = \frac{f_0}{\rho_0}\partial_z\left(\rho_0 \frac{-k_l V_T q_r^{(0)}\Gamma(1 - \Gamma z)^{-1}}{d\theta_1/dz}\right) - \frac{f_0}{d\theta_1/dz}\partial_z \mathbf{u} \cdot \boldsymbol{\nabla}_\parallel q_v^{(0)}. \tag{82}$$

This enables a formulation of our model in terms of potential vorticity inversion, as mentioned in the introduction: given Q and q_v, we can rewrite the definition of Q to yield an elliptic partial differential equation for the pressure perturbation, which is given in its dimensional form in (16) above. The related PV-inversion problem has a unique solution if we specify boundary conditions for p. Horizontal flow and potential temperature can then diagnostically be recovered from the geostrophic and hydrostatic balances, respectively. With a given cloud water content q_c, we can also use the diagnostic relation (80) to compute the rainwater mixing ratio, and thus, we obtain the leading-order solutions of *all* model variables.

h. *Interpretation of the cloud-free limit*

As we already mentioned in our scaling of q_c, we will have $q_c^{(0)} \to 0$ quite frequently in a realistic setting (this formal limit

simply describes atmospheric environments with a thin cloud cover, it is not meant to imply assumptions on microphysical processes, such as fast autoconversion)—what will be the immediate consequences of this limit for our model? First, we observe that only the evaporation term remains as a sink in the equation for rain:

$$\partial_z(\rho_0 q_r^{(0)}) = \frac{\rho_0}{V_T} S_{\mathrm{ev}}^{(0)}. \tag{83}$$

With the constraint

$$q_r^{(0)} \to 0 \tag{84}$$

as $z \to \infty$ and $S_{\mathrm{ev}}^{(0)} \geq 0$, this forces us to conclude

$$q_r^{(0)} \equiv 0, \tag{85}$$

which in turn means that the water vapor mixing ratio is purely advected by the geostrophic flow:

$$D_t^{(0)} q_v^{(0)} = 0. \tag{86}$$

Thus, *all* moisture components vanish in the leading-order temperature equation. The QG dynamics then becomes that of dry air as expected.

7. Properties of PQG$_{\mathrm{DL}}$: The omega equation

As we have emphasized repeatedly, PQG$_{\mathrm{DL}}$ is set up to develop a more general model, covering synoptic dynamics through the lower troposphere and all the way to the planetary boundary layer. Yet, this model can also stand on its own as a valid extension of established QG theory and as a variant of the PQG family of models. Therefore, we will illustrate some of its properties in this section, using the *omega equation.*

The omega equation is a diagnostic Poisson-type equation for the QG vertical velocity that constitutes a widely used tool in synoptic meteorology (Hoskins et al. 1978, 1985, 2003). Since the relationship between moist processes and up- or downdrafts is of general meteorological interest, we will present the omega equation in its PQG$_{\mathrm{DL}}$ form and discuss its qualitative properties, also in comparison with PQG. Appendix B sketches a derivation of the omega equation in the context of our model.

a. General form of the equation

As laid out in appendix B, the omega equation in QG with an arbitrary heat source S_θ takes the form

$$N^2\Delta_\parallel \tilde{w} + f^2 \frac{1}{\overline{\rho}} \partial_z(\overline{\rho}\partial_z \tilde{w}) = 2\boldsymbol{\nabla}_\parallel \cdot \mathbf{Q} + f\beta v + \Delta_\parallel S_b, \tag{87}$$

where the buoyancy frequency $N = \sqrt{(g/\theta_{\mathrm{ref}})(d\overline{\theta}/dz)}$ is traditionally assumed constant and we have introduced the Q vector

$$\mathbf{Q} = -(\boldsymbol{\nabla}_\parallel \tilde{b} \cdot \partial_x \mathbf{u})\mathbf{i} - (\boldsymbol{\nabla}_\parallel \tilde{b} \cdot \partial_y \mathbf{u})\mathbf{j}, \tag{88}$$

where $\mathbf{i}$ and $\mathbf{j}$ are unit vectors in the x and y directions, respectively, and $\tilde{b} = (g/\theta_{\mathrm{ref}})\tilde{\theta}$ denotes the buoyancy. The second term on the right in (87) is due to the β effect, which is frequently neglected.

As demonstrated in (B6)–(B8), the source term S_b in PQG$_{\mathrm{DL}}$ reads

$$S_b = \frac{g}{\theta_{\mathrm{ref}}}\left[c_l V_r q_r \frac{R_d}{c_{\mathrm{pd}}} \partial_z \ln\overline{p} - \frac{L_{\mathrm{ref}}}{c_{\mathrm{pd}}}(S_{\mathrm{ev}} - S_{\mathrm{cd}})\right], \tag{89}$$

which leads to

$$N^2\Delta_\parallel \tilde{w} + f^2 \frac{1}{\overline{\rho}} \partial_z(\overline{\rho}\partial_z \tilde{w}) = 2\boldsymbol{\nabla}_\parallel \cdot \mathbf{Q} + f\beta v + \frac{g}{\theta_{\mathrm{ref}}}\Delta_\parallel\left[c_l V_r q_r \frac{R_d}{c_{\mathrm{pd}}} \partial_z \ln\overline{p} - \frac{L_{\mathrm{ref}}}{c_{\mathrm{pd}}}(S_{\mathrm{ev}} - S_{\mathrm{cd}})\right] \tag{90}$$

as the omega equation in PQG$_{\mathrm{DL}}$.

As is apparent from this formulation, the incorporation of cloud microphysics via parameterization of the various phase conversions allows moisture to influence vertical motions in multiple ways:

- By condensation in saturated air
- By "negative condensation" (evaporation of cloud water) as well as evaporation of rain in undersaturated air
- By falling rain (regardless of saturation), as indicated by the rightmost term in (90)

In PQG variants that only consider one dynamical moisture variable, such as the model derived in section 5, no such variety of interactions is possible: in undersaturated air, moisture cannot influence the dynamics at all.

In the following, we want to make the connection between vertical velocity and the moist constituents more palpable:

b. Estimating moist contributions: A sample solution

We can isolate the component of vertical velocity that is *directly* due to moist processes by writing any solution of (90) as

$$\tilde{w} = w_d + w_m, \tag{91}$$

where w_d solves the "dry equation," (87), without any heat sources. Then, w_m will be a solution of

$$N^2\Delta_\parallel w_m + f^2\partial_z\left(\frac{1}{\overline{\rho}}\partial_z(\overline{\rho}w_m)\right) = \frac{g}{\theta_{\mathrm{ref}}}\Delta_\parallel\left[c_l V_r q_r \frac{R_d}{c_{\mathrm{pd}}} \partial_z \ln\overline{p} - \frac{L_{\mathrm{ref}}}{c_{\mathrm{pd}}}(S_{\mathrm{ev}} - S_{\mathrm{cd}})\right]. \tag{92}$$

Let us now prescribe a moisture distribution with a particularly convenient vertical structure that permits an explicit representation of w_m in terms of the sources on the right-hand side: in a saturated atmosphere, assume a state of *incipient condensation*, such that $S_{\mathrm{ev}} = q_r = 0$ and

$$S_{\mathrm{cd}} = C_{\mathrm{cn}} q_{\mathrm{cn}} (q_v - q_{\mathrm{vs}})^+; \tag{93}$$

i.e., no significant amount of cloud has emerged yet and all condensation is due to the presence of condensation kernels.

We now investigate the case in which S_{cd} assumes a vertical structure as follows:

$$S_{cd}(t, \mathbf{x}, z) = C_{cn} T_0(z) K(t, \mathbf{x}) \sigma(t, \mathbf{x}), \tag{94}$$

where K and σ are horizontal distributions of condensation kernels and supersaturation, respectively. Provided such a distribution, we can then assume that w_m also takes such a vertical structure; we therefore look for solutions of the form

$$w_m(t, \mathbf{x}, z) = T_0(z) W_m(t, \mathbf{x}). \tag{95}$$

Substituting this ansatz into (92), we get for the left-hand side

$$N^2 \Delta_\parallel w_m + f^2 \partial_z \left(\frac{1}{\overline{\rho}} \partial_z (\overline{\rho} w_m) \right) = T_0 \Delta_\parallel N^2 W_m + f_0^2 \partial_z \left(\frac{1}{\overline{\rho}} \partial_z (\overline{\rho} T_0) \right) W_m = T_0 \Delta_\parallel N^2 W_m, \tag{96}$$

since $\partial_z(\overline{\rho} T_0) = \partial_z \overline{p} = -\overline{\rho}$. Thus, the vertical component drops out of the equation and, using (94), we are left with

$$T_0 \Delta_\parallel N^2 W_m = T_0 \Delta_\parallel \left[\frac{L_{ref}}{c_{pd}} C_{cn} K \sigma \right], \tag{97}$$

which implies

$$\Delta_\parallel \left[N^2 W_m - \frac{L_{ref}}{c_{pd}} C_{cn} K \sigma \right] = 0. \tag{98}$$

Finally, making the assumption that condensation is horizontally restricted to the interior of the domain under consideration, (98) can be formulated as a Laplace equation with homogeneous Dirichlet boundary conditions (Evans 2010), and its unique solution is simply

$$W_m = \frac{L_{ref} C_{cn}}{c_{pd} N^2} K \sigma. \tag{99}$$

Thus, if (94) holds, updrafts due to condensation intensify *in proportion* with both supersaturation and the concentration of condensation kernels. We emphasize that this result only pertains to updrafts directly related to condensation, not the vertical velocity as a whole.

8. Conclusions

In this note, we have demonstrated how to derive the PQG model of Smith and Stechmann (2017) in its anelastic form systematically from equations for compressible moist atmospheric flow with bulk microphysics closures. In doing so, we have not introduced a soundproof limit from the outset, but relied only on the distinguished limit for the Rossby, Mach, and Froude numbers proposed in Klein (2010), and on a heuristic correspondence principle for the asymptotic rescaling of the moist parameters. The derivation was carried out by systematic asymptotic analysis.

Motivated by the recent introduction of the diabatic layer in the context of QG theory by Klein et al. (2022), we then put forward a modified scaling ansatz, designed to yield a system of equations that can connect to this new intermediate layer (located between the bulk troposphere and the Ekman friction layer) in a mathematically sound and physically meaningful way. In contrast to the PQG model, the new PQG_{DL} model allows for a straightforward PV inversion, essentially analogous to that of the classical QG theory. In turn, PQG_{DL} only models the upper 3–12 km of the troposphere, while stronger diabatic effects of moisture at lower levels are to be addressed by the diabatic layer equations, which we intend to work out in a future publication. Properties of the PQG_{DL} system were illustrated using the omega equation, an equation that allows us to illuminate the relationship between vertical air motions and moist temperature sources.

We hope to gain more insight into moisture dynamics in the midlatitude atmosphere on the synoptic scale from future investigations of this system, regarding, for example, baroclinic instability, cyclogenesis, and the associated moist processes.

Acknowledgments. D.B. and S.H. acknowledge support by the Austrian Science Fund (FWF) via the SFB "Taming Complexity in Partial Differential Systems" with Project F65. S.H. also acknowledges support by the Austrian Science Fund via the previous Hertha-Firnberg Project T-764. R.K. acknowledges support by Deutsche Forschungsgemeinschaft through Grant CRC 1114 "Scaling Cascades in Complex Systems," Project 235221301, Project (C06) "Multi-scale structure of atmospheric vortices." The authors are grateful to the Wolfgang Pauli Institute Vienna for continuous support, e.g., the Pauli fellowship for R.K. and for scientific discussions with its director, N.J. Mauser. The authors thank Leslie Smith and Sam Stechmann for helpful comments, in particular regarding potential vorticity inversion.

Data availability statement. The paper presents theoretical work and all derivations should be described in sufficient detail. No further data are required to reproduce the findings.

APPENDIX A

The Moist Anelastic Buoyancy

In this appendix, we do not aim to derive the full set of anelastic equations; we only want to derive the anelastic buoyancy in the form of Hernandez-Duenas et al. (2013) under a minimal set of scaling assumptions. In this, we will try to stay true to the spirit of the traditional derivation, as it can be found, e.g., in Vallis (2017).

1) The first assumption is that all state variables *as well as the moisture components* can be decomposed into a background state $\tilde{f} = \tilde{f}(z)$ and a perturbation $f' = f'(t, x, y, z)$, where $f' \ll \tilde{f}$. This roughly corresponds to our asymptotic expansion, with the crucial difference that only

two terms are considered; however, f' corresponds to $f^{(2)}$ in our regime. Therefore, f_0 and f_1 here appear "bundled together," which leads to a less refined approximation. This is the chief reason for the discrepancy that we encountered in the main text.

2) All thermodynamic relations for the perturbation variables are linearized. This corresponds to only considering the first dynamically relevant term in our asymptotic expansion.
3) The water content relative to dry air in the atmosphere is always small, that is, $q_v \ll 1$. Furthermore, we consider an unsaturated background state, implying $\tilde{q}_T = \tilde{q}_v$; as an additional consequence, the contribution of water vapor e to the total atmospheric pressure is also small, i.e., $e \ll p$. This does not specify the order of q_v or e relative to the perturbations of the state variables, again in contrast to our regime.
4) The depth of the vertical motion is comparable to the density scale height $-\tilde{\rho}(d\tilde{\rho}/dz)^{(-1)}$; the (potential) temperature scale height is one order of magnitude larger. The first part of this assumption is explicitly stated in Hernandez-Duenas et al. (2013); the second part makes up for the fact that we do not differentiate between a leading-order *constant* temperature and a first-order background stratification, which again goes back to assumption 1.
5) Moisture is present at leading order and does not drop off too quickly at higher altitudes, that is, we require $\tilde{q_v}/\tilde{q_{vs}} = O(1)$ as well as $(d\tilde{q_v}/dz)/(d\tilde{q_{vs}}/dz) = O(1)$.

a. Relations for potential temperature

Since the ideal gas law holds in the form

$$p = R_d \frac{1 + \frac{q_v}{E}}{1 + q_T} \rho T, \tag{A1}$$

we can utilize the definition of the potential temperature to derive the relation

$$\ln\theta = \ln C + \frac{1}{\gamma} \ln p - \ln\rho - \ln\overline{R}, \tag{A2}$$

where C is a constant and

$$\overline{R} = R_d \frac{1 + \frac{q_v}{E}}{1 + q_T}. \tag{A3}$$

Now, since (A2) has to hold for the background variables alone, differentiating with respect to z yields

$$\frac{1}{\tilde{\theta}}\frac{d\tilde{\theta}}{dz} = \frac{1}{\gamma\tilde{p}}\frac{d\tilde{p}}{dz} - \frac{1}{\tilde{\rho}}\frac{d\tilde{\rho}}{dz} - \frac{1}{E\left(1 + \frac{\tilde{q}_v}{E}\right)}\frac{d\tilde{q}_v}{dz} + \frac{1}{1 + \tilde{q}_T}\frac{d\tilde{q}_T}{dz}. \tag{A4}$$

Since we assume an unsaturated background state, it holds

$$\tilde{q}_T = \tilde{q}_v; \tag{A5}$$

utilizing hydrostatic balance then yields

$$\frac{1}{\tilde{\rho}}\frac{d\tilde{\rho}}{dz} = -\frac{g\tilde{\rho}}{\gamma\tilde{p}} - \frac{1}{\tilde{\theta}}\frac{d\tilde{\theta}}{dz} - (E - 1)\frac{1}{1 + \tilde{q}_v}\frac{d\tilde{q}_v}{dz}. \tag{A6}$$

Now, turning to the perturbations, by linearizing (A2) we obtain

$$\frac{\theta'}{\tilde{\theta}} = \frac{1}{\gamma}\frac{p'}{\tilde{p}} - \frac{\rho'}{\tilde{\rho}} - \frac{q_v'}{E} + q_T'. \tag{A7}$$

b. Derivation of the buoyancy term

The assumption of hydrostatic balance for the background profiles yields

$$\frac{Dw}{Dt} + \frac{1}{\tilde{\rho}}\frac{\partial\rho'}{\partial z} = -g\frac{\rho'}{\tilde{\rho}} \tag{A8}$$

in the vertical momentum balance, which can be rewritten as

$$\frac{Dw}{Dt} + \frac{\partial}{\partial z}\left(\frac{p'}{\tilde{\rho}}\right) = -\frac{p'}{\tilde{\rho}^2}\frac{d\tilde{\rho}}{dz} - g\frac{\rho'}{\tilde{\rho}}; \tag{A9}$$

substituting (A6), we then arrive at

$$\frac{Dw}{Dt} + \frac{\partial}{\partial z}\left(\frac{p'}{\tilde{\rho}}\right) = -\frac{p'}{\tilde{\rho}}\left[-\frac{g\tilde{\rho}}{\gamma\tilde{p}} - \frac{1}{\tilde{\theta}}\frac{d\tilde{\theta}}{dz} - \left(\frac{1}{E} - 1\right)\frac{1}{1 + \tilde{q}_v}\frac{d\tilde{q}_v}{dz}\right] - g\frac{\rho'}{\tilde{\rho}}. \tag{A10}$$

With our assumption on the scale heights, the second term in brackets on the rhs is clearly asymptotically small; the moisture term can be rewritten in the form

$$\frac{1}{\frac{1}{\tilde{q}_v} + 1}\frac{1}{\tilde{q}_v}\frac{d\tilde{q}_v}{dz} = \frac{1}{\frac{1}{\tilde{q}_v} + 1}\frac{d\ln\tilde{q}_v}{dz}; \tag{A11}$$

due to $\tilde{q}_v \ll 1$, it therefore suffices to show that $d\ln\tilde{q}_v/dz$ is not asymptotically large in order to justify the neglect of this term.

To this end, we can use the Clausius–Clapeyron equation for the (background) saturation vapor pressure $\tilde{e}_s$:

$$\frac{d\ln\tilde{e}_s}{dT} = \frac{1}{R_v}\frac{L(\tilde{T})}{\tilde{T}^2}. \tag{A12}$$

The saturation vapor pressure, in turn, is related to the (background) saturation mixing ratio $\tilde{q}_{vs}$ by the formula

$$\tilde{q}_{vs} = \frac{E\tilde{e}_s}{\tilde{p} - \tilde{e}_s}. \tag{A13}$$

In our setting, it holds $d\ln\tilde{q}_v/dz \sim d\ln\tilde{q}_{vs}/dz$, due to assumption 5. It therefore suffices to estimate the latter:

$$\begin{aligned}\frac{d\ln\tilde{q}_v}{dz} &= \frac{d\tilde{T}}{dz}\frac{d\ln\tilde{e}_s}{d\tilde{T}} + \frac{g\tilde{\rho}}{\tilde{p} - \tilde{e}_s} + \frac{\tilde{e}_s}{\tilde{p} - \tilde{e}_s}\frac{d\tilde{T}}{dz}\frac{d\ln\tilde{e}_s}{d\tilde{T}} \\ &= \frac{g\tilde{\rho}}{\tilde{p} - \tilde{e}_s} + \left(\frac{\tilde{q}_{vs}}{E} + 1\right)\frac{d\tilde{T}}{dz}\frac{d\ln\tilde{e}_s}{d\tilde{T}};\end{aligned} \tag{A14}$$

the first term here is clearly bounded, while we can employ Clausius–Clapeyron for the second:

$$\frac{d\tilde{T}}{dz}\frac{d\ln\tilde{e}_s}{d\tilde{T}} = \frac{d\tilde{T}}{dz}\frac{1}{R_v}\frac{L(\tilde{T})}{\tilde{T}^2} = \frac{1}{R_v}\frac{L(\tilde{T})}{\tilde{T}}\frac{1}{\tilde{T}}\frac{d\tilde{T}}{dz}. \tag{A15}$$

Due to our assumption on the temperature scale height, we can infer that this term is not just bounded from above, but actually asymptotically small.

Going back to (A10), the remaining terms yield the expression

$$g\left[\frac{1}{\gamma}\frac{p'}{\tilde{p}} - \frac{\rho'}{\tilde{\rho}}\right], \tag{A16}$$

which by (A7) can be rewritten as

$$g\left[\frac{\theta'}{\tilde{\theta}} + \left(\frac{1}{E} - 1\right)q_v' - q_c' - q_r'\right]. \tag{A17}$$

This is the exact form of the buoyancy force in the anelastic system of Hernandez-Duenas et al. (2013).

APPENDIX B

Derivation of the Omega Equation

In any version of PQG, the hydrostatic and geostrophic balances, (5a) and (5b), hold, as well as the vorticity equation, (9). Since these relations are equivalent to those in standard QG theory and no vertical velocity appears in the moist transport equations of $\mathrm{PQG_{DL}}$, any changes in the result will stem from the temperature equation. The latter can be reformulated in terms of potential temperature such that all moist terms appear as sources; thus, it suffices to sketch a derivation that is analogous to one for *dry* QG with a heat source. While the latter can be considered generally known, most references on the omega equation make use of the Boussinesq approximation and neglect the β effect. Therefore, we show the main steps of a derivation without these a priori simplifications.

Our starting point are the geostrophic and hydrostatic balances, (5a) and (5b), respectively, and the transport equations for vorticity and the equivalent potential temperature perturbation, (15a) and (15b), respectively, which we restate here for the reader's convenience:

$$f\mathbf{k}\times\mathbf{u} = -\boldsymbol{\nabla}_\parallel\phi, \tag{B1}$$

$$g\frac{\tilde{\theta}}{\theta_{\mathrm{ref}}} = \partial_z\phi, \tag{B2}$$

$$D_t^g[\zeta + \beta y] = \frac{f}{\overline{\rho}}\partial_z(\overline{\rho}\tilde{w}), \tag{B3}$$

$$D_t^g\tilde{\theta}_e + \tilde{w}\frac{d\overline{\theta}_e}{dz} = c_l V_r q_r \frac{R_d}{c_{\mathrm{pd}}}\partial_z\ln\overline{p}. \tag{B4}$$

As usual, the pressure perturbation ϕ assumes the role of a streamfunction (up to a constant factor); in particular it holds

$$\zeta = \frac{1}{f}\Delta_\parallel\phi. \tag{B5}$$

Observing that $\overline{\theta_e} = \overline{\theta}$ in $\mathrm{PQG_{DL}}$, since there is no moist background in this version of PQG and rewriting (B4) in terms of θ, we get

$$D_t^g\tilde{\theta} + \tilde{w}\frac{d\overline{\theta}}{dz} = c_l V_r q_r \frac{R_d}{c_{\mathrm{pd}}}\partial_z\ln\overline{p} - \frac{L_{\mathrm{ref}}}{c_{\mathrm{pd}}}D_t^g q_v \tag{B6}$$

and, employing (15c),

$$D_t^g\tilde{\theta} + \tilde{w}\frac{d\overline{\theta}}{dz} = c_l V_r q_r \frac{R_d}{c_{\mathrm{pd}}}\partial_z\ln\overline{p} - \frac{L_{\mathrm{ref}}}{c_{\mathrm{pd}}}(S_{\mathrm{ev}} - S_{\mathrm{cd}}). \tag{B7}$$

Finally, assuming a constant Brunt–Väisälä frequency $N = \sqrt{(g/\theta_{\mathrm{ref}})(d\overline{\theta}/dz)}$, we can write the above in the form

$$D_t^g\tilde{b} + N^2\tilde{w} = \frac{g}{\theta_{\mathrm{ref}}}\left[c_l V_r q_r \frac{R_d}{c_{\mathrm{pd}}}\partial_z\ln\overline{p} - \frac{L_{\mathrm{ref}}}{c_{\mathrm{pd}}}(S_{\mathrm{ev}} - S_{\mathrm{cd}})\right] =: S_b, \tag{B8}$$

where $\tilde{b} := g(\tilde{\theta}/\theta_{\mathrm{ref}})$.

Now, starting with the actual derivation, we can combine (B3) and (B5) to obtain

$$D_t^g(\Delta_\parallel\phi) = \frac{f^2}{\overline{\rho}}\partial_z(\overline{\rho}\tilde{w}) - f\beta v. \tag{B9}$$

Taking the vertical derivative of this equation and using hydrostatic balance, (B2), we get

$$\begin{aligned} D_t^g(\Delta_\parallel\tilde{b}) &= -\partial_z\mathbf{u}\cdot\boldsymbol{\nabla}_\parallel(\Delta_\parallel\phi) + \frac{f^2}{\overline{\rho}}\partial_z(\overline{\rho}\tilde{w}) - f\beta v \\ &= -\mathbf{k}\times\boldsymbol{\nabla}_\parallel\tilde{b}\cdot\boldsymbol{\nabla}_\parallel\zeta + \frac{f^2}{\overline{\rho}}\partial_z(\overline{\rho}\tilde{w}) - f\beta v. \end{aligned} \tag{B10}$$

In the next step, we take $\Delta_\parallel$ of (B4) and get

$$D_t^g(\Delta_\parallel\tilde{b}) + \Delta_\parallel(\mathbf{u}\cdot\boldsymbol{\nabla}_\parallel\tilde{b}) - \mathbf{u}\cdot\boldsymbol{\nabla}_\parallel(\Delta_\parallel\tilde{b}) = -N^2\Delta_\parallel\tilde{w} + \Delta_\parallel S_b. \tag{B11}$$

A laborious, but straightforward calculation then shows

$$\Delta_\parallel(\mathbf{u}\cdot\boldsymbol{\nabla}_\parallel\tilde{b}) = \mathbf{u}\cdot\boldsymbol{\nabla}_\parallel(\Delta_\parallel\tilde{b}) - \boldsymbol{\nabla}_\parallel\tilde{b}\cdot\boldsymbol{\nabla}_\parallel\mathbf{u} - 2\boldsymbol{\nabla}_\parallel\cdot\mathbf{Q}, \tag{B12}$$

where the Q vector is defined as in (88). Thus, we obtain

$$D_t^g(\Delta_\parallel\tilde{b}) = \boldsymbol{\nabla}_\parallel\tilde{b}\cdot\boldsymbol{\nabla}_\parallel\mathbf{u} + 2\boldsymbol{\nabla}_\parallel\cdot\mathbf{Q} + \Delta_\parallel S_b - N^2\Delta_\parallel\tilde{w}. \tag{B13}$$

To conclude, we want to combine (B10) and (B13) in order to arrive at a diagnostic equation; checking that it holds

$$-\mathbf{k}\times\boldsymbol{\nabla}_\parallel\tilde{b}\cdot\boldsymbol{\nabla}_\parallel\zeta = \boldsymbol{\nabla}_\parallel\tilde{b}\cdot\Delta_\parallel\mathbf{u}, \tag{B14}$$

thanks to the incompressibility of $\mathbf{u}$, these two terms cancel when subtracting (B10) from (B13) and rearranging yields

$$N^2\Delta_\parallel\tilde{w} + f^2\frac{1}{\overline{\rho}}\partial_z(\overline{\rho}\partial_z\tilde{w}) = 2\boldsymbol{\nabla}_\parallel\cdot\mathbf{Q} + f\beta v + \Delta_\parallel S_b, \tag{B15}$$

the $\mathrm{PQG_{DL}}$ version of the omega equation.

REFERENCES

Bannon, P. R., 1995: Potential vorticity conservation, hydrostatic adjustment, and the anelastic approximation. *J. Atmos. Sci.*, **52**, 2302–2312, https://doi.org/10.1175/1520-0469(1995)052<2302:PVCHAA>2.0.CO;2.

Cotton, W., G. Bryan, and S. van den Heever, 2011: *Storm and Cloud Dynamics*. 2nd ed. Elsevier, 820 pp.

De Vries, H., J. Methven, T. Frame, and B. Hoskins, 2010: Baroclinic waves with parameterized effects of moisture interpreted using Rossby wave components. *J. Atmos. Sci.*, **67**, 2766–2784, https://doi.org/10.1175/2010JAS3410.1.

Evans, L., 2010: *Partial Differential Equations*. 2nd ed. American Mathematical Society, 749 pp.

Fleishauer, R., V. Larson, and T. Vonder Haar, 2002: Observed microphysical structure of midlevel, mixed-phase clouds. *J. Atmos. Sci.*, **59**, 1779–1804, https://doi.org/10.1175/1520-0469(2002)059<1779:OMSOMM>2.0.CO;2.

Grabowski, W., and P. Smolarkiewicz, 1996: Two-time-level semi-Lagrangian model for precipitating clouds. *Mon. Wea. Rev.*, **124**, 487–497, https://doi.org/10.1175/1520-0493(1996)124<0487:TTLSLM>2.0.CO;2.

Hernandez-Duenas, G., A. Majda, L. Smith, and S. Stechmann, 2013: Minimal models for precipitating turbulent convection. *J. Fluid Mech.*, **717**, 576–611, https://doi.org/10.1017/jfm.2012.597.

Hittmeir, S., and R. Klein, 2018: Asymptotics for moist deep convection I: Refined scalings and self-sustaining updrafts. *Theor. Comput. Fluid Dyn.*, **32**, 137–164, https://doi.org/10.1007/s00162-017-0443-z.

Hoskins, B., I. Draghici, and H. Davies, 1978: A new look at the ω-equation. *Quart. J. Roy. Meteor. Soc.*, **104**, 31–38, https://doi.org/10.1002/qj.49710443903.

——, M. McIntyre, and A. Robertson, 1985: On the use and significance of isentropic potential vorticity maps. *Quart. J. Roy. Meteor. Soc.*, **111**, 877–946, https://doi.org/10.1002/qj.49711147002.

——, M. Pedder, and D. Jones, 2003: The omega equation and potential vorticity. *Quart. J. Roy. Meteor. Soc.*, **129**, 3277–3303, https://doi.org/10.1256/qj.02.135.

Houze, R. A., Jr., 2014: *Cloud Dynamics*. 2nd ed. Elsevier, 496 pp.

Kessler, E., 1995: On the continuity and distribution of water substance in atmospheric circulations. *Atmos. Res.*, **38**, 109–145, https://doi.org/10.1016/0169-8095(94)00090-Z.

Kevorkian, J., and J. Cole, 1996: *Multiple Scale and Singular Perturbation Methods*. Springer-Verlag, 634 pp.

Khvorostyanov, V., and J. Curry, 2014: *Thermodynamics, Kinetics and Microphysics of Clouds*. Cambridge University Press, 782 pp.

Klein, R., 2010: Scale-dependent models for atmospheric flows. *Annu. Rev. Fluid Mech.*, **42**, 249–274, https://doi.org/10.1146/annurev-fluid-121108-145537.

——, and A. Majda, 2006: Systematic multiscale models for deep convection on mesoscales. *Theor. Comput. Fluid Dyn.*, **20**, 525–551, https://doi.org/10.1007/s00162-006-0027-9.

——, L. Schielicke, S. Pfahl, and B. Khouider, 2022: QG–DL–Ekman: Dynamics of a diabatic layer in the quasi-geostrophic framework. *J. Atmos. Sci.*, **79**, 887–905, https://doi.org/10.1175/JAS-D-21-0110.1.

Lapeyre, G., and I. Held, 2004: The role of moisture in the dynamics and energetics of turbulent baroclinic eddies. *J. Atmos. Sci.*, **61**, 1693–1710, https://doi.org/10.1175/1520-0469(2004)061<1693:TROMIT>2.0.CO;2.

Monteiro, J., and J. Sukhatme, 2016: Quasi-geostrophic dynamics in the presence of moisture gradients. *Quart. J. Roy. Meteor. Soc.*, **142**, 187–195, https://doi.org/10.1002/qj.2644.

Parkins, C. J., P. A. Blythe, and D. G. Crighton, 2000: Hot spot ignition: The Newtonian limit. *Proc. Roy. Soc.*, **456A**, 2857–2882, https://doi.org/10.1098/rspa.2000.0644.

Pedlosky, J., 1987: *Geophysical Fluid Dynamics*. 2nd ed. Springer-Verlag, 710 pp.

Smith, L., and S. Stechmann, 2017: Precipitating quasigeostrophic equations and potential vorticity inversion with phase changes. *J. Atmos. Sci.*, **74**, 3285–3303, https://doi.org/10.1175/JAS-D-17-0023.1.

Vallis, G., 2017: *Atmospheric and Oceanic Fluid Dynamics*. 2nd ed. Cambridge University Press, 946 pp.

Weischet, W., and W. Endlicher, 2018: *Einführung in die allgemeine Klimatologie*. 9th ed. Gebr. Borntraeger, 370 pp.

Wetzel, A., L. Smith, S. Stechmann, and J. Martin, 2019: Balanced and unbalanced components of moist atmospheric flows with phase changes. *Chin. Ann. Math. Ser.*, **40B**, 1005–1038, https://doi.org/10.1007/s11401-019-0170-4.

Zhang, W., G. Xu, B. Xi, J. Ren, X. Wan, L. Zhou, C. Cui, and D. Wu, 2020: Comparative study of cloud liquid water and rain liquid water obtained from microwave radiometer and Micro Rain Radar observations over central China during the monsoon. *J. Geophys. Res. Atmos.*, **125**, e2020JD032456, https://doi.org/10.1029/2020JD032456.

Zhao, Z., and H. Lei, 2014: Observed microphysical structure of nimbostratus in northeast cold vortex over China. *Atmos. Res.*, **142**, 91–99, https://doi.org/10.1016/j.atmosres.2013.09.008.

PQG-DL-Ekman: a triple-deck boundary layer theory for large-scale atmospheric flow with moist process closures

Daniel Bäumer,[a] Rupert Klein[b]

[a] *Research platform MMM, c/o Fakultät für Mathematik, Universität Wien, Vienna, Austria*

[b] *FB Mathematik und Informatik, Freie Universität Berlin, Berlin, Germany*

Corresponding author: Daniel Bäumer, daniel.baeumer@univie.ac.at

ABSTRACT: Reduced mathematical models for atmospheric dynamics at various scales have a long and rich history. However, versions of such models that explicitly incorporate moisture and phase changes have been developed only fairly recently. This work merges one of said modeling innovations, namely Smith and Stechmann's *precipitating quasigeostrophic* (PQG) model family, with a triple-deck boundary layer theory due to Klein et al. that extends the classical QG-Ekman theory by an intermediate *diabatic layer* (DL). A detailed analysis of the Clausius-Clapeyron relation and Kessler-type bulk microphysics closures is included in the systematic derivation of the resulting PQG-DL-Ekman theory. Furthermore, to illustrate some of the model's properties, explicit axisymmetric solutions of the precipitating diabatic layer equations are derived and combined with numerical sample solutions for the bulk flow.

1. Introduction

Moist processes, from nucleation on the smallest cloud condensation kernels to large-scale precipitation systems, play a pivotal role in the dynamics of our planet's atmosphere. In the theoretical treatment of said dynamics, scale analysis, boundary layer theory and, more recently, the method of multiple scales have played a central role for many decades, leading to reduced models such as the ubiquitous quasi-geostrophic (QG) theory for the midlatitudes, the Matsuno-Gill models for the tropics and many more. The explicit incorporation of the most important moist processes, such as cloud formation and rain production, as well as the associated cloud microphysics, in these models thus promises to further our understanding of the highly complex interactions between the bulk flow and its (moist) thermodynamics at various scales - yet, first steps in this direction have been taken only relatively recently: the first multiscale model that systematically investigated transport equations for moisture species *and* the corresponding bulk microphysics closures in the context of asymptotic analysis was proposed by Klein and Majda (2006). Numerous studies on moist convection by Majda and coauthors followed - we only mention (Hernandez-Duenas et al. 2013), where a cloud-resolving model was proposed that later served as the starting point for the derivation of the original precipitating QG equations, one of the building blocks for the present work. The dynamics of convective cloud towers in the tropics was further studied by Hittmeir and Klein (2018).

Regarding synoptic-scale flow in the midlatitudes, the first systematic extension of classical QG theory by transport equations for water vapor and precipitation is due to Smith and Stechmann (2017), who derived the family of *precipitating QG* (PQG) models in a manner that was consistent with the textbook treatment of dry QG as in, e.g., (Pedlosky 1987). A different, but intimately related ansatz was pursued by Klein et al. (2022): in this work, the observation that diabatic processes tend to be systematically stronger at lower tropospheric levels, more frequently allowing for neutral or even unstable stratification, led to the extension of the well-known QG-Ekman theory (Pedlosky 1987; Vallis 2017) to a *triple-deck* boundary layer theory. This theory augments QG-Ekman with the novel *diabatic layer* (DL) as an intermediary between the free troposphere, which is governed by QG, and the (frictional) planetary boundary layer, where Ekman theory is applied. While also applicable to a dry atmosphere, this modeling innovation was motivated in large part by empirical evidence that processes such as cooling by evaporation at lower tropospheric

levels often significantly exceed the strength of heat sources that the scaling assumptions of QG theory permit. Therefore, it should be a worthwhile endeavor to combine the modeling efforts of Smith and Stechmann (2017) and Klein et al. (2022) and to derive a refined *PQG-DL-Ekman* model that takes into account the varying strengths of both spatiotemporal moisture perturbations and their associated phase changes across the various tropospheric layers. The foundation for this undertaking was laid by Bäumer et al. (2023), where the authors first showed how Smith and Stechmann's PQG equations can be embedded into the framework of Klein (2010) for model hierarchies in atmospheric flows, and subsequently derived a new variant of PQG that was designed specifically to connect to a diabatic layer with matching moist process closures.

In the present work, we build on said foundation and derive the previously announced PQG-DL-Ekman model, strictly in keeping with the tenets of singular perturbation theory (Kevorkian and Cole 1996).

2. The governing equations

As we are building on the $\mathrm{PQG_{DL}}$ model derived in (Bäumer et al. 2023), specifically for the purpose of extending it to the diabatic layer, we start from the same set of equations as in the cited article, supplemented by a priori unspecified closures for turbulent friction and diffusion. As stated by Bäumer et al. (2023), this model formulation goes back to Hittmeir and Klein (2018), and it includes established bulk microphysics closures as proposed and investigated by Kessler (1995); Grabowski and Smolarkiewicz (1996); Klein and Majda (2006). In its fully viscous, diffusive form,

its local wellposedness has recently been established by Doppler et al. (2024):

$$D_t\mathbf{u} + 2(\mathbf{\Omega}\times\mathbf{v})_{\parallel} + \frac{1}{\rho}\boldsymbol{\nabla}_{\parallel} p = \frac{\rho_d}{\rho} q_r V_r \partial_z \mathbf{u} + \mathcal{D}_{\mathbf{u}}, \tag{1a}$$

$$D_t w + 2(\mathbf{\Omega}\times\mathbf{v})_{\perp} + \frac{1}{\rho}\partial_z p = -g + \frac{\rho_d}{\rho} q_r V_r \partial_z w + \mathcal{D}_w, \tag{1b}$$

$$D_t \rho_d + \rho_d(\boldsymbol{\nabla}\cdot\mathbf{v}) = 0, \tag{1c}$$

$$C D_t \ln\left(\frac{\theta}{\theta_{\text{ref}}}\right) + \Sigma D_t \ln\left(\frac{p}{p_{\text{ref}}}\right) + \frac{L(T)}{T} D_t q_v = c_l V_r q_r \left(\partial_z \ln\left(\frac{\theta}{\theta_{\text{ref}}}\right) + \frac{R_d}{c_{\text{pd}}}\partial_z \ln\left(\frac{p}{p_{\text{ref}}}\right)\right) + Q + \mathcal{D}_\theta, \tag{1d}$$

$$D_t q_v = S_{\text{ev}} - S_{\text{cd}} + \mathcal{D}_v, \tag{1e}$$

$$D_t q_c = S_{\text{cd}} - S_{\text{cr}} - S_{\text{ac}} + \mathcal{D}_c, \tag{1f}$$

$$D_t q_r - \frac{1}{\rho_d}\partial_z(\rho_d V_r q_r) = S_{\text{cr}} + S_{\text{ac}} - S_{\text{ev}} + \mathcal{D}_r, \tag{1g}$$

with the additional relations

$$\rho = \rho_d(1 + q_v + q_c + q_r), \tag{2a}$$

$$p = R_d \rho_d T\left(1 + \frac{q_v}{R_d/R_v}\right), \tag{2b}$$

$$T = \theta\left(\frac{p}{p_{\text{ref}}}\right)^{\frac{\gamma-1}{\gamma}} \equiv \theta\pi, \tag{2c}$$

$$\mathbf{v} = \mathbf{u} + w\mathbf{k}, \tag{2d}$$

$$S_{\text{ev}} = C_{\text{ev}}\frac{p}{\rho}(q_{\text{vs}} - q_v)^+ q_r, \tag{2e}$$

$$S_{\text{cd}} = C_{\text{cn}}(q_v - q_{\text{vs}})^+ q_{\text{cn}} + C_{\text{cd}}(q_v - q_{\text{vs}}) q_c, \tag{2f}$$

$$S_{\text{ac}} = C_{\text{ac}}(q_c - q_{\text{ac}})^+, \tag{2g}$$

$$S_{\text{cr}} = C_{\text{cr}} q_c q_r, \tag{2h}$$

$$C = c_{\text{pd}} + c_{\text{pv}} q_v + c_l(q_c + q_r), \tag{2i}$$

$$\Sigma = \left(\frac{c_{\text{pv}}}{c_{\text{pd}}} R_d - R_v\right) q_v + \frac{c_l}{c_{\text{pd}}} R_d (q_c + q_r), \tag{2j}$$

$$L(T) = L_{\text{ref}} - (c_l - c_{\text{pv}})(T - T_{\text{ref}}) \equiv L_{\text{ref}}\phi(T). \tag{2k}$$

In the above equations, $(\mathbf{u} = (u, v, 0), w, \rho, \rho_d, T, \theta, p, \pi, q_v, q_c, q_r, q_{\text{vs}})$ denote horizontal and vertical velocity, density, dry air density, temperature, potential temperature, pressure, the dimensionless Exner pressure and the mixing ratios of water vapor, cloud water and rain, as well as the saturation mixing ratio, respectively; $g \approx 9.8$ m s^{-2} is the gravitational acceleration, $\mathbf{\Omega}$ the earth rotation vector, and the subscripts $\|$ and $\perp$ indicate horizontal and vertical components of a vector, respectively. We denote the positive part of a function f by f^+. As usual, c_{pd} and c_{pv} denote the specific heat capacities at constant pressure of dry air and water vapor, while c_l is the heat capacity of liquid water, here assumed constant for simplicity, and V_r is the terminal rainfall velocity; R_d and R_v are the gas constants for dry air and water vapor, $\gamma = c_{\text{pd}}/(c_{\text{pd}} - R_d)$ is the isentropic exponent of dry air, $\mathbf{k}$ the vertical unit vector, $p_{\text{ref}} \approx 10^5$ Pa the reference pressure and the material derivative D_t is given by

$$D_t = \partial_t + \mathbf{v} \cdot \boldsymbol{\nabla} = \partial_t + \mathbf{u} \cdot \boldsymbol{\nabla}_{\|} + w\partial_z. \tag{3}$$

In line with usual assumptions (Cotton et al. 2011), the dry air mass obeys the continuity equation (1c). Notice that the density appearing on the left-hand sides of the momentum equations (1a), (1b) is the full density from (2a) and not the dry air density. Therefore, the effect of moisture on (total) density is properly accounted for. Individual contributions from the moist constituents are the following: in the momentum equations (1a)-(1b), momentum changes due to falling rain appear on the right-hand side; in the thermodynamic equation (1d), C denotes the "total moist heat capacity", specified in (2i); Σ, defined in (2j), collects moist contributions related to the work done by pressure forces and $L(T)$ is the latent heat (enthalpy) of vaporization, which can be written as a linear function of temperature under the assumption of constant c_l. The reference values L_{ref} for latent heat and T_{ref} for temperature are listed in Table 1, while Q represents all diabatic heat sources other than latent heating. Finally, the right-hand side represents temperature changes due to precipitation falling relative to its environment. In the transport equations for the respective mixing ratios (1e)-(1g), terms of the form $S_\star$ denote the usual Kessler-type closures for the microphysical processes of evaporation (ev), condensation (cd), autoconversion (ac) and collection (cr), respectively. In (2e)-(2h),parameters of the form $C_\star$ denote rate constants of the respective processes, while q_{cn} represents the local density of condensation kernels and q_{ac} denotes an activation threshold for the autoconversion of cloud droplets into raindrops.

Turbulent closures for the quantity $\star$ are indicated by $\mathcal{D}_\star$. We defer a discussion of their respective importance and explicit formulas to subsection 4.3.

We do not explicitly consider cold (cirrus) clouds that would necessitate parametrization of the ice phase. While the importance of ice formation and the associated phase changes in the formation of stratiform cloud decks is undisputed (Houze 2014), their systematic incorporation would give rise to a host of additional modeling difficulties. For that reason, we reserve this endeavor for future work.

$T_{\mathrm{ref}} = \theta_{\mathrm{ref}}$	288.15	K	Typical midlatitude surface temperature
R_d	287	J/kg/K	Dry air gas constant
c_{pd}	1005	J/kg/K	Specific heat capacity of dry air at constant pressure
R_v	462	J/kg/K	Water vapor gas constant
c_{pv}	1850	J/kg/K	Specific heat capacity of water vapor at constant pressure
c_l	4186	J/kg/K	Specific heat capacity of liquid water
L_{ref}	2.466×10^6	J/kg	Latent heat (enthalpy) of vaporization at $T = T_{\mathrm{ref}}$

TABLE 1. Thermodynamic state parameters for a mixture of dry air, water vapor and liquid water.

3. Overview of resulting model equations

Here, for the reader's convenience, we summarize the results of the derivations in sections 4 and 5 in dimensional form. We adopt the following notational conventions: for any model variable f that admits a decomposition into a leading-order background profile and a higher-order perturbation, we write $\bar{f} = \bar{f}(z)$ for the former and $\tilde{f} = \tilde{f}(t, \mathbf{x}, z)$ for the latter. Perturbations that appear both in the quasigeostrophic regime, henceforth denoted by $\mathrm{PQG}_{\mathrm{DL}}$, and in the diabatic layer are assigned superscripts accordingly. We denote the material derivative with respect to the leading-order geostrophic velocity by

$$D_t^g = \partial_t + \mathbf{u} \cdot \boldsymbol{\nabla}_{\parallel}, \tag{4}$$

where it will always be clear from the context whether $\mathbf{u}$ stands for the horizontal velocity field in $\mathrm{PQG}_{\mathrm{DL}}$ or that in the DL. Finally, we account for the two different distinguished limits introduced

by Hittmeir and Klein (2018) and discussed below in section 4 by allowing for $\alpha \in \{0, 1\}$, leading to varying forms of the dynamical buoyancy perturbation.

a. The PQG_{DL} equations

These take a form very close to, but not identical with the equations proposed by Bäumer et al. (2023). We refer to sections 4 and 5 for a detailed discussion of the differences in the scaling, which are mainly felt in the appearance of the vertical velocity in the transport equation for water vapor.

(i) Diagnostic relations from momentum equations: As in all PQG model variants proposed thus far, geostrophic balance takes the usual form, while the hydrostatic relation incorporates water vapor buoyancy in the regime $\alpha = 0$:

$$f\mathbf{k}\times\mathbf{u}^{\mathrm{QG}} = -\boldsymbol{\nabla}_{\parallel}\tilde{\phi}^{\mathrm{QG}} \tag{5a}$$

$$\partial_z\tilde{\phi}^{\mathrm{QG}} = g\left(\frac{\tilde{\theta}^{\mathrm{QG}}}{\theta_{\mathrm{ref}}} + (1-\alpha)\frac{R_v}{R_d}\tilde{q}_v^{\mathrm{QG}}\right). \tag{5b}$$

Here, $\tilde{\phi}^{\mathrm{QG}} = \frac{\tilde{p}^{\mathrm{QG}}}{\bar{\rho}}$ (up to background terms).

(ii) Transport equations: The equation for the geostrophic vorticity ζ^{QG} also appears formally unchanged relative to the classical model,

$$D_t^g\left[\zeta^{\mathrm{QG}} + \beta y\right] = \frac{f}{\bar{\rho}}\partial_z\left(\bar{\rho}\tilde{w}^{\mathrm{QG}}\right), \tag{6}$$

with the small vertical velocity $\tilde{w}^{\mathrm{QG}}$.

The leading-order thermodynamic evolution is best expressed in terms of the (linearized) equivalent potential temperature $\theta_e = \theta + Lq_v$, which here plays a role analogous to that of θ in a dry air regime:

$$D_t^g\tilde{\theta}_e^{\mathrm{QG}} + \tilde{w}^{\mathrm{QG}}\frac{d\bar{\theta}_e}{dz} = Q^{\mathrm{QG}} + \mathcal{D}_\theta^{\mathrm{QG}}. \tag{7}$$

Turning to the moist constituents, transport of water vapor reads

$$D_t^g\tilde{q}_v^{\mathrm{QG}} + \tilde{w}^{\mathrm{QG}}\frac{d\bar{q}_{\mathrm{vs}}}{dz} = S_{\mathrm{ev}}^{\mathrm{QG}} - S_{\mathrm{cd}}^{\mathrm{QG}} + \mathcal{D}_v^{\mathrm{QG}}. \tag{8}$$

As in Smith and Stechmann's original PQG equations, but in contrast with Bäumer et al. (2023), the water vapor mixing ratio here has a leading-order background component; see section 4 for the reasoning behind this change. The cloud water mixing ratio obeys

$$D_t^g q_c^{\mathrm{QG}} = S_{\mathrm{cd}}^{\mathrm{QG}} - S_{\mathrm{ac}}^{\mathrm{QG}} - S_{\mathrm{cr}}^{\mathrm{QG}} + \mathcal{D}_c^{\mathrm{QG}} \tag{9}$$

at leading order, while the respective phase changes $S_\star^{\mathrm{QG}}$ are given by

$$S_{\mathrm{ev}}^{\mathrm{QG}} = \bar{C}_{\mathrm{ev}} \left(\tilde{q}_{\mathrm{vs}}^{\mathrm{QG}} - \tilde{q}_v^{\mathrm{QG}} \right)^+ q_r^{\mathrm{QG}} \tag{10a}$$

$$S_{\mathrm{cd}}^{\mathrm{QG}} = \bar{C}_{\mathrm{cn}} \left(\tilde{q}_v^{\mathrm{QG}} - \tilde{q}_{\mathrm{vs}}^{\mathrm{QG}} \right)^+ q_{\mathrm{cn}} + \bar{C}_{\mathrm{cd}} \left(\tilde{q}_v^{\mathrm{QG}} - \tilde{q}_{\mathrm{vs}}^{\mathrm{QG}} \right) q_c \tag{10b}$$

$$S_{\mathrm{ac}}^{\mathrm{QG}} = \bar{C}_{\mathrm{ac}} \left(q_c^{\mathrm{QG}} - q_{\mathrm{ac}} \right)^+ \tag{10c}$$

$$S_{\mathrm{cr}}^{\mathrm{QG}} = \bar{C}_{\mathrm{cr}} q_c^{\mathrm{QG}} q_r^{\mathrm{QG}}. \tag{10d}$$

Crucially, the local saturation status *and* the saturation threshold itself here are determined by spatiotemporal perturbations, with the first-order correction to the saturation mixing ratio being a function of potential temperature anomalies by systematic expansion of the Clausius-Clapeyron relation.

(iii) Diagnostic relation for rain: As in (Bäumer et al. 2023), our scaling of the terminal velocity of raindrops yields the quasi-1D equation

$$-\frac{1}{\bar{\rho}} \partial_z \left(\bar{\rho} V_r q_r^{\mathrm{QG}} \right) = S_{\mathrm{ac}}^{\mathrm{QG}} + S_{\mathrm{cr}}^{\mathrm{QG}} - S_{\mathrm{ev}}^{\mathrm{QG}} \tag{11}$$

for the rain water mixing ratio. Since geostrophic transport does not come into play at leading order here, the only auxiliary condition needed to specify a unique solution is a one-sided boundary condition in z that can be imposed at the top of the domain.

Having collected the relevant balances, we proceed in the usual fashion, focusing on the regime $\alpha = 1$: the vertical velocity can be eliminated from (5a)-(11) by introduction of a suitable notion of *potential vorticity* (PV) and a suitable moisture variable (cf. Smith and Stechmann (2017)). As

detailed in section 5, this process leads to the system

$$D_t^g \mathrm{PV}_e = -\frac{f}{d\bar{\theta}_e/dz}\partial_z \mathbf{u}^{\mathrm{QG}} \cdot \boldsymbol{\nabla}_\parallel \left(\frac{L_{\mathrm{ref}}}{c_{\mathrm{pd}}}\tilde{q}_v^{\mathrm{QG}}\right) + \frac{f}{\bar{\rho}}\partial_z\left(\frac{\bar{\rho}\left(Q^{\mathrm{QG}} + \mathcal{D}_\theta^{\mathrm{QG}}\right)}{d\bar{\theta}_e/dz}\right) \tag{12a}$$

$$D_t^g \tilde{M} = B(z)\left[S_{\mathrm{ev}}^{\mathrm{QG}} - S_{\mathrm{cd}}^{\mathrm{QG}} + \mathcal{D}_v^{\mathrm{QG}}\right] + Q^{\mathrm{QG}} + \mathcal{D}_\theta^{\mathrm{QG}} \tag{12b}$$

$$D_t^g q_c^{\mathrm{QG}} = S_{\mathrm{cd}}^{\mathrm{QG}} - S_{\mathrm{ac}}^{\mathrm{QG}} - S_{\mathrm{cr}}^{\mathrm{QG}} + \mathcal{D}_c^{\mathrm{QG}} \tag{12c}$$

$$-\frac{1}{\bar{\rho}}\partial_z\left(\bar{\rho}V_r q_r^{\mathrm{QG}}\right) = S_{\mathrm{ac}}^{\mathrm{QG}} + S_{\mathrm{cr}}^{\mathrm{QG}} - S_{\mathrm{ev}}^{\mathrm{QG}} \tag{12d}$$

$$\frac{1}{f}\Delta_\parallel \tilde{\phi}^{\mathrm{QG}} + \frac{f}{\bar{\rho}}\partial_z\left(\frac{\bar{\rho}}{d\bar{\theta}_e/dz}\frac{B(z)}{L_{\mathrm{ref}}/c_{\mathrm{pd}} + B(z)}\partial_z\tilde{\phi}^{\mathrm{QG}}\right) = \mathrm{PV}_e - \beta y - \frac{f}{\bar{\rho}}\partial_z\left(\frac{\bar{\rho}}{d\bar{\theta}_e/dz}\frac{L_{\mathrm{ref}}/c_{\mathrm{pd}}}{L_{\mathrm{ref}}/c_{\mathrm{pd}} + B(z)}\tilde{M}\right) \tag{12e}$$

$$f\mathbf{k}\times\mathbf{u}^{\mathrm{QG}} = -\boldsymbol{\nabla}_\parallel \tilde{\phi}^{\mathrm{QG}} \tag{12f}$$

$$\partial_z\tilde{\phi}^{\mathrm{QG}} = g\frac{\tilde{\theta}^{\mathrm{QG}}}{\theta_{\mathrm{ref}}}, \tag{12g}$$

where PV_e is the QG potential vorticity based on equivalent potential temperature θ_e, the moisture variable $\tilde{M}$ is a linear combination of $\tilde{\theta}_e^{\mathrm{QG}}$ and q_v^{QG} and the following additional relations hold:

$$B(z) = -\frac{d\bar{\theta}_e/dz}{d\bar{q}_{\mathrm{vs}}/dz} \tag{13a}$$

$$\tilde{q}_v^{\mathrm{QG}} = \frac{1}{L_{\mathrm{ref}}/c_{\mathrm{pd}} + B(z)}\left(\tilde{M} - \tilde{\theta}^{\mathrm{QG}}\right). \tag{13b}$$

It is important to note that, even though the system as a whole is clearly nonlinear, the elliptic inversion equation (12e) *is* linear in a diagnostic setting, where we can assume the quantities PV_e and $\tilde{M}$ to be given. See the discussion at the end of section 5a concerning the relevance of this statement.

A formally equivalent alternative to the formulation (12) that mirrors the *dry* QG theory more closely takes the form

$$D_t^g \mathrm{PV} = -\frac{f}{\bar{\rho}}\partial_z\left(\frac{\bar{\rho}L\left(S_{\mathrm{ev}}^{\mathrm{QG}} - S_{\mathrm{cd}}^{\mathrm{QG}} + \mathcal{D}_v^{\mathrm{QG}}\right)}{d\bar{\theta}/dz}\right) + \frac{f}{\bar{\rho}}\partial_z\left(\frac{\bar{\rho}\left(Q^{\mathrm{QG}} + \mathcal{D}_\theta^{\mathrm{QG}}\right)}{d\bar{\theta}/dz}\right) \tag{14a}$$

$$D_t^g \tilde{M} = B(z)\left[S_{\mathrm{ev}}^{\mathrm{QG}} - S_{\mathrm{cd}}^{\mathrm{QG}} + \mathcal{D}_v^{\mathrm{QG}}\right] + \mathcal{D}_\theta^{\mathrm{QG}} + Q^{\mathrm{QG}} \tag{14b}$$

$$D_t^g q_c^{\mathrm{QG}} = S_{\mathrm{cd}}^{\mathrm{QG}} - S_{\mathrm{ac}}^{\mathrm{QG}} - S_{\mathrm{cr}}^{\mathrm{QG}} + \mathcal{D}_c^{\mathrm{QG}} \tag{14c}$$

$$-\frac{1}{\bar{\rho}}\partial_z(\bar{\rho}V_r q_r^{\mathrm{QG}}) = S_{\mathrm{ac}}^{\mathrm{QG}} + S_{\mathrm{cr}}^{\mathrm{QG}} - S_{\mathrm{ev}}^{\mathrm{QG}} \tag{14d}$$

$$\frac{1}{f}\Delta_\parallel\tilde{\phi} + \frac{f}{\bar{\rho}}\partial_z\left(\frac{\bar{\rho}}{d\bar{\theta}/dz}\partial_z\tilde{\phi}\right) = \mathrm{PV} - \beta y \tag{14e}$$

$$f\mathbf{k}\times\mathbf{u}^{\mathrm{QG}} = -\boldsymbol{\nabla}_\parallel\tilde{\phi}^{\mathrm{QG}} \tag{14f}$$

$$\partial_z\tilde{\phi}^{\mathrm{QG}} = g\frac{\tilde{\theta}^{\mathrm{QG}}}{\theta_{\mathrm{ref}}}, \tag{14g}$$

where we used the usual QG PV based on potential temperature. A less attractive feature of this formulation is that one has to contend with a discontinuous right hand side due to the moisture source terms in (14a). The investigation of PV formulations for $\alpha = 0$ is deferred to future publications.

b. The precipitating DL equations

In a DL of intermediate height (roughly 3 km), we start from the assumption that diabatic effects systematically exceed the strength allowed for in the QG context. In the original QG-DL-Ekman model of Klein et al. (2022), this led to a system that preserved both geostrophic and hydrostatic balance, but was governed dynamically exclusively by the thermodynamic equation with an external heat source. Here, the inclusion of moist process closures naturally extends the dry system by an evolution equation for water vapor, with the key assumption being that *subsaturation* in the DL (relative to the saturation mixing ratio) can also exceed the strength implicitly prescribed by PQG scaling. Thus, rain evaporation in dry air below cloud base emerges as the central new mechanism

in the novel *precipitating DL* (PDL) equations. Cloud water, on the other hand, drops out of the leading-order dynamics, necessitating more involved matching conditions to connect to the $\mathrm{PQG_{DL}}$ regime correctly, see section 5b for details and an outlook on viable alternatives. By a systematic derivation based on the scaling summarized above, the PDL equations read

$$D_t^g \tilde{\theta}_e^{\mathrm{DL}} = Q^{\mathrm{DL}} + \mathcal{D}_\theta^{\mathrm{DL}} \tag{15a}$$

$$D_t^g \tilde{q}_v^{\mathrm{DL}} = S_{\mathrm{ev}}^{\mathrm{DL}} + \mathcal{D}_v^{\mathrm{DL}} \tag{15b}$$

$$0 = S_{\mathrm{cd}}^{\mathrm{DL}} \tag{15c}$$

$$-\partial_z (V_r q_r^{\mathrm{DL}}) = -S_{\mathrm{ev}}^{\mathrm{DL}} \tag{15d}$$

$$f\mathbf{k}\times\mathbf{u}^{\mathrm{DL}} = -\boldsymbol{\nabla}_\parallel \tilde{\phi}^{\mathrm{DL}} \tag{15e}$$

$$\partial_z \tilde{\phi}^{\mathrm{DL}} = g\left(\frac{\tilde{\theta}^{\mathrm{DL}}}{\theta_{\mathrm{ref}}} + (1-\alpha)\frac{R_v}{R_d}\tilde{q}_v^{\mathrm{DL}}\right), \tag{15f}$$

with the top boundary condition for the rain water mixing ratio given by matching to the $\mathrm{PQG_{DL}}$ flow. As in (Klein et al. 2022), the vertical velocity does not directly influence the reduced dynamics and stays *constant* throughout the layer due to the velocity divergence constraint implied by the pertinent low Mach number of the flow.

c. The Ekman layer

In the large-scale mean, moist processes do not influence the leading-order balances in the frictional boundary layer. Therefore, the generation of an Ekman pumping velocity by mass fluxes near the surface constitutes its only contribution to the coupled dynamics, fully analogous to the classical theory (Pedlosky 1987; Vallis 2017). This mechanism is encapsulated in the formula

$$\tilde{w}^{\mathrm{QG}}|_{z=0} = \frac{d^{\mathrm{Ek}}}{2}\frac{1}{f}\Delta_\parallel \tilde{\phi}^{\mathrm{DL}}|_{z=0}, \tag{16}$$

with the Ekman layer height d^{Ek}. Notice that the pressure which is imprinted on the Ekman layer is that at the bottom of the DL. Inserting (16) into the thermodynamic equation (7), evaluated at

the bottom of the $\mathrm{PQG_{DL}}$ domain, we obtain the time-dependent bottom boundary condition

$$D_t^g\left(\partial_z\tilde{\phi}^{\mathrm{QG}}\right)|_{z=0} = -g\frac{L_{\mathrm{ref}}}{c_{\mathrm{pd}}T_{\mathrm{ref}}}\frac{1}{B(0)}D_t^g\tilde{M}|_{z=0} - \frac{L_{\mathrm{ref}}/c_{\mathrm{pd}}+B(0)}{B(0)}\frac{d^{\mathrm{Ek}}}{2}\frac{1}{f}\Delta_{\parallel}\tilde{\phi^{\mathrm{DL}}}|_{z=0}\frac{d\bar{\theta}_e}{dz}(0) + Q^{\mathrm{QG}}|_{z=0} + \mathcal{D}_\theta^{\mathrm{QG}}|_{z=0} \tag{17}$$

for the regime $\alpha = 1$. Supplementing either of the PV formulations derived for $\mathrm{PQG_{DL}}$ and the PDL equations (15) with (17) yields a complete description of the governing equations of the PQG-DL-Ekman model in dimensional form. This boundary condition would take a different form when $\alpha = 0$, but as already mentioned, we reserve a detailed investigation of this regime for future studies.

4. Scaling: non-dimensionalization and choice of a distinguished limit

As in (Bäumer et al. 2023), we base our derivation on the distinguished limit for dry airflows of Klein (2010): with ϵ representing a generic small, dimensionless parameter, corresponding to a numerical value of ~ 0.1, we scale the Mach, external Froude and Rossby numbers as

$$\mathrm{M} = \frac{u_{\mathrm{ref}}}{\sqrt{p_{\mathrm{ref}}/\rho_{\mathrm{ref}}}} = \epsilon^{3/2} = \frac{u_{\mathrm{ref}}}{\sqrt{g h_{\mathrm{sc}}}} = \mathrm{Fr_{ext}}, \qquad \mathrm{Ro} = \frac{u_{\mathrm{ref}}}{2\Omega l_{\mathrm{ref}}} = O(\epsilon), \tag{18}$$

where the relevant parameters are summarized in Table 2. With an appropriately defined synoptic length scale, we then have

$$\frac{h_{\mathrm{sc}}}{l_{\mathrm{ref}}} = \epsilon^2 \tag{19}$$

as our scaling for the aspect ratio of the flow, which further implies that w_{ref} obeys

$$w_{\mathrm{ref}} = \epsilon^2 u_{\mathrm{ref}}. \tag{20}$$

u_{ref}	~ 10	m s^{-1}	Typical horizontal wind speed
l_{ref}	$\sim 10^6$	m	Synoptic length scale
$h_{\text{sc}} = \frac{R_d T_{\text{ref}}}{g}$	$\sim 8.5 \times 10^3$	m	Pressure scale height
$w_{\text{ref}} = u_{\text{ref}} \frac{h_{\text{sc}}}{l_{\text{ref}}}$	~ 0.1	m s^{-1}	Reference vertical velocity

TABLE 2. Synoptic reference lengths and velocities.

In our treatment of the Coriolis force, we employ the traditional β-plane approximation (Pedlosky 1987), linearizing the (vertical) Coriolis parameter about a reference latitude $\sim 45°$:

$$\frac{1}{\Omega}\boldsymbol{\Omega} \sim (f_0 + \epsilon\beta\frac{y}{l_{\text{ref}}})\mathbf{k} + o(\epsilon). \tag{21}$$

Next, we supplement our distinguished limit with scalings for the thermodynamic parameters of moist, cloudy air. In doing so, we consider the two options first identified by Hittmeir and Klein (2018) as viable choices, shown in Table 3 below:

	Value	Regime $\alpha = 1$	Regime $\alpha = 0$
Nondimensional parameters			
$\frac{R_d}{c_{\text{pd}}}$	0.29	$\epsilon\Gamma$	$\epsilon\Gamma$
$\frac{c_{\text{pv}}}{c_{\text{pd}}}$	1.8	k_v	$\epsilon^{-1}k_v$
$\frac{R_v}{c_{\text{pd}}}$	0.46	$1/A$	$1/A$
$\frac{c_l}{c_{\text{pd}}}$	4.2	$\epsilon^{-1}k_l$	$\epsilon^{-1}k_l$
$\frac{L_{\text{ref}}}{c_{\text{pd}}T_{\text{ref}}}$	8.5	$\epsilon^{-1}L$	$\epsilon^{-1}L$
Derived nondimensional parameters			
$\frac{R_d}{R_v}$	0.62	E	ϵE
$\frac{c_{\text{pv}}}{c_{\text{pd}}}\frac{R_d}{c_{\text{pd}}} - \frac{R_v}{c_{\text{pd}}}$	0.067	$\epsilon\kappa_v$	κ_v

TABLE 3. Two viable moist extensions of the distinguished limit for dry air

In the two right-most columns, all parameters are bounded *independent* of ϵ - in other words, they are $O(1)$ in the limit $\epsilon \to 0$. Let us now first discuss the regime labeled $\alpha = 1$, which assigns asymptotic rescalings based on the numerical magnitudes of the respective parameters. Here, we are faced with the following dilemma: if we were to adhere to the tenets of similarity theory, the distinguished limit defined by the top five rows would imply that the derived quantity

$$\frac{R_d}{R_v} = \frac{R_d}{c_{\mathrm{pd}}} \Big/ \frac{R_v}{c_{\mathrm{pd}}} = \epsilon \Gamma A \tag{22}$$

is asymptotically small, while

$$\frac{c_{\mathrm{pv}}}{c_{\mathrm{pd}}} \frac{R_d}{c_{\mathrm{pd}}} - \frac{R_v}{c_{\mathrm{pd}}} = k_v \epsilon \Gamma - \frac{1}{A} \tag{23}$$

attains a negative value in the limit $\epsilon \to 0$. However, R_d/R_v is actually *larger* than R_v/c_{pd}, which we assigned a bounded value, while the derived expression at the bottom of Table 3 is a small *positive* quantity. In proposing the value-based regime $\alpha = 1$, we therefore take the following position: *accurate representation of the numerical values takes precedence over strict formal consistency,* and the ad hoc scalings for the two derived quantities are thus viewed as justified. From the perspective of dimensional analysis, the resulting formal inconsistency is of course worrisome, but the dynamics obtained in this fashion extend the classical QG theory in a very natural way and are compatible with the PQG model family. Moreover, to quote directly from Hittmeir and Klein (2018):

> "The second regime, in contrast, has been defined purely on the basis of the actual magnitudes of the dimensionless parameters. Numbers between 0.4 and 3.0 are considered of order unity, while smaller or larger values are associated with asymptotic rescalings in terms of ϵ. This provides a scaling that better matches with the actual numbers than the first regime, but it is not strictly consistent with similarity theory. Although this is at odds with the usual procedures, it may actually open up an interesting route of investigation. The thermodynamics of moist air may just be asymptotically compatible with a family of equation systems that features the same functional forms in the constitutive equations as those of moist air, but whose set of determining parameters is less constrained. The results of Sect. 4.2, in which we compare asymptotic and error-controlled numerical approximations to the moist adiabatic distribution, corroborate this point of view."

We therefore adopt said regime as the basis for our investigations in the present work. Nevertheless, the formally consistent distinguished limit labeled $\alpha = 0$, which does not match as well with the numerical values, might also have merit, and while we utilize the value-based regime in the derivation of sample solutions and numerical calculations in this article, we present all model equations in a form that includes the additional terms that would arise from adoption of $\alpha = 0$ by introduction of a switching function.

Remark: While we base our model equations in the quasigeostrophic regime largely on the $\mathrm{PQG_{DL}}$ model of Bäumer et al. (2023), we have made one important adjustment: the scaling $R_d/c_{\mathrm{pd}} \sim \epsilon$, known as the *Newtonian limit* for dry air (Parkins et al. 2000), was *not* adopted in the derivation of that model. The reason for which we revert to the Newtonian limit in the present work is the incorporation of the fundamental Clausius-Clapeyron relation (CC) into our scaling procedure, which we will discuss in detail in the following subsection.

a. The Clausius-Clapeyron relation

We recall that CC for an ideal gas reads

$$\frac{d\ln e_s}{dT} = \frac{L(T)}{R_v T^2}, \tag{24}$$

expressing the dependence of the saturation vapor pressure e_s on temperature T. Further recalling that we assumed a *linear* dependence of latent heat on temperature at the outset,

$$L(T) = L_{\mathrm{ref}} - (c_l - c_{\mathrm{pv}})(T - T_{\mathrm{ref}}), \tag{25}$$

with constant heat capacities, (24) can be integrated exactly to yield the formula

$$e_s(T) = e_{s\mathrm{ref}} \left(\frac{T_{\mathrm{ref}}}{T}\right)^{\frac{c_l - c_{\mathrm{pv}}}{R_v}} \exp\left\{\left(\frac{L_{\mathrm{ref}}}{R_v T_{\mathrm{ref}}} + \frac{c_l - c_{\mathrm{pv}}}{R_v}\right)\left(1 - \frac{T_{\mathrm{ref}}}{T}\right)\right\}. \tag{26}$$

As explained in (Klein and Majda 2006), the standard scaling

$$\frac{R_d}{c_{\mathrm{pd}}} = O(1), \tag{27}$$

when combined with reasonable scalings for the moist thermodynamical parameters, causes the saturation vapor pressure to vanish *at all orders* away from the surface in the asymptotics. In brief, this is due to the fact that the leading-order solution for the background temperature stratification in this event leads to an expansion for e_s dominated by a term of the form

$$\exp\left\{-\frac{\lambda}{\epsilon}\left(\frac{\Gamma z}{1-\Gamma z}\right)\right\}, \tag{28}$$

with bounded λ, Γ in the limit $\epsilon \to 0$. This term vanishes faster than any finite power of ϵ, i.e. it is *transcendentally small* in the terminology of singular perturbation theory (Kevorkian and Cole 1996). Therefore, this scaling would imply that any non-negligible amount of moisture crosses the saturation threshold away from the planetary boundary layer, which is clearly at odds with observations.

The Newtonian limit introduced above provides a remedy to this counterintuitive behavior: as we will see in section 5, the background temperature in the resulting regime is *constant* at leading order, removing the exponential sensitivity of the saturation vapor pressure with respect to height. Moreover, the asymptotic models of, e.g., Hittmeir and Klein (2018), which utilize the Newtonian limit, have shown that it leads to realistic approximations to various moist atmospheric flow phenomena. For those reasons, we have decided to proceed with the supplementary distinguished limits listed in Table 3, both of which yield $O(1)$ variations of e_s across the depth of the troposphere.

Now, it only remains to fix the asymptotic magnitude of the saturation vapor pressure. While typical values of e_s in the midlatitudes are significantly lower than in the tropics, the reference value

$$e_{s\mathrm{ref}} = e_s(T_{\mathrm{ref}}) \approx 1704 \text{ Pa} \tag{29}$$

still clearly suggests

$$\frac{e_{s\mathrm{ref}}}{p_{\mathrm{ref}}} = O(\epsilon^2) \tag{30}$$

as the most reasonable choice. This is the same scaling in ϵ that was found appropriate for the tropics in the cited earlier work when working with the value-based regime ($\alpha = 1$). If one wishes to fully retain consistency with similarity theory (regime $\alpha = 0$), however, the scaling $R_d/R_v = \epsilon E$ necessitates raising the asymptotic magnitude of the saturation vapor pressure by one order in ϵ *if*

stronger moist processes in the DL are assumed. Including this alternative, we thus have

$$\frac{e_{s\mathrm{ref}}}{p_{\mathrm{ref}}} = O(\epsilon^{1+\alpha}). \tag{31}$$

b. Moist constituents and phase changes

We now turn to the task of determining appropriate asymptotic rescalings for the terminal fall velocity, the spatiotemporal perturbations in the atmospheric water reservoir and the corresponding conversion terms in the transport eqs. (1e)-(1g). In the friction-dominated Ekman layer, moist processes cannot be present at leading order unless we assume a further increase in their asymptotic strength relative to the DL. This is at odds with both theory and observations and therefore, no discussion of moist constituents in this layer is required.

1) Terminal rainfall velocity

The terminal velocity V_r of raindrops strongly depends on the size that they attain during their passage through the cloud inside of which they originated. In the context of large-scale dynamics, where we indiscriminately put *all* hydrometeors with non-negligible fall speeds in one basket, represented by the mixing ratio q_r, we cannot account for this dependence and, as is customary in asymptotic models, assume a *constant* value of V_r, to be understood as a weighted average of the individual terminal velocities over the size spectrum of a typical cloud in a midlatitude cyclone. As argued in (Bäumer et al. 2023), stratiform precipitation (which is dominant in midlatitude cyclones) tends to be gentler and produces smaller raindrops than convective precipitation - see also, e.g., Niu et al. (2010) for a comparison of raindrop size distributions and fall speeds in convective versus stratiform rain. Therefore, V_r will not exceed a few meters per second on average and the scaling

$$\frac{V_r}{w_{\mathrm{ref}}} = \epsilon^{-1} V_T, \tag{32}$$

with V_T bounded independent of ϵ, suggests itself. Here, we should point out that $V_r/u_{\mathrm{ref}} \sim \epsilon$, while $V_r \sim u_{\mathrm{ref}}$ in the convective cloud towers of Hittmeir and Klein (2018). In a future multiscale regime, one might therefore need to incorporate the dependence of the average fall speed on local atmospheric conditions.

2) Water vapor

Since the saturation mixing ratio of water vapor q_{vs} and the saturation vapor pressure e_s are related by the formula

$$q_{\mathrm{vs}} = \frac{R_d}{R_v}\frac{e_s}{p - e_s}, \tag{33}$$

our considerations in the previous subsection already fix the asymptotic rescaling of the saturation mixing ratio,

$$q_{\mathrm{vs}} = O(\epsilon^2), \tag{34}$$

which remains valid in *both* regimes that we discussed earlier since $\frac{R_d}{R_v} = \epsilon^{1-\alpha}E$ with $E = O(1)$. From the Clausius-Clapeyron relation, we get the formula (26) for the saturation vapor pressure as a function of temperature. The presence of a purely vertical background distribution of temperature (and pressure) consequently implies that q_{vs} only varies in the vertical at leading order. It thus remains to determine appropriate scalings for perturbations about this "moist background". Here, we should keep the following in mind:

1. It is well known that supersaturation (i.e. excess relative humidity) actually attained in our planet's atmosphere tends to be quite small, typically not exceeding 1% (Houze 2014). It would thus appear unreasonable to permit *positive* perturbations of the water vapor mixing ratio comparable to q_{vs} in magnitude.

2. Subsaturation, on the other hand, frequently is substantial: to provide a representative example, surface relative humidities in Germany averaged 78.6% in the time period from 1971-2000 (Razafimaharo et al. 2020). Thus, the assumption of a consistently (almost) saturated troposphere might prove overly restrictive.

In the $\mathrm{PQG_{DL}}$ model of Bäumer et al. (2023), the authors were guided by 2, assuming variations of q_v unrestricted by a moist background. Due to the scaling assumptions of QG theory, however, this necessitated the scaling $q_v \sim q_{\mathrm{vs}} \sim \epsilon^3$ for the bulk troposphere; since this is not realistic close to the surface, it was then envisioned that q_{vs} should increase in asymptotic magnitude as we pass through the DL and the Ekman layer. Unfortunately, it turned out upon closer inspection that such a vertical variability of the saturation mixing ratio would not be derivable from Clausius-Clapeyron without changing our approach to the vertical layering of the atmosphere altogether.

This, while theoretically viable, would force us to rebuild our distinguished limit and would further make comparisons to previously derived models difficult - in short, it would be rather impractical. Ultimately, we therefore decided to opt for a different approach for the time being, keeping the scaling (34) for the saturation mixing ratio throughout. For the perturbations

$$\tilde{q}_v := q_v - q_{\mathrm{vs}}, \tag{35}$$

we based our decision on the following observations:

1. Since we are interested in phenomena that are nontrivially influenced by moist processes (primarily latent heating and cooling), transport of water vapor needs to feed into the transport of potential temperature in Eq. (1d), that is, it needs to enter the asymptotic expansion scheme for this equation at the same order.

2. Phenomenologically, the primary mechanism that has been identified as responsible for the production of liquid water on the synoptic scale is *warm frontal lifting* (Houze 2014), where moist air is transported over long distances on a gentle upward slope, producing clouds by continually lifting air parcels just above their lifting condensation levels. Therefore, the corresponding transport operator for water vapor should incorporate *both* horizontal and vertical advection at leading order (in the regime for the bulk troposphere).

In conclusion, recalling the respective strengths of potential temperature perturbations in QG and DL, it can be straightforwardly deduced that the only scaling in agreement with both of the above is

$$\tilde{q}_v^{\mathrm{QG}} = O(\epsilon^3) \text{ and} \tag{36a}$$

$$\tilde{q}_v^{\mathrm{DL}} = O(\epsilon^{5/2}). \tag{36b}$$

3) Cloud liquid water

In asymptotic models involving clouds and precipitation, the mixing ratio of cloud water is commonly scaled as a perturbation of the total water reservoir of the atmosphere, since the ratio of cloud liquid water content (CLWC) to water vapor content is almost invariably small. This

immediately suggests the scaling

$$q_c^{\mathrm{QG}} = O(\epsilon^3), \tag{37}$$

which is in good agreement with the highest CLWCs typically observed in stratiform clouds (Zhao and Lei 2014; Zhang et al. 2020).

In the diabatic layer, the already established scaling in (36b) seems to imply a progression toward significantly *higher* CLWCs, i.e. $q_c \sim \epsilon^{5/2}$. However, this scaling assumption would correspond to mixing ratios of several g/kg, which is not supported by the observational record. Hence, we stay with the scaling chosen in QG and assume

$$q_c^{\mathrm{DL}} = O(\epsilon^3). \tag{38}$$

This asymptotic rescaling, as we will see in section 5, leads to the transport of cloud water dropping out of the leading-order dynamics in DL. - The *initial formation* of clouds is thus relegated to the middle and upper troposphere in our model.

4) Rain

Stratiform precipitation, which is the dominant form of precipitation in midlatitude cyclones, has markedly different characteristics than convective precipitation (Houze 2014): updrafts are significantly weaker, raindrops grow to smaller sizes and, accordingly, they exhibit slower average fall speeds (as already discussed above). Furthermore, the percentage of cloud droplets that grow to precipitable size is greatly diminished relative to the situation in convective cells or mesoscale convective systems.

Thus, the asymptotic magnitude of the rain water mixing ratio will certainly need to be smaller than that usually assumed in reduced models on convective and mesoscales (Klein and Majda 2006; Hittmeir and Klein 2018). In (Bäumer et al. 2023), it was already argued that

$$q_r^{\mathrm{QG}} = O(\epsilon^4), \tag{39}$$

which looks prohibitively small at first glance, in fact constitutes the "proper" scaling in the context of our target model. Other than conjectured in that work, however, it turned out that the magnitude

of q_r needs to remain the same in the diabatic layer, i.e.

$$q_r^{\mathrm{DL}} = O(\epsilon^4). \tag{40}$$

This can be understood as follows: while the mixing ratio of rain in the DL remains comparable to that higher up in the troposphere, its *change at leading order*, e.g., by evaporation below cloud base, which occurs over an asymptotically shorter vertical distance, is sufficient to contribute to the stronger thermodynamical perturbations present in DL.

Remark: Even though we scaled the rain water mixing ratio as $O(\epsilon^4)$, this should *not* be taken to be representative of synoptic-scale mean rainfall rates in the midlatitudes. Rather, it represents the rainfall rate that is *directly due to synoptic-scale processes,* i.e., the synoptic precipitation regions arising from warm frontal lifting. As can be seen in Table 5 of Austin and Houze (1972), this rate is actually quite small, in the range of $\sim 0.5 - 1$mm/h, with embedded mesoscale precipitation areas contributing a much higher amount of rain. One should also keep in mind that the magnitudes actually attained by the moist constituents are determined by the evolution of a nonlinear system in time - our scaling choices first and foremost express the assumption that interactions between all of the moisture species are present in the reduced model.

5) Phase changes

First looking at the PQG regime, we point out that our asymptotic rescalings, except for that of the saturation mixing ratio, agree with those of Bäumer et al. (2023). Thus, one might already expect that the scalings for the bulk microphysics closures obtained therein carry over to the present regime. This is in fact the case, but here, we argue for them from a more general point of view:

The Kessler-style bulk microphysics closures in (2e)-(2h) have already been successfully incorporated into models for moist convection (Klein and Majda 2006; Hittmeir and Klein 2018). When constructing a model for moist *large-scale* flow, the corresponding closures for condensation, evaporation etc. (possibly excepting autoconversion) should therefore be interpreted as large-scale averages over the smaller-scale perturbations at the appropriate order, even though we do not explicitly construct a multiscale model in this specific instance. In particular, while we will use the Kessler-type scheme indicated in (2e)-(2h) in the PQG regime, the (scaled) rate constants appearing therein should *not* be identified with those in the original equations. Rather, one should

imagine that we consider said large-scale averages and, purely for simplicity, re-parameterize them in a form fully analogous to the original scheme. Keeping this in mind, we now state the central assumption: *all phase transitions are present in the asymptotic expansion at leading order* (as in the $\mathrm{PQG}_{\mathrm{DL}}$-model of Bäumer et al. (2023)).

As for the scaling in the DL, the lack of leading-order transport of cloud water due to (38) implies that the autoconversion term S_{ac} should likewise drop out of the reduced model, as well as the collection term S_{cr}. Due to the assumption of stronger variability in relative humidity expressed in (36b), Eq. (1f) therefore reduces to the constraint that no condensation occurs at leading order. We will thoroughly explore the consequences of this systematic reduction in section 5.

c. Closures for friction and turbulent mixing

The impact of turbulent mixing on large-scale atmospheric flow, specifically the reduced versions of Eqs. (1d)-(1g), certainly is significant. Unfortunately, due to the breakdown of scale separation in turbulent flow (Klein 2010), such effects cannot be described with the tool chest of asymptotic analysis on multiple scales, and we therefore resort to generic closures in the form of Fickian diffusion. As far as the relative strengths of these terms are concerned, we will proceed purely pragmatically, assuming that they enter the asymptotic expansion at the same order as the corresponding transport terms of the form $D_t(\cdot)$.

d. Scaled governing equations

Nondimensionalizing the governing equations and implementing the distinguished limits laid out above, we arrive at

$$D_t\mathbf{u} + \frac{1}{\epsilon} f\mathbf{k}\times\mathbf{u} + \frac{1}{\epsilon^3}\frac{1}{\rho}\boldsymbol{\nabla}_{\|} p = \epsilon^3 \frac{\rho_d}{\rho} q_r V_r \partial_z \mathbf{u} + \mathcal{D}_{\mathbf{u}}, \tag{41a}$$

$$D_t w + \frac{1}{\epsilon^5}\frac{1}{\rho}\partial_z p = -\frac{1}{\epsilon^5} + \epsilon^3 \frac{\rho_d}{\rho} q_r V_r \partial_z w + \mathcal{D}_w, \tag{41b}$$

$$\partial_t \rho_d + \nabla_{\|}\cdot(\rho_d \mathbf{u}) + \partial_z(\rho_d w) = 0, \tag{41c}$$

$$C_\epsilon D_t \ln\theta + \epsilon^3 \Sigma_\epsilon D_t \ln p + \epsilon \frac{L\phi_\epsilon}{T} D_t q_v = \epsilon^2 k_l V_T q_r (\partial_z \ln\theta + \epsilon\Gamma\partial_z \ln p) + Q + \mathcal{D}_\theta, \tag{41d}$$

$$D_t q_v = S_{\text{ev}} - S_{\text{cd}} + \mathcal{D}_v, \tag{41e}$$

$$D_t q_c = S_{\text{cd}} - S_{\text{cr}} - S_{\text{ac}} + \mathcal{D}_c, \tag{41f}$$

$$D_t q_r - \frac{1}{\epsilon}\frac{1}{\rho_d}\partial_z(\rho_d V_r q_r) = \frac{1}{\epsilon}\left[S_{\text{cr}} + S_{\text{ac}} - S_{\text{ev}}\right] + \mathcal{D}_r, \tag{41g}$$

where

$$\rho = \rho_d(1 + \epsilon^2(q_v + \epsilon q_c + \epsilon^2 q_r)), \tag{42a}$$

$$p = \rho_d T\left(1 + \epsilon^{1+\alpha}\frac{q_v}{E}\right), \tag{42b}$$

$$T = \theta p^{\epsilon\Gamma} \equiv \theta\pi, \tag{42c}$$

$$C_\epsilon = 1 + \epsilon^{1+\alpha} k_v q_v + \epsilon^2(k_l(q_c + \epsilon q_r)), \tag{42d}$$

$$S_{\text{ev}} = \bar{C}_{\text{ev}}\frac{p}{\rho}(q_{\text{vs}} - q_v)^+ q_r, \tag{42e}$$

$$S_{\text{cd}} = \bar{C}_{\text{cn}}(q_v - q_{\text{vs}})^+ q_{\text{cn}} + \bar{C}_{\text{cd}}(q_v - q_{\text{vs}}) q_c, \tag{42f}$$

$$S_{\text{ac}} = \bar{C}_{\text{ac}}(q_c - q_{\text{ac}})^+, \tag{42g}$$

$$S_{\text{cr}} = \bar{C}_{\text{cr}} q_c q_r, \tag{42h}$$

$$\Sigma_\epsilon = \epsilon^\alpha \kappa_v q_v + \Gamma k_l(q_c + \epsilon q_r), \tag{42i}$$

$$\phi_\epsilon = 1 - \frac{k_l - \epsilon^\alpha k_v}{L}(T - 1). \tag{42j}$$

Notice the bars in (42e)-(42h), which serve as reminders that the constants $\bar{C}_\star$ are not necessarily the same as those in the original system; the prefactor $1/\epsilon$ in (41g) will raise the corresponding

leading-order terms in the equation for q_r to the same order in the asymptotic scheme as those in (41e) and (41f). Both the value-based regime and the formally consistent one are included by the choice of either $\alpha = 1$ or $\alpha = 0$, respectively.

5. Asymptotic expansion and derivation of PQG-DL-Ekman

We now proceed with the derivation of our model equations from a standard formal expansion ansatz, starting with the $\mathrm{PQG_{DL}}$ regime for the bulk flow. We remind the reader that this regime is an *updated* version of the $\mathrm{PQG_{DL}}$ model of Bäumer et al. (2023), with significant departures from the latter in the transport of water vapor and its potential vorticity (PV) formulation. For that reason, we show all important steps of the derivation, skipping only tedious, but elementary calculations. Furthermore, we reemphasize that the assumptions inherent in $\mathrm{PQG_{DL}}$ only hold at tropospheric heights > 3 km, due to the presence of the intermediate diabatic layer. Whenever a comparison to the model of Bäumer et al. (2023) is made, we will denote the latter by $\mathrm{PQG_{DL}^{weak}}$, referring to its lack of a strong moist background.

a. The PQG_{DL} equations

As usual, we begin by expanding all model variables in terms of the asymptotically small parameter ϵ. In parallel to classical QG, we assume purely vertical background profiles for the thermodynamical variables p, ρ, T and θ, respectively, indicating the corresponding terms in the expansion by *single* subscripts. If some background distribution is constant altogether at some given order, this is indicated by a *double* subscript. Finally, perturbation variables with unrestricted dependence on $(t, \mathbf{x}, z)$ carry bracketed superscripts.

For the model variables that also occur in dry air, we thus make the ansatz

$$p = p_0 + \epsilon p_1 + \epsilon^2 p^{(2)} + \epsilon^3 p^{(3)} + o(\epsilon^3), \tag{43a}$$

$$\pi = \pi_0 + \epsilon \pi_1 + \epsilon^2 \pi_2 + \epsilon^3 \pi^{(3)} + o(\epsilon^3), \tag{43b}$$

$$\rho = \rho_0 + \epsilon \rho_1 + \epsilon^2 \rho^{(2)} + o(\epsilon^2), \tag{43c}$$

$$\theta = \theta_{00} + \epsilon \theta_1 + \epsilon^2 \theta^{(2)} + o(\epsilon^2), \tag{43d}$$

$$T = T_{00} + \epsilon T_1 + \epsilon^2 T^{(2)} + o(\epsilon^2), \tag{43e}$$

$$\mathbf{u} = \mathbf{u}^{(0)} + \epsilon \mathbf{u}^{(1)} + o(\epsilon), \tag{43f}$$

$$w = w^{(0)} + \epsilon w^{(1)} + o(\epsilon), \tag{43g}$$

where the constants T_{00}, θ_{00} are not introduced ad hoc, but rather a consequence of the Newtonian limit (Klein and Majda 2006; Hittmeir and Klein 2018). The latter also implies that spatiotemporal perturbations in the expansion of the Exner pressure π only start to come into play at third order, even though dynamical pressure perturbations are $O(\epsilon^2)$.

As for the moist constituents, we recall (34) and (36a), which translate to the ansatz

$$q_v = q_{\mathrm{vs}0} + \epsilon q_v^{(1)} + o(\epsilon). \tag{44}$$

Here, $q_{\mathrm{vs}0}$ is the leading-order term in the asymptotic expansion of the saturation mixing ratio, which can readily be obtained from (26) and (33) in the form

$$q_{\mathrm{vs}0}(z) = E \frac{e_{s0}(z)}{p_0(z)} = E e_{s_{ref}} \frac{\exp\{LAT_1(z)\}}{p_0(z)}. \tag{45}$$

Saturation in this ansatz thus is equivalent to

$$q_v^{(1)} > q_{\mathrm{vs}}^{(1)}, \tag{46}$$

with the first-order correction $q_{\mathrm{vs}}^{(1)}$ to the leading-order saturation mixing ratio. This correction depends on the temperature perturbation $T^{(2)}$ and thus is *not* a given quantity, nor part of the static background. We will show the exact form of this dependence when deriving the reduced moisture balances later in this section.

Remark: The presence of the moist background profile q_{vs0} obviously restricts the applicability of our model to atmospheric regions with a uniformly large supply of water vapor, a limitation the model shares with the original PQG equations of Smith and Stechmann (2017). It should be possible to overcome this restriction by introducing a *transition* or *internal layer* (in the sense of singular perturbation theory) at the interface separating dry and moist regions, with dry regions obeying classical QG. This is an endeavor that we plan to pursue in future work.

The liquid water species q_c and q_r expand as

$$q_c = q_c^{(0)} + o(1), \tag{47a}$$

$$q_r = q_r^{(0)} + o(1), \tag{47b}$$

in accordance with our heuristic scaling assumptions from subsection 4.2.

Now, inserting the ansatz (43)-(47) into the scaled governing equations and collecting terms of equal order in ϵ, we can deduce:

(i) Horizontal momentum and mass balances: Since friction does not *directly* impact the bulk flow, i.e. $\mathcal{D}_{\mathbf{u}} \equiv 0$ outside the Ekman layer, the leading-order contributions to eqs. (41a) and (41c) are formally equivalent to those in the model for dry air, except for the pressure perturbation $p^{(2)}$, which depends on the moist background distribution via (42b). We therefore obtain geostrophic balance,

$$f_0 \mathbf{k} \times \mathbf{u}^{(0)} = -\frac{1}{\rho_0} \boldsymbol{\nabla}_{\parallel} p^{(2)}, \tag{48}$$

from the horizontal momentum Eq. (41a) and incompressibility of the horizontal geostrophic velocity,

$$\nabla_{\parallel} \cdot \mathbf{u}^{(0)} = 0, \tag{49}$$

as an immediate consequence. By a standard argument, evaluation of the continuity equation at leading order then yields the constraint

$$w^{(0)} \equiv 0, \tag{50}$$

also characteristic of QG theory. At next order, we get

$$\nabla_{\parallel} \cdot \mathbf{u}^{(1)} + \frac{1}{\rho_0} \partial_z (\rho_0 w^{(1)}) = 0, \tag{51}$$

which is an *anelastic constraint.*

In the horizontal momentum equation, the $O(\epsilon)$ contributions read

$$D_t^{(0)}\mathbf{u}^{(0)} + \beta y\mathbf{k}\times\mathbf{u}^{(0)} + f_0\mathbf{k}\times\mathbf{u}^{(1)} + \frac{1}{\rho_0}\boldsymbol{\nabla}_\parallel p^{(3)} - \frac{\rho_1}{\rho_0^2}\boldsymbol{\nabla}_\parallel p^{(2)} = 0. \tag{52}$$

Taking the vertical component of the curl, this leads to

$$D_t^{(0)}\left[\zeta^{(0)} + \beta y\right] + f_0\nabla_\parallel\cdot\mathbf{u}^{(1)} = D_t^{(0)}\left[\zeta^{(0)} + \beta y\right] - \frac{f_0}{\rho_0}\partial_z(\rho_0 w^{(1)}) = 0, \tag{53}$$

the transport equation for the absolute quasigeostrophic vorticity $\zeta^{(0)} + \beta y$, with the relative vorticity $\zeta^{(0)} := \partial_x v^{(0)} - \partial_y u^{(0)}$. Here, $D_t^{(0)} = \partial_t + (\mathbf{u}^{(0)}\cdot\boldsymbol{\nabla}_\parallel)$ is the material derivative with respect to the geostrophic flow.

(ii) Vertical momentum balance: The vertical momentum Eq. (41b) is dominated by hydrostatic balance at all relevant orders. Here, the regimes $\alpha = 1$ and $\alpha = 0$ lead to markedly different outcomes: first investigating the former, as in the derivation of the $\mathrm{PQG}_{\mathrm{DL}}^{\mathrm{weak}}$ model (Bäumer et al. 2023), asymptotic expansion at the relevant orders and utilization of the ideal gas law (2b) result in the leading-order explicit solution

$$T_{00}\rho_0(z) = p_0(z) = p_0(0)e^{-\frac{z}{T_{00}}} \tag{54}$$

and the relation

$$\partial_z\left(\frac{p_1}{\rho_0}\right) = T_1 = \theta_1 - \pi_1 \tag{55}$$

for the static background. In (54), we included the constant factors $T_{00} = p_0(0) = 1$ for clarity. At next order, we obtain

$$\partial_z\left(\frac{p^{(2)}}{\rho_0}\right) = \theta^{(2)} + \pi_1\theta_1 + \pi_2 + \frac{\rho_1}{\rho_0}T_1 + \left(\frac{1}{E} - 1\right)q_{\mathrm{vs0}} \tag{56}$$

as an expression for the leading-order *buoyancy* perturbation. In order to get to the usual form of this relation, we again proceed as Bäumer et al. (2023), recognizing that all terms on the right-hand

side except for $\theta^{(2)}$ depend on z only - therefore, setting

$$\tilde{\phi} := \frac{p^{(2)}}{\rho_0} - \int_0^z \left[\pi_1 \theta_1 + \pi_2 + \frac{\rho_1}{\rho_0} T_1 + \left(\frac{1}{E} - 1 \right) q_{\mathrm{vs}0} \right] d\zeta, \tag{57}$$

we can write

$$\partial_z \tilde{\phi} = \theta^{(2)} \tag{58}$$

as our buoyancy relation for the adjusted pressure perturbation $\tilde{\phi}$, scaled by the background density. We can also rewrite the geostrophic balance relation (48) as

$$f_0 \mathbf{k} \times \mathbf{u}^{(0)} = -\boldsymbol{\nabla}_{\parallel} \tilde{\phi}, \tag{59}$$

since the horizontal gradient annihilates the added background terms.

In the regime $\alpha = 0$, the first-order correction to the static background reads

$$\partial_z \left(\frac{p_1}{\rho_0} \right) = \theta_1 + \pi_1 + \frac{1}{E} q_{\mathrm{vs}_0}, \tag{60}$$

which reveals a systematically stronger impact of moisture onto buoyancy in this regime. The dynamical buoyancy perturbation now can be written in the form

$$\partial_z \left(\frac{p^{(2)}}{\rho_0} \right) = \theta^{(2)} + \frac{1}{E} q_v^{(1)} + \pi_1 \theta_1 + \pi_2 + \frac{\rho_1}{\rho_0} (\theta_1 - \pi_1) + \left[\frac{1}{E} \left(\frac{\rho_1}{\rho_0} + \theta_1 + \pi_1 \right) - 1 \right] q_{\mathrm{vs}_0}. \tag{61}$$

Due to the appearance of $q_v^{(1)}$ on the right-hand side, we have a clear deviation from the traditional form of the hydrostatic relationship. Defining $\tilde{\phi}$ appropriately to absorb the background contributions, we obtain

$$\partial_z \tilde{\phi} = \theta^{(2)} + \frac{1}{E} q_v^{(1)}. \tag{62}$$

Even though - as previously mentioned - we do not study this regime further in the present article, we would like to point out that there is evidence that the contribution of water vapor to buoyancy fluctuations is considerable at least in the tropics (Yang et al. 2022), which lends credibility to this modified form of the hydrostatic relationship.

(iii) Transport of potential temperature: Recalling (50) and (54), expanding (41d) yields

$$D_t^{(0)}\theta^{(2)} + w^{(1)}\frac{d\theta_1}{dz} + LD_t^{(0)}q_v^{(1)} + Lw^{(1)}\frac{dq_{\mathrm{vs}0}}{dz} = Q^{(0)} + \mathcal{D}_\theta^{(0)}. \tag{63}$$

Introducing the (linearized) equivalent potential temperature

$$\theta_e := \theta + Lq_v, \tag{64}$$

we can equivalently write

$$D_t^{(0)}\theta_e^{(2)} + w^{(1)}\frac{d\theta_{e1}}{dz} = Q^{(0)} + \mathcal{D}_\theta^{(0)}. \tag{65}$$

We remark that, while we do not consider the inclusion of turbulent mixing crucial for the model, it might be necessary for its rigorous mathematical validation, since the thermodynamics encoded in (65) depend on the nonsmooth phase changes in the reduced version of (41e).

(iv) Transport of water vapor: With the scaling assumptions laid out in section 4, we obtain

$$\begin{aligned} D_t^{(0)}q_v^{(1)} + w^{(1)}\frac{dq_{\mathrm{vs}0}}{dz} =& \bar{C}_{\mathrm{ev}}T_{00}\left[q_{\mathrm{vs}}^{(1)} - q_v^{(1)}\right]^+ q_r^{(0)} \\ &- \bar{C}_{\mathrm{cn}}\left[q_v^{(1)} - q_{\mathrm{vs}}^{(1)}\right]^+ q_{\mathrm{cn}}^{(0)} - \bar{C}_{\mathrm{cd}}\left[q_v^{(1)} - q_{\mathrm{vs}}^{(1)}\right] q_c^{(0)} + \mathcal{D}_v^{(0)}, \end{aligned} \tag{66}$$

where the turbulent closure $\mathcal{D}_v^{(0)}$ again might prove helpful in order to prove the general existence of (strong) solutions, as in previous work on moist transport equations with phase changes (Hittmeir et al. 2017, 2020, 2023; Doppler et al. 2024). Remember that q_v and q_{vs} are identical at leading order, which is why the first-order correction $q_{\mathrm{vs}}^{(1)}$ to the saturation mixing ratio shows up on the right-hand side. This quantity can be written in the form

$$E\frac{e_s^{(1)}}{p_0} - E\frac{p_1}{p_0^2}e_{s0}, \tag{67}$$

where

$$e_s^{(1)} = A\left[LT^{(2)} - \left(L + \frac{k_l + (1-\alpha)k_v}{2}\right)T_1^2\right]e_{s0}. \tag{68}$$

Thus, $q_{\mathrm{vs}}^{(1)}$ varies linearly with the unknown $T^{(2)}$ or, equivalently, $\theta^{(2)}$, and the saturation threshold is *unknown* a priori.

(v) Transport of cloud water: Since there is no "background liquid water", the leading-order transport of cloud water is purely horizontal:

$$\begin{aligned} D_t^{(0)} q_c^{(0)} =& \bar{C}_{\mathrm{cn}} \left[q_v^{(1)} - q_{\mathrm{vs}}^{(1)} \right]^+ q_{\mathrm{cn}}^{(0)} + \bar{C}_{\mathrm{cd}} \left[q_v^{(1)} - q_{\mathrm{vs}}^{(1)} \right] q_c^{(0)} \\ & - \bar{C}_{\mathrm{ac}} \left[q_c^{(0)} - q_{\mathrm{ac}}^{(0)} \right]^+ - \bar{C}_{\mathrm{cr}} q_c^{(0)} q_r^{(0)} + \mathcal{D}_c^{(0)}, \end{aligned} \tag{69}$$

where the same remarks as above apply with regard to the sources on the right-hand side.

(vi) Quasi-steady column of rain: From the scaled Eq. (41g), we obtain - as in section 6 of Bäumer et al. (2023) - a *diagnostic* relationship for the mixing ratio of rain at leading order:

$$\begin{aligned} -\frac{1}{\rho_0} \partial_z (\rho_0 V_T q_r^{(0)}) =& \bar{C}_{\mathrm{ac}} \left[q_c^{(0)} - q_{\mathrm{ac}}^{(0)} \right]^+ + \bar{C}_{\mathrm{cr}} q_c^{(0)} q_r^{(0)} \\ & - \bar{C}_{\mathrm{ev}} T_{00} \left[q_{\mathrm{vs}}^{(1)} - q_v^{(1)} \right]^+ q_r^{(0)}. \end{aligned} \tag{70}$$

This equation exhibits a mathematically straightforward, but in this context unusual structure: since it is essentially a first-order ODE that depends on $(t, \mathbf{x})$ only parametrically, the only data that we need to prescribe in order to specify a unique solution is

$$q_r^{(0)}(t, \mathbf{x}, h)$$

at a fixed height h, for all $(t, \mathbf{x})$. The physically sensible choice here is to set the rain water mixing ratio to zero at the top of the layer, since (almost) all precipitation in the earth's atmosphere is generated below the tropopause.

We now present the $\mathrm{PQG_{DL}}$ system in its preliminary form, where $\alpha \in \{0,1\}$ and the latter yields the traditional form of the hydrostatic relationship:

$$f_0 \mathbf{k} \times \mathbf{u}^{(0)} = -\boldsymbol{\nabla}_{\parallel} \tilde{\phi}, \tag{71a}$$

$$\partial_z \tilde{\phi} = \theta^{(2)} + (1-\alpha)\frac{1}{E} q_v^{(1)}, \tag{71b}$$

$$D_t^{(0)} \left[\zeta^{(0)} + \beta y \right] = \frac{f_0}{\rho_0} \partial_z (\rho_0 w_1), \tag{71c}$$

$$D_t^{(0)} \theta_e^{(2)} + w^{(1)} \frac{d\theta_{e1}}{dz} = Q^{(0)} + \mathcal{D}_\theta^{(0)}, \tag{71d}$$

$$D_t^{(0)} q_v^{(1)} + w^{(1)} \frac{dq_{\mathrm{vs0}}}{dz} = S_{\mathrm{ev}}^{(0)} - S_{\mathrm{cd}}^{(0)} + \mathcal{D}_v^{(0)}, \tag{71e}$$

$$D_t^{(0)} q_c^{(0)} = S_{\mathrm{cd}}^{(0)} - S_{\mathrm{ac}}^{(0)} - S_{\mathrm{cr}}^{(0)} + \mathcal{D}_c^{(0)}, \tag{71f}$$

$$-\frac{1}{\rho_0} \partial_z (\rho_0 V_T q_r^{(0)}) = S_{\mathrm{ac}}^{(0)} + S_{\mathrm{cr}}^{(0)} - S_{\mathrm{ev}}^{(0)}, \tag{71g}$$

with

$$q_{\mathrm{vs}}^{(1)} = \left[AL(\theta^{(2)} + \pi_1 \theta_1 + \pi_2) - A(L + (k_l + (1-\alpha)k_v)/2) T_1^2 - \frac{p_1}{p_0} \right] q_{\mathrm{vs0}} \tag{72a}$$

$$S_{\mathrm{ev}}^{(0)} = \bar{C}_{\mathrm{ev}} T_{00} \left[q_{\mathrm{vs}}^{(1)} - q_v^{(1)} \right]^+ q_r^{(0)} \tag{72b}$$

$$S_{\mathrm{cd}}^{(0)} = \bar{C}_{\mathrm{cn}} \left[q_v^{(1)} - q_{\mathrm{vs}}^{(1)} \right]^+ q_{\mathrm{cn}}^{(0)} + \bar{C}_{\mathrm{cd}} \left[q_v^{(1)} - q_{\mathrm{vs}}^{(1)} \right] q_c^{(0)} \tag{72c}$$

$$S_{\mathrm{ac}}^{(0)} = \bar{C}_{\mathrm{ac}} \left[q_c^{(0)} - q_{\mathrm{ac}}^{(0)} \right]^+ \tag{72d}$$

$$S_{\mathrm{cr}}^{(0)} = \bar{C}_{\mathrm{cr}} q_c^{(0)} q_r^{(0)}. \tag{72e}$$

Here, all (subscripted) background terms are given, and the turbulent closures $\mathcal{D}_\star$ can be specified, e.g., as proportional to (horizontal) Laplacians of the respective transported quantities when needed.

Once more analogous to classical QG (and previous investigations of PQG dynamics as in, e.g., (Wetzel et al. 2019)), we aim to reformulate this system based on a suitable notion of *potential vorticity* (PV). This task will be a fair bit more involved than in the dry regime, owing to the presence of the various moisture species and phase changes.

1) Potential vorticity formulation of $\mathrm{PQG_{DL}}$

We recall the *quasigeostrophic potential vorticity,* here indicated by PV for simplicity, and given by

$$\mathrm{PV} = \zeta^{(0)} + \beta y + \frac{f_0}{\rho_0}\partial_z\left(\frac{\rho_0\theta^{(2)}}{d\theta_1/dz}\right). \tag{73}$$

It permits a formulation of classical QG in terms of only one horizontal transport equation,

$$D_t^{(0)}\mathrm{PV} = \frac{f_0}{\rho_0}\partial_z\left(\frac{\rho_0 Q^{(0)}}{d\theta_1/dz}\right), \tag{74}$$

while the pressure perturbation $\tilde{\phi}$ (and consequently $\mathbf{u}^{(0)}$ and $\theta^{(2)}$) can be recovered from the linear Poisson-type equation

$$\frac{1}{f_0}\Delta_\parallel\tilde{\phi} + \frac{f_0}{\rho_0}\partial_z\left(\frac{\rho_0\partial_z\tilde{\phi}}{d\theta_1/dz}\right) = \mathrm{PV} - \beta y, \tag{75}$$

given appropriate boundary conditions. In particular, this reformulation completely eliminates the small QG vertical velocity $w^{(1)}$ from the system, which actively shapes the dynamics solely via the bottom boundary condition. This becomes relevant when we couple QG to a boundary layer, that is, the Ekman layer - we will thoroughly explain the analogous situation in PQG-DL-Ekman in the next two subsections.

Now, we intend to find an analogous formulation for the $\mathrm{PQG_{DL}}$ system (71). Here, we carry out the derivations for the regime $\alpha = 1$ *only,* in order not to overwhelm the reader with equations and since this is the one used throughout the remainder of this paper. We will devote future work to the study of PV formulations for $\alpha = 0$, which can be derived straightforwardly by taking into account the modified buoyancy perturbation. - Returning to the problem at hand, at least two contrasting approaches are viable: in the first, proceeding along similar lines as Smith and Stechmann (2017), we need to determine a suitable notion of PV analogous to the QG potential vorticity. Here, basing PV on the equivalent potential temperature θ_e seems natural, since its evolution equation (71d) mirrors that of θ in dry air. We therefore define PV_e as

$$\mathrm{PV}_e = \zeta^{(0)} + \beta y + \frac{f_0}{\rho_0}\partial_z\left(\frac{\rho_0\theta_e^{(2)}}{d\theta_{e1}/dz}\right). \tag{76}$$

Observing that all equations involved in the derivation of the evolution equation of PV_e are (up to source terms) the same in our model as in the original PQG equations (Smith and Stechmann 2017), we immediately arrive at

$$D_t^{(0)}\mathrm{PV}_e = -\frac{f_0}{d\theta_{e1}/dz}\partial_z \mathbf{u}^{(0)} \cdot \boldsymbol{\nabla}_\parallel \theta_e^{(2)} + \frac{f_0}{\rho_0}\partial_z\left(\frac{\rho_0(Q^{(0)} + \mathcal{D}_\theta^{(0)})}{d\theta_{e1}/dz}\right). \tag{77}$$

The presence of $d\theta_{e1}/dz$ in the denominator indicates that the validity of this formulation requires an *unconditionally stably stratified* atmosphere in the large-scale mean, i.e.

$$\frac{d\theta_{e1}}{dz} > 0 \tag{78}$$

throughout. This condition might seem quite restrictive - however, thanks to the inclusion of the diabatic layer, we only need it to apply at altitudes greater than ~ 3 km, while even neutral stratification can be attained below (Klein et al. 2022). If one wants to preserve the less restrictive condition $d\theta_1/dz > 0$, one can still revert to "dry" PV as a dynamical variable. The alternative formulation resulting from this ansatz is shown after this one. We should remark that, as pointed out to the authors by Sam Stechmann, (78) should still be assumed in any formulation of the model in order to guarantee the validity of QG theory in the first place.

Clearly, due to the incorporation of the moist constituents q_v, q_c and q_r, we need more than one transport equation to fully determine the $\mathrm{PQG_{DL}}$ flow. We would like to not use $q_v^{(1)}$, whose transport equation (71e) depends on $w^{(1)}$, and therefore, again following Smith and Stechmann (2017), introduce an auxiliary moist variable: defining

$$\tilde{M} := \theta_e^{(2)} - \frac{d\theta_{e1}/dz}{dq_{\mathrm{vs0}}/dz} q_v^{(1)} \equiv \theta_e^{(2)} + B(z) q_v^{(1)}, \tag{79}$$

it is straightforward to check that

$$D_t^{(0)}\tilde{M} = B(z)\left[S_{\mathrm{ev}}^{(0)} - S_{\mathrm{cd}}^{(0)} + \mathcal{D}_v^{(0)}\right] + \mathcal{D}_\theta^{(0)} + Q^{(0)}, \tag{80}$$

which does not involve the vertical velocity.

The evolution equation for cloud water (71f) and the diagnostic relation (71g) for rain do not depend on $w^{(1)}$ in the first place, so no reformulation is needed there.

Next, we turn to the moist analogue of the elliptic recovery equation (75) for the pressure perturbation $\tilde{\phi}$. Here, a linear combination of PV_e and the vertical derivative of $\tilde{M}$ does the trick: by direct calculation, one can verify that

$$\frac{1}{f_0}\Delta_{\parallel}\tilde{\phi} + \frac{f_0}{\rho_0}\partial_z\left(\frac{\rho_0}{d\theta_{e1}/dz}\frac{B(z)}{L+B(z)}\partial_z\tilde{\phi}\right) = \mathrm{PV}_e - \frac{f_0}{\rho_0}\partial_z\left(\frac{\rho_0}{d\theta_{e1}/dz}\frac{L}{L+B(z)}\tilde{M}\right) - \beta y, \qquad (81)$$

which, given PV_e and $\tilde{M}$, is a linear elliptic equation for $\tilde{\phi}$. (The term $B(z)$, implicitly defined in (79), will always be positive when (78) holds.)

Remark: Linearity here holds for given *balanced* or low-frequency components of the flow, which in this context means that their respective evolution equations do not incorporate vertical advection; see Wetzel et al. (2019) for a thorough discussion of this concept. The PV formulations of Smith and Stechmann (2017) and Wetzel et al. (2019) are *nonlinear* when only balanced quantities are given. This nonlinearity is, in fact, a consequence of the fast phase transitions that the authors prescribe from the outset. The present full microphysics approach - while more complicated overall - therefore leads to a structurally *simpler* inversion equation for the stream function, that is, the pressure perturbation. In particular, Eq. (81) does not exhibit a jump in the (background) buoyancy frequency, which physically is caused by the passage of air parcels from undersaturated to saturated air. This might be puzzling at first glance, since $d\theta/dz$ and $d\theta_e/dz$ *do* differ at $O(\epsilon)$ also in the present scaling. In the context of QG theory with time resolved, non-singular source terms, however, *vertical motion is too weak to make this jump affect the temperature of an idealized rising or falling air parcel at the same order.* This discontinuity can therefore be expected to come into play only at the level of the dynamical perturbations, which can be seen from the structure of (80) and (81) ($\partial_z\tilde{M}$ will be discontinuous at a horizontally aligned phase interface).

The transition from our full microphysics model to that of Wetzel et al. can formally be achieved by altering our asymptotic scheme to include a prefactor of the form $1/\epsilon^n$ with sufficiently large exponent, n, in the condensation term; in order to clarify the connection between the two approaches, we sketch the corresponding derivation at the end of this subsection.

In conclusion, we obtain

$$D_t^{(0)}\mathrm{PV}_e = -\frac{f_0}{d\theta_{e1}/dz}\partial_z \mathbf{u}^{(0)}\cdot\boldsymbol{\nabla}_{\parallel} L q_v^{(1)} + \frac{f_0}{\rho_0}\partial_z\left(\frac{\rho_0(Q^{(0)}+\mathcal{D}_\theta^{(0)})}{d\theta_{e1}/dz}\right) \tag{82a}$$

$$D_t^{(0)}\tilde{M} = B(z)\left[S_{\mathrm{ev}}^{(0)} - S_{\mathrm{cd}}^{(0)} + \mathcal{D}_v^{(0)}\right] + \mathcal{D}_\theta^{(0)} + Q^{(0)} \tag{82b}$$

$$D_t^{(0)} q_c^{(0)} = S_{\mathrm{cd}}^{(0)} - S_{\mathrm{ac}}^{(0)} - S_{\mathrm{cr}}^{(0)} + \mathcal{D}_c^{(0)} \tag{82c}$$

$$-\frac{1}{\rho_0}\partial_z(\rho_0 V_T q_r^{(0)}) = S_{\mathrm{ac}}^{(0)} + S_{\mathrm{cr}}^{(0)} - S_{\mathrm{ev}}^{(0)} \tag{82d}$$

$$\frac{1}{f_0}\Delta_{\parallel}\tilde{\phi} + \frac{f_0}{\rho_0}\partial_z\left(\frac{\rho_0}{d\theta_{e1}/dz}\frac{B(z)}{L+B(z)}\partial_z\tilde{\phi}\right) = \mathrm{PV}_e - \frac{f_0}{\rho_0}\partial_z\left(\frac{\rho_0}{d\theta_{e1}/dz}\frac{L}{L+B(z)}\tilde{M}\right) - \beta y \tag{82e}$$

$$f_0\mathbf{k}\times\mathbf{u}^{(0)} = -\boldsymbol{\nabla}_{\parallel}\tilde{\phi} \tag{82f}$$

$$\theta^{(2)} = \partial_z\tilde{\phi} \tag{82g}$$

as the first PV formulation of $\mathrm{PQG_{DL}}$, supplemented by the relations

$$q_{\mathrm{vs}}^{(1)} = \left[AL(\theta^{(2)} + \pi_1\theta_1 + \pi_2) - A(L + k_l/2)T_1^2 - \frac{p_1}{p_0}\right] q_{\mathrm{vs0}} \tag{83a}$$

$$q_v^{(1)} = \frac{1}{L+B(z)}(\tilde{M} - \theta^{(2)}) \tag{83b}$$

$$S_{\mathrm{ev}}^{(0)} = \bar{C}_{\mathrm{ev}} T_{00}\left[q_{\mathrm{vs}}^{(1)} - q_v^{(1)}\right]^+ q_r^{(0)} \tag{83c}$$

$$S_{\mathrm{cd}}^{(0)} = \bar{C}_{\mathrm{cn}}\left[q_v^{(1)} - q_{\mathrm{vs}}^{(1)}\right]^+ q_{\mathrm{cn}}^{(0)} + \bar{C}_{\mathrm{cd}}\left[q_v^{(1)} - q_{\mathrm{vs}}^{(1)}\right] q_c^{(0)} \tag{83d}$$

$$S_{\mathrm{ac}}^{(0)} = \bar{C}_{\mathrm{ac}}\left[q_c^{(0)} - q_{\mathrm{ac}}^{(0)}\right]^+ \tag{83e}$$

$$S_{\mathrm{cr}}^{(0)} = \bar{C}_{\mathrm{cr}} q_c^{(0)} q_r^{(0)} \tag{83f}$$

$$B(z) = -\frac{d\theta_{e1}/dz}{dq_{\mathrm{vs0}}/dz}. \tag{83g}$$

2) An alternative PV formulation

Purely formally, the leading-order thermodynamic equation in $\mathrm{PQG_{DL}}$ can be written in a form equivalent to dry QG with a heat source, the difference of course being that this "source" is not given externally. Therefore, in terms of the classical QG potential vorticity, we can also write this

system in the form

$$D_t^{(0)}\mathrm{PV} = -\frac{f_0}{\rho_0}\partial_z\left(\frac{\rho_0 L\left(S_{\mathrm{ev}}^{(0)} - S_{\mathrm{cd}}^{(0)} + \mathcal{D}_v^{(0)}\right)}{d\theta_1/dz}\right) + \frac{f_0}{\rho_0}\partial_z\left(\frac{\rho_0\left(Q^{(0)} + \mathcal{D}_\theta^{(0)}\right)}{d\theta_1/dz}\right) \tag{84a}$$

$$D_t^{(0)}\tilde{M} = B(z)\left[S_{\mathrm{ev}}^{(0)} - S_{\mathrm{cd}}^{(0)} + \mathcal{D}_v^{(0)}\right] + \mathcal{D}_\theta^{(0)} + Q^{(0)} \tag{84b}$$

$$D_t^{(0)} q_c^{(0)} = S_{\mathrm{cd}}^{(0)} - S_{\mathrm{ac}}^{(0)} - S_{\mathrm{cr}}^{(0)} + \mathcal{D}_c^{(0)} \tag{84c}$$

$$-\frac{1}{\rho_0}\partial_z(\rho_0 V_T q_r^{(0)}) = S_{\mathrm{ac}}^{(0)} + S_{\mathrm{cr}}^{(0)} - S_{\mathrm{ev}}^{(0)} \tag{84d}$$

$$\frac{1}{f_0}\Delta_\parallel\tilde{\phi} + \frac{f_0}{\rho_0}\partial_z\left(\frac{\rho_0}{d\theta_1/dz}\partial_z\tilde{\phi}\right) = \mathrm{PV} - \beta y \tag{84e}$$

$$f_0\mathbf{k}\times\mathbf{u}^{(0)} = -\boldsymbol{\nabla}_\parallel\tilde{\phi} \tag{84f}$$

$$\theta^{(2)} = \partial_z\tilde{\phi}, \tag{84g}$$

where the relations (83) hold as before. This formulation exhibits a discontinuous right-hand side in the PV transport equation (84a), but it has the advantage of representing a natural extension of traditional QG models in which latent heating is incorporated as a source term in the "dry" thermodynamic equation.

3) The fast condensation limit

Let us first clarify the notion of "fast condensation", which corresponds to the following implicit definition of the condensation term:

$$\begin{cases} q_v = q_{\mathrm{vs}}, \quad q_c = q_t - q_{\mathrm{vs}} - q_r & \text{in saturated air} \\ q_v < q_{\mathrm{vs}}, \quad q_c = 0 & \text{in undersaturated air,} \end{cases} \tag{85}$$

where q_t denotes the total water content. This definition effectively reduces the number of prognostic variables by one, since q_c can be calculated explicitly from q_t and q_r at any given time (and q_{vs}, which in our model is a function of the potential temperature perturbation, but often is

assumed to be given as a function of z):

$$q_c = \max\left(q_t - q_{\mathrm{vs}} - q_r, 0\right). \tag{86}$$

By the same token, we have

$$q_v = \min\left(q_{\mathrm{vs}}, q_t - q_r\right). \tag{87}$$

On a formal level, this alternative can be recovered systematically simply by rescaling the respective nucleation and condensation rates appropriately: instead of assuming continuous reparameterization, as described in section 4b, we straightforwardly identify both C_{cn} and C_{cd} as asymptotically fast with respect to the chosen timescale and make the ansatz

$$C_{\mathrm{cn}} t_{\mathrm{ref}} \sim C_{\mathrm{cd}} t_{\mathrm{ref}} \sim \epsilon^{-n}, \tag{88}$$

for some $n \gg 1$. The leading-order balance in the scaled moisture equations then results as

$$S_{\mathrm{cd}}^{(0)} = C_{\mathrm{cn}}(q_v^{(1)} - q_{\mathrm{vs}}^{(1)})^{+} q_{\mathrm{cn}}^{(0)} + C_{\mathrm{cd}}(q_v^{(1)} - q_{\mathrm{vs}}^{(1)}) q_c^{(0)} = 0, \tag{89}$$

which, due to the nonnegativity of $q_c^{(0)}$ and $q_{\mathrm{cn}}^{(0)}$, immediately enforces (85). We thus obtain a formal derivation of the alternative that was prescribed by Wetzel et al. (2019) from the outset. Notice that our model also differs from that of Wetzel and coauthors in the scaling of the terminal fall velocity.

Now, let us sketch how the anelastic PQG equations of Wetzel et al. (2019) can be derived from the leading-order balances on the synoptic timescale. In doing so, we first need to take into consideration the deviating scalings in the cited article: Wetzel et al. assumed a terminal rainfall velocity comparable to the vertical reference velocity,

$$V_r \sim w_{\mathrm{ref}}, \tag{90}$$

and consequently a rain mixing ratio of the same order of magnitude as the overall moisture anomaly,

$$q_r^{\mathrm{QG}} \sim \tilde{q}_v^{\mathrm{QG}}. \tag{91}$$

Finally, Wetzel and coauthors assumed a saturation mixing ratio that was given as a background profile at *all* orders, which simplifies the further treatment. With these scalings in place and proceeding purely formally from a regular asymptotic expansion ansatz, the leading-order equations for the moist thermodynamics read in our notation

$$D_t^{(0)}\theta_e^{(2)} + w^{(1)}\frac{d\theta_{e_1}}{dz} = 0 \tag{92a}$$

$$D_t^{(0)}q_v^{(1)} + w^{(1)}\frac{dq_{\mathrm{vs}_0}}{dz} = S_{\mathrm{ev}}^{(0)} - S_{\mathrm{cd}}^{(n)} \tag{92b}$$

$$D_t^{(0)}q_c^{(0)} = S_{\mathrm{cd}}^{(n)} - S_{\mathrm{ac}}^{(0)} - S_{\mathrm{cr}}^{(0)} \tag{92c}$$

$$D_t^{(0)}q_r^{(0)} - \frac{1}{\rho_0}\partial_z\left(\rho_0 V_T q_r^{(0)}\right) = S_{\mathrm{ac}}^{(0)} + S_{\mathrm{cr}}^{(0)} - S_{\mathrm{ev}}^{(0)}, \tag{92d}$$

where we assumed a non-diffusive regime. Since, upon taking the fast condensation limit, $q_v^{(1)}$ and $q_c(0)$ become functions of $q_t^{(1)} = q_v^{(1)} + q_c^{(0)} + q_r^{(0)}$ and $q_r^{(0)}$, we rewrite (92) accordingly in a reduced form, taking the sum of (92b)-(92d) to obtain an equation for $q_t^{(1)}$:

$$D_t^{(0)}\theta_e^{(2)} + w^{(1)}\frac{d\theta_{e_1}}{dz} = 0 \tag{93a}$$

$$D_t^{(0)}q_t^{(1)} = \frac{1}{\rho_0}\partial_z\left(\rho_0 V_T q_r^{(0)}\right) \tag{93b}$$

$$D_t^{(0)}q_r^{(0)} - \frac{1}{\rho_0}\partial_z\left(\rho_0 V_T q_r^{(0)}\right) = S_{\mathrm{ac}}^{(0)} + S_{\mathrm{cr}}^{(0)} - S_{\mathrm{ev}}^{(0)}. \tag{93c}$$

These equations - together with geostrophic and hydrostatic balances, as well as the QG vorticity equation - form a closed system in the limit $\tau \to \infty$.

Concerning the details of the derivation of a suitable PV formulation, we refer the reader to Wetzel et al. (2019). The key point here is that (87) can be written in the form

$$q_v = H_u(q_t - q_r) + H_s q_{\mathrm{vs}}, \tag{94}$$

where H_u and H_s denote indicator functions of undersaturated and saturated states, respectively; however, when rewriting (93) in terms of balanced quantities, the local saturation state cannot be determined without knowledge of θ, which is part of the *output* of the PV-and-moisture inversion equation. The nonlinearity of said equation (and the appearance of a switch in the buoyancy

frequency therein) can thus be seen as a consequence of the combination of a moist background with fast microphysics.

Remark: The analytical and numerical investigation of piecewise elliptic operators with switches at the phase interface certainly poses numerous challenges. We do want to mention, however, that progress on the analysis front has been made recently: Remond-Tiedrez et al. (2024) have established the well-posedness of weak solutions of the original PQG PV-M inversion equation of Smith and Stechmann (2017).

b. Precipitating DL dynamics

All (P)QG models rely on a stable background stratification of θ or θ_e and small deviations of these variables from their background states of, at most, order $O(\epsilon^2)$. As a consequence, the diabatic heating rates they permit are quite modest, in the range of ~ 3 K/day. As argued by Klein et al. (2022), such heating rates agree well with the synoptic-scale averages found in reanalysis data across most of the free troposphere - see also the references mentioned in the cited work. Near the surface, however, diabatic effects can be seen to significantly exceed the strength that QG scaling implicitly assumes. This observation motivated the introduction of the diabatic layer equations by Klein et al. to extend the classical QG-Ekman model to a triple-deck boundary layer theory in which the layer of intermediate height is both dynamically and thermodynamically active. In the sequel, we show how the "dry" DL equations that incorporate strong diabatic heating only via an external heat source can be systematically augmented by moist (thermo)dynamics, asymptotically matched to the $\mathrm{PQG_{DL}}$ flow just derived in an overlap region.

The characteristic height of the DL can be estimated as $\sim \sqrt{\epsilon} h_{\mathrm{sc}}$, which corresponds to a physical value of about 3 km. Adopting the notation of Klein et al. (2022), we abbreviate $\delta = \sqrt{\epsilon}$ and introduce the stretched layer coordinate $\eta = z/\delta$. This suggests the generic ansatz

$$f^{\mathrm{DL}} = f^{\mathrm{DL}}(t, \mathbf{x}, \eta) = f^{(0/2)}(t, \mathbf{x}, \eta) + \delta f^{(1/2)}(t, \mathbf{x}, \eta) + \dots \tag{95}$$

for all DL model variables. In the original DL equations of Klein et al. (2022), the diabatic layer was characterized by the assumption that potential temperature perturbations could *dynamically change* the lower-level stratification of the troposphere, e.g., toward a neutral state. Mathematically,

this implied an expansion of the (nondimensional) form

$$\theta^{\mathrm{DL}} = 1 + \delta^2\theta_1(0) + \delta^3\theta^{(3/2)} + o(\delta^3), \tag{96}$$

with $\theta^{(3/2)} = \theta^{(3/2)}(t, \mathbf{x}, \eta)$.

As we have seen in the derivation of $\mathrm{PQG_{DL}}$, the equivalent potential temperature $\theta_e = \theta + Lq_v$ plays a role in the moist dynamics that is largely analogous to that of θ in the dry regime. Therefore, it seems plausible that θ_e should expand in the same fashion in a moist DL regime, and this is compatible with the scaling assumption on $\tilde{q}_v^{\mathrm{DL}}$ expressed in (36b).

We thus state the formal expansion ansatz for the precipitating DL (PDL) dynamics without further ado:

$$p^{\mathrm{DL}} = p_{0/2} + \delta p_{1/2} + \delta^2 p_{2/2} + \delta^3 p_{3/2} + \delta^4 p^{(4/2)} + \delta^5 p^{(5/2)} + o(\delta^5), \tag{97a}$$

$$\rho^{\mathrm{DL}} = \rho_{0/2} + \delta\rho_{1/2} + \delta^2\rho_{2/2} + \delta^3\rho^{(3/2)} + o(\delta^3), \tag{97b}$$

$$\theta^{\mathrm{DL}} = 1 + \delta^2\theta_{2/2} + \delta^3\theta^{(3/2)} + o(\delta^3), \tag{97c}$$

$$T^{\mathrm{DL}} = 1 + \delta^2 T_{2/2} + \delta^3 T^{(3/2)} + o(\delta^3), \tag{97d}$$

$$\mathbf{u}^{\mathrm{DL}} = \mathbf{u}^{(0/2)} + \delta\mathbf{u}^{(1/2)} + o(\delta), \tag{97e}$$

$$w^{\mathrm{DL}} = w^{(0/2)} + \delta w^{(1/2)} + \delta^2 w^{(2/2)} + o(\delta^2), \tag{97f}$$

$$q_v^{\mathrm{DL}} = q_{\mathrm{vs}0/2} + \delta q_v^{(1/2)} + o(\delta), \tag{97g}$$

$$q_c^{\mathrm{DL}} = q_c^{(0/2)} + o(1), \tag{97h}$$

$$q_r^{\mathrm{DL}} = q_r^{(0/2)} + o(1). \tag{97i}$$

Here, we have omitted terms in the expansions of the temperature variables that can easily be shown to vanish by preliminary matching considerations. The ansatz (97) can now be inserted into (41), where we only need to rewrite any vertical derivatives in terms of η:

(i) Horizontal momentum and mass balances: As in the "dry" DL equations of Klein et al. (2022), geostrophic balance is preserved in the diabatic layer at all relevant orders. We obtain

$$f_0\mathbf{k}\times\mathbf{u}^{(0/2)} = -\boldsymbol{\nabla}_{\parallel}p^{(4/2)} \tag{98}$$

and

$$f_0 \mathbf{k} \times \mathbf{u}^{(1/2)} = -\boldsymbol{\nabla}_\parallel p^{(5/2)}, \tag{99}$$

by inserting the expansion ansatz (97) into the horizontal momentum Eq. (41a).

Evaluation of the continuity equation at the relevant orders provides constraints on the vertical velocity: again following Klein et al. (2022), we get

$$w^{(0/2)} = w^{(1/2)} = 0 \tag{100}$$

and

$$\partial_\eta w^{(2/2)} = 0, \tag{101}$$

i.e., a vertical velocity that is imprinted on (P)DL by the bulk flow and stays constant throughout the layer:

$$w^{(2/2)} = w^{(2/2)}(t, \mathbf{x}) = w^{(1)}(t, \mathbf{x}, 0). \tag{102}$$

(ii) Vertical momentum balance: Treating the regime $\alpha = 1$ first, the expansion of the static background (up to $p_{3/2}$) is still identical to that of the dry DL regime, and of no particular interest. At the level of the perturbation, a closer look is warranted:

$$\partial_\eta p^{(4/2)} = -\rho^{(3/2)} = \theta^{(3/2)} - p_{3/2} - (\Gamma + \theta_1(0))\,\eta \tag{103}$$

again suggests the introduction of an adjusted pressure perturbation in order to avoid unnecessary clutter:

$$\tilde{\phi}^{\mathrm{DL}} := p^{(4/2)} + \int_0^\eta \left(p_{3/2} + (\Gamma + \theta_1(0))\,\eta'\right) d\eta'. \tag{104}$$

We can now write

$$f_0 \mathbf{k} \times \mathbf{u}^{(0/2)} = -\boldsymbol{\nabla}_\parallel \tilde{\phi}^{\mathrm{DL}}, \tag{105a}$$

$$\partial_\eta \tilde{\phi}^{\mathrm{DL}} = \theta^{(3/2)} \tag{105b}$$

for the geostrophic and hydrostatic balances in PDL.

When $\alpha = 0$, as in $\mathrm{PQG_{DL}}$, moisture already contributes to the static background (not shown); at the level of dynamical perturbations, the same steps as in previous derivations then yield

$$\partial_\eta \tilde{\phi}^{\mathrm{DL}} = \theta^{(3/2)} + \frac{1}{E} q_v^{(1/2)}. \tag{106}$$

(iii) Transport of potential temperature: Here, before we derive the reduced equation, written in terms of the equivalent potential temperature θ_e, we need to make clear the expansion of the saturation mixing ratio in the diabatic layer: systematic expansion of (33) and (26) yields

$$q_{\mathrm{vs}0/2} = E e_{s_{00}} = E e^{LA\theta_1(0)} \tag{107}$$

and

$$q_{\mathrm{vs}}^{(1/2)} = ELA e_{s_{00}} T^{(3/2)} + E e_{s_{00}} \eta; \tag{108}$$

the static moist background is thus *constant* in the precipitating DL, while the first-order correction that determines the local saturation threshold again depends on the temperature perturbation and consequently is part of the *output* of the PDL system.

Due to the constancy of $q_{\mathrm{vs}0/2}$, vertical advection drops out of the leading-order balance and the reduced version of (41d) now reads

$$(\partial_t + \mathbf{u}^{(0/2)} \cdot \nabla_\parallel)\theta_e^{(3/2)} \equiv D_t^{(0/2)} \theta_e^{(3/2)} = Q^{(0/2)} + \mathcal{D}_\theta^{(0/2)}, \tag{109}$$

where any heat sources that one might consider beyond latent heating resp. cooling are now permitted to attain (dimensional) rates

$$Q^{\mathrm{DL}} \sim \frac{\delta^3 T_{\mathrm{ref}}}{t_{\mathrm{ref}}} \approx 10 \text{ K/day}. \tag{110}$$

(iv) Moist constituents: In determining the evolution of the moisture species q_v^{DL}, q_c^{DL} and q_r^{DL}, we first need to resolve one crucial issue: by our scaling assumptions, the evolution equation for cloud water reduces to the constraint

$$S_{\mathrm{cd}}^{(0/2)} = \bar{C}_{\mathrm{cn}} \left[q_v^{(1/2)} - q_{\mathrm{vs}}^{(1/2)} \right]^+ q_{\mathrm{cn}}^{(0/2)} + \bar{C}_{\mathrm{cd}} \left[q_v^{(1/2)} - q_{\mathrm{vs}}^{(1/2)} \right] q_c^{(0/2)} = 0, \tag{111}$$

which leads to the alternative

$$\begin{cases} q_v^{(1/2)} = q_{\mathrm{vs}}^{(1/2)} & \text{in saturated air} \\ q_c^{(0/2)} = 0 & \text{in undersaturated air.} \end{cases} \tag{112}$$

Since we have not imposed any restrictions on the generation of leading-order cloud water in $\mathrm{PQG}_{\mathrm{DL}}$, this constraint will necessitate additional conditions on the initial data for water vapor perturbations in the DL to guarantee matching to the bulk flow. First, let us discuss the saturated case:

Since we require $q_v^{(1/2)} = q_{\mathrm{vs}}^{(1/2)}$ in saturated regions, the initial data for water vapor (and potential temperature) need to be chosen such that

$$q_v^{(1/2)}|_{t=0} \leq q_{\mathrm{vs}}^{(1/2)}|_{t=0} \tag{113}$$

everywhere. Due to the structure of the (independently derived) Eqs. (115d) and (115c) (see below), this constraint will then be obeyed for all times, as long as we choose the heat source $Q^{(0/2)}$ such that no (leading-order) external cooling is applied to saturated air parcels.

In the respective balances for q_v and q_r, only the evaporation term survives at leading order. Additionally, the vertical velocity drops out of (41e), since the saturation mixing ratio becomes constant at leading order in the DL, and the resulting moisture dynamics in PDL read

$$D_t^{(0/2)} q_v^{(1/2)} = S_{\mathrm{ev}}^{(0/2)} + \mathcal{D}_v^{(0/2)}, \tag{114a}$$

$$S_{\mathrm{cd}}^{(0/2)} = 0, \tag{114b}$$

$$-\partial_\eta (V_T q_r^{(0/2)}) = -S_{\mathrm{ev}}^{(0/2)}. \tag{114c}$$

We can now state the complete, closed set of equations for $\alpha \in \{0, 1\}$,

$$f_0 \mathbf{k} \times \mathbf{u}^{(0/2)} = -\boldsymbol{\nabla}_{\parallel} \tilde{\phi}^{\mathrm{DL}} \tag{115a}$$

$$\partial_\eta \tilde{\phi}^{\mathrm{DL}} = \theta^{(3/2)} + (1-\alpha)\frac{1}{E} q_v^{(1/2)} \tag{115b}$$

$$D_t^{(0/2)} \theta_e^{(3/2)} = Q^{(0/2)} + \mathcal{D}_\theta^{(0/2)} \tag{115c}$$

$$D_t^{(0/2)} q_v^{(1/2)} = S_{\mathrm{ev}}^{(0/2)} + \mathcal{D}_v^{(0/2)} \tag{115d}$$

$$S_{\mathrm{cd}}^{(0/2)} = 0 \tag{115e}$$

$$-\partial_\eta (V_T q_r^{(0/2)}) = -S_{\mathrm{ev}}^{(0/2)}, \tag{115f}$$

with the supplementary relations

$$\theta^{(3/2)} = \theta_e^{(3/2)} - L q_v^{(1/2)}, \tag{116a}$$

$$q_{\mathrm{vs}}^{(1/2)} = E e^{AL\theta_1(0)} \left[AL\theta^{(3/2)} - (AL\Gamma - 1)\eta \right], \tag{116b}$$

$$S_{\mathrm{cd}}^{(0/2)} = = \bar{C}_{\mathrm{cn}} \left[q_v^{(1/2)} - q_{\mathrm{vs}}^{(1/2)} \right]^+ q_{\mathrm{cn}}^{(0/2)} + \bar{C}_{\mathrm{cd}} \left[q_v^{(1/2)} - q_{\mathrm{vs}}^{(1/2)} \right] q_c^{(0/2)}, \tag{116c}$$

$$S_{\mathrm{ev}}^{(0/2)} = \bar{C}_{\mathrm{ev}} T_{00} (q_{\mathrm{vs}}^{(1/2)} - q_v^{(1/2)})^+ q_r^{(0/2)}. \tag{116d}$$

These are the *precipitating DL equations.*

To clarify how rain influences the large-scale flow in this system, let us ignore additional heat sources and turbulent mixing for the moment and substitute the sum of (115d) and (115f) in the temperature equation (115c), which yields

$$D_t^{(0/2)} \theta^{(3/2)} = -L \partial_\eta (V_T q_r^{(0/2)}). \tag{117}$$

Latent heating (cooling) in the moist, precipitating DL regime is therefore *directly proportional to the downward change of the rainfall mixing ratio,* as in section 6 of Smith and Stechmann (2017). However, the internal structure of the moisture dynamics is markedly different in our regime, which is only meant to hold at lower tropospheric levels anyways.

1) Matching to the $\mathrm{PQG_{DL}}$ flow

In the original DL equations of Klein et al. (2022), the crucial condition for matching to the QG flow could be formulated in terms of the pressure difference over the depth of the diabatic layer. Since this condition - except for minor differences in notation - is formally unchanged in PDL for $\alpha = 1$, we only state the result, referring the interested reader to Klein et al. (2022) for a detailed derivation: it must hold

$$\left| \int_0^\infty \left(\theta^{(3/2)} - \left. \frac{d\theta_1}{dz} \right|_{z=0} \eta' \right) d\eta' \right| < \infty, \tag{118}$$

which is equivalent to the condition that $\theta^{(3/2)}$ approaches its limiting expression sufficiently fast, at a rate faster than $1/\eta$. This will certainly hold if it does so initially *and* all diabatic heating terms vanish at the same rate. In the following, we once again focus on the value-based regime - however, the conditions derived here can easily be seen to be sufficient when $\alpha = 0$ as well.

Clearly, the validity of (118) in PDL depends on the evolution of the moist constituents, and the logical next step is to derive appropriate matching conditions for $q_v^{(1/2)}$ and $q_r^{(0/2)}$. Observing that the strength of (negative) latent heating $LD_t^{(0/2)} q_v^{(1/2)}$ in (115c) is determined by evaporation $S_{\mathrm{ev}}^{(0/2)}$ in undersaturated air, while no latent heating is felt at leading order in saturated air, the matching condition (118) will certainly be fulfilled if

$$q_{\mathrm{vs}}^{(1/2)} - q_v^{(1/2)} = o\left(\frac{1}{\eta}\right) \quad \text{as } \eta \to \infty, \tag{119}$$

i.e., if the limit is achieved at a rate faster than $1/\eta$. This condition *will* hold if it does so initially, since no additional sources of moisture appear in (115d) (turbulent mixing only redistributes the transported quantity). To be more precise, we observe that, in the source-free non-diffusive case, (108) implies

$$D_t^{(0/2)} q_{\mathrm{vs}}^{(1/2)} = ALEe_{s_{00}} D_t^{(0/2)} \theta^{(3/2)}, \tag{120}$$

which combined with (115c) yields

$$D_t^{(0/2)} \left[q_{\mathrm{vs}}^{(1/2)} - q_v^{(1/2)} \right] = -\left(AL^2 Ee_{s_{00}} + 1 \right) D_t^{(0/2)} q_v^{(1/2)}, \tag{121}$$

which by (115d) is equivalent to

$$D_t^{(0/2)}\left[q_{\mathrm{vs}}^{(1/2)}-q_v^{(1/2)}\right]=-\left(AL^2Ee_{s_{00}}+1\right)\bar{C}_{\mathrm{ev}}q_r^{(0/2)}\left(q_{\mathrm{vs}}^{(1/2)}-q_v^{(1/2)}\right). \tag{122}$$

Thus, subsaturation can only decrease along (horizontal) particle trajectories. The addition of external heat sources *can* compensate for this, but the behavior for $\eta \gg 1$ will be unaffected as long as these source terms decay at the appropriate rate.

Now, we check the necessary conditions for matching of the moisture species themselves. To that end, first recall the expansion of q_v in the bulk layer:

$$q_v^{\mathrm{QG}}=q_{\mathrm{vs}0}+\epsilon q_v^{(1)}+o(\epsilon); \tag{123}$$

in PDL, we assumed stronger spatiotemporal variations of atmospheric water, translating to

$$q_v^{\mathrm{DL}}=q_{\mathrm{vs}0/2}+\delta q_v^{(1/2)}+o(\delta). \tag{124}$$

Taylor expansion of (123) for $z \ll 1$ and substitution of $z=\delta\eta$ yield

$$q_v^{\mathrm{QG}}(t,\mathbf{x},\delta\eta)=q_{\mathrm{vs}0}(0)+\delta\left.\frac{dq_{\mathrm{vs}0}}{dz}\right|_{z=0}\eta+o(\delta), \tag{125}$$

which must agree with the corresponding terms in (124) in the limit $\eta \to \infty$. Thus, matching the water vapor mixing ratio at leading order is equivalent to requiring

$$q_v^{(1/2)}-\left.\frac{dq_{\mathrm{vs}0}}{dz}\right|_{z=0}\eta=o\left(\frac{1}{\eta}\right)\quad \text{as } \eta\to\infty\,. \tag{126}$$

However, we already stated (119) as a necessary condition. Next, recall that

$$\begin{aligned} q_{\mathrm{vs}}^{(1/2)}=e^{LA\theta_1(0)}\left[ELAT^{(3/2)}+E\eta\right]&=e^{LA\theta_1(0)}\left[ELA\theta^{(3/2)}-E(LA\Gamma-1)\eta\right]\\ &\sim e^{LA\theta_1(0)}E\left[LA\theta_1'(0)-\Gamma LA+1\right]\eta \end{aligned} \tag{127}$$

in the limit $\eta \to \infty$, while a straightforward calculation yields

$$\left.\frac{dq_{\mathrm{vs0}}}{dz}\right|_{z=0} = e^{LA\theta_1(0)} E\left[LA\theta_1'(0) - \Gamma LA + 1\right], \tag{128}$$

which shows that (126) is fulfilled *automatically* when (119) is. This completes our discussion of the matching conditions for the water vapor mixing ratio.

Turning to the constraint (112) for cloud water, we need to impose the following additional conditions for matching to the bulk flow:

In undersaturated PDL regions, the mixing ratio of cloud water must vanish to leading order. Since clouds might still be generated at the bottom of the bulk (QG) layer over time, even in initially undersaturated regions, we need to choose the initial state of the system such that *there is a finite DL height h above which no significant subsaturation occurs.* This is needed in order to make sure that q_c remains continuous across the layers. We thus require that

$$q_v^{(1/2)} = q_{\mathrm{vs}}^{(1/2)} \tag{129}$$

for all $\eta \geq h$. Furthermore, we need to prescribe vanishing diabatic heating, i.e.

$$Q^{(0/2)} = 0 \tag{130}$$

for all $\eta \geq h$, owing to the dependence of $q_{\mathrm{vs}}^{(1/2)}$ on potential temperature perturbations (see Eq. (127)). If (129) holds initially for some finite h and (130) is prescribed accordingly, this condition will hold for all times. Thus, there is a "sublayer" at the top of the DL where clouds that formed in the bulk layer dissolve as we approach strongly undersaturated lower-level air. In other words, $q_c^{(0/2)}$ will continuously tend to zero in said sublayer wherever it is required by (115e), in a manner that otherwise is not specified by the leading-order PDL solution.

Physically, this technical condition can be interpreted as follows: clouds that form at lower tropospheric levels extend down into the DL, where their base can be found at finite height. This is consistent with the observed thickness of nimbostratus clouds, which are known to attain a vertical extent of 8 – 12 km (Houze 2014, Chapter 6).

Remark: The fact that the decay of q_c in the DL is not fully specified by the model equations strictly speaking constitutes a loss of mathematical well-posedness. It is possible to formulate a PDL system that does not suffer from this drawback if the scaling $q_c^{\mathrm{DL}} \sim \epsilon^{5/2}$ is assumed. This actually leads to an interesting alternative that we intend to present in a future publication. Another option that could be considered a refinement of the theory would be to let the thermodynamic and moisture perturbations in the DL connect not just to the static PQG background, but to the corresponding perturbations in the bulk flow. This approach requires dealing with technical hurdles, e.g., related to the augmentation of the asymptotic expansion by logarithmic terms, that we also intend to tackle in the near future.

Last, but not least, we go over the matching of the respective rain mixing ratios: since this includes only zeroth-order terms, the matching reduces to requiring continuity across the layers,

$$q_r^{(0/2)}(t,\mathbf{x},\eta) \to q_r^{(0)}(t,\mathbf{x},0) \quad \text{as } \eta \to \infty. \tag{131}$$

In PDL, q_r is determined by the first-order quasi-1D equation

$$-\partial_\eta q_r^{(0/2)} = -\frac{1}{V_T}\bar{C}_{\mathrm{ev}}\left(q_{\mathrm{vs}}^{(1/2)} - q_v^{(1/2)}\right)^+ q_r^{(0/2)}, \tag{132}$$

which leads to the representation formula

$$q_r^{(0/2)}(t,\mathbf{x},\eta) = q_r^{(0)}(t,\mathbf{x},0)\exp\left\{\frac{\bar{C}_{\mathrm{ev}}}{V_T}\int_\infty^\eta \left(q_{\mathrm{vs}}^{(1/2)} - q_v^{(1/2)}\right)^+ d\eta'\right\}. \tag{133}$$

Again, this solution will be valid as long as the integral in the exponent converges, which is already guaranteed by the previously stated matching condition (119).

c. The Ekman layer: Ekman pumping in PQG-DL-Ekman

As already stated earlier, the leading-order balances in the Ekman layer are not affected by the incorporation of moist processes: at altitudes < 1 km, while clouds can be present, they are most certainly not dense enough over a synoptic region to raise latent heating to a leading-order effect. Thus, the only microphysical mechanism that might be of relevance is evaporation of rain in dry boundary-layer air. Even though this can certainly be very impactful locally, such effects are too

weak in the large-scale mean to play a role at leading order. Moreover, recalling that fully developed stratiform clouds typically have their base in the diabatic layer (at altitudes $\sim 1-3$ km, cf. Xu et al. (2019)), we have already incorporated evaporation below cloud base as a strong diabatic effect where it matters the most, i.e., in the PDL equations (115).

We thus adopt *classical* Ekman theory (Pedlosky 1987; Vallis 2017) as the final component of our model, as it was done in (Klein et al. 2022). Briefly summarizing the main points, the Ekman solution for the horizontal velocity field provides an expression for the vertical velocity generated in the Ekman layer; matching to the DL solution then allows us to derive the relation

$$w^{(1)}|_{z=0} = \frac{\sqrt{\mathrm{Ek}}}{2}\,\Delta_\parallel \tilde{\phi}^{\mathrm{DL}}\big|_{\eta=0}\,, \tag{134}$$

with the *Ekman number* Ek that is proportional to the turbulent friction coefficient of the flow.

This relation now provides the bottom boundary condition for the $\mathrm{PQG_{DL}}$ pressure perturbation (shown only for $\alpha = 1$, since we did not cover PV formulations of the $\alpha = 0$ regime): evaluating the thermodynamic equation (71d) at $z = 0$ and substituting hydrostatic balance as well as (134) and (83a), we obtain

$$\begin{aligned}\left(\partial_t + \mathbf{u}^{(0)}|_{z=0}\cdot\nabla_\parallel\right)\left.\frac{\partial\tilde{\phi}^{\mathrm{QG}}}{\partial z}\right|_{z=0} = &-\frac{L}{B(0)}\left(\partial_t + \mathbf{u}^{(0)}|_{z=0}\cdot\nabla_\parallel\right)\tilde{M}|_{z=0}\\ &-\frac{L+B(0)}{B(0)}\frac{\sqrt{\mathrm{Ek}}}{2}\frac{1}{f_0}\Delta_\parallel\tilde{\phi}^{\mathrm{DL}}|_{\eta=0}\frac{d\theta_{e1}}{dz}(0) + \mathcal{Q}^{(0)}|_{z=0} + \mathcal{D}_\theta^{(0)}|_{z=0}.\end{aligned} \tag{135}$$

This completes the derivation of our model equations based on the regime $\alpha = 1$, consisting of the $\mathrm{PQG_{DL}}$ system (82)-(83), the PDL equations (115)-(116) and the matching conditions (118), (119), (129)-(130), (131) and (135).

To illustrate how the bulk flow interacts with the lower-lying boundary layers in a nontechnical manner, Fig. 1 provides a visual representation of the matching conditions:

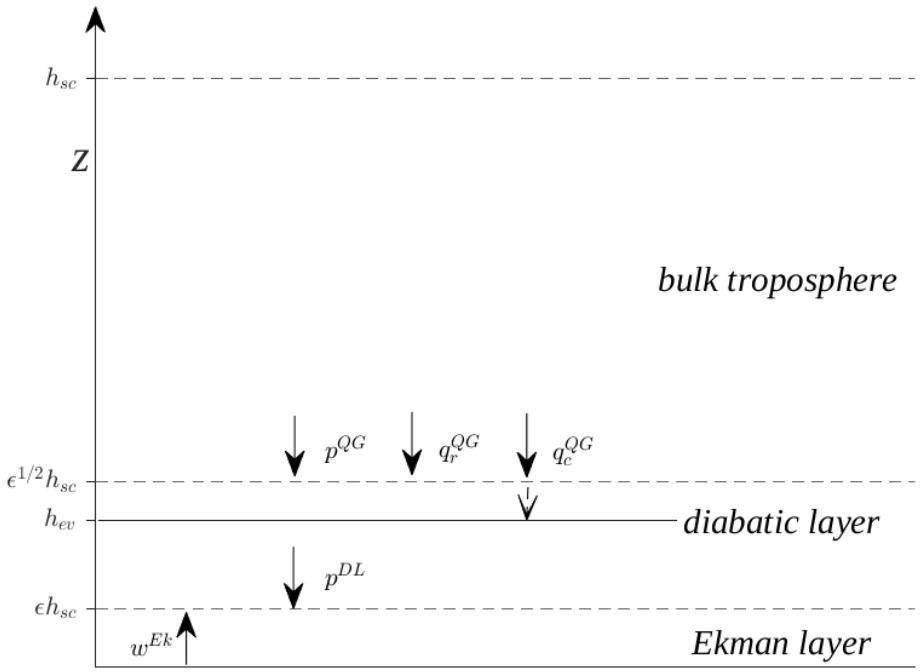

FIG. 1. Visual overview of the feedback mechanisms between the individual layers in PQG-DL-Ekman. The vertical arrows are to be interpreted as follows: the value of the variable indicated next to the arrow is imprinted onto the layer it points towards as a consequence of the matching conditions. All interactions of the dry QG-DL-Ekman theory are preserved, with the added effect of rain falling into the DL, where it may partially evaporate. The sublayer between h_{sc} and h_{ev} only serves to let clouds dissolve, indicated by the short dashed arrow - note that h_{ev} can, in principle, also vary in the horizontal.

6. Explicit PDL solutions for axisymmetric flow

From here on out, both in the derivation of explicit solutions and in the numerical simulations, we will only utilize the regime $\alpha = 1$.

It is a useful property of flow in geostrophic balance that certain symmetries annihilate all advection terms in the associated transport equations. In particular, utilizing cylindrical coordinates (r, ϕ, η) in the DL and seeking axisymmetric solutions of the form

$$\mathbf{U} = \mathbf{U}(t, r, \eta), \tag{136}$$

it immediately follows from (99) that

$$\mathbf{u}^{\mathrm{DL}} = u_{\phi}^{\mathrm{DL}} \mathbf{e}_{\phi}, \tag{137}$$

i.e., the horizontal velocity field is purely azimuthal. Since all transported scalars are independent of ϕ, the material derivative D_t reduces to a time derivative and the PDL system without diffusion or external heating reduces to

$$\partial_t \tilde{\theta}_e^{\mathrm{DL}} = 0, \tag{138a}$$

$$\partial_t \tilde{q}_v^{\mathrm{DL}} = S_{\mathrm{ev}}^{\mathrm{DL}} = \bar{C}_{\mathrm{ev}}(\tilde{q}_{\mathrm{vs}}^{\mathrm{DL}} - \tilde{q}_v^{\mathrm{DL}})^+ q_r^{\mathrm{DL}}, \tag{138b}$$

$$-\partial_\eta q_r^{\mathrm{DL}} = -\frac{1}{V_T} S_{\mathrm{ev}}^{\mathrm{DL}}, \tag{138c}$$

$$\tilde{q}_{\mathrm{vs}}^{\mathrm{DL}} = E e^{AL\bar{\theta}(0)} \left[AL\tilde{\theta}_e^{\mathrm{DL}} - AL^2 \tilde{q}_v^{\mathrm{DL}} - (AL\Gamma - 1)\eta \right], \tag{138d}$$

while pressure and velocity can be diagnostically recovered from the hydrostatic and geostrophic balances, respectively, at any given time. As we shall see shortly, this simplified system can be solved *explicitly* in terms of the solution of the $\mathrm{PQG}_{\mathrm{DL}}$ flow.

Remark: Axisymmetric solutions are only consistent with the $\mathrm{PQG}_{\mathrm{DL}}$ flow if we neglect the β-effect. While working on an f-plane certainly entails a loss of physical realism, it is common to do so in theoretical models based on QG theory, for example in the famous Eady model for baroclinic instability. We therefore expect the f-plane approximation to be sufficient to capture the essentials of the mechanisms that we want to illustrate.

(i) Representation formula for the rain mixing ratio: Prescribing an arbitrary initial state that is compatible with the matching conditions, we can write

$$q_r^{\mathrm{DL}}(t, r, \eta) = q_r^{\mathrm{QG}}(t, r, 0) \exp\left\{ \frac{\bar{C}_{\mathrm{ev}}}{V_T} \int_\infty^\eta (\tilde{q}_{\mathrm{vs}}^{\mathrm{DL}} - \tilde{q}_v^{\mathrm{DL}}) d\eta' \right\}, \tag{139}$$

where the integrand vanishes at *finite* height for all (t, r).

(ii) Moist thermodynamics: We can reformulate (138b) as an equation for the saturation deficit $\tilde{q}_{\mathrm{vs}}^{\mathrm{DL}} - \tilde{q}_v^{\mathrm{DL}}$, using (138a) and (138d):

$$\partial_t \tilde{\theta}_e^{\mathrm{DL}} = 0 \tag{140}$$

implies

$$\partial_t \tilde{q}_{\mathrm{vs}}^{\mathrm{DL}} = -AEL^2 e^{AL\bar{\theta}(0)} \partial_t \tilde{q}_v^{\mathrm{DL}} \equiv -C_1 \partial_t \tilde{q}_v^{\mathrm{DL}}. \tag{141}$$

Further substituting (139) for q_r^{DL}, we arrive at

$$\partial_t(\tilde{q}_{\mathrm{vs}}^{\mathrm{DL}} - \tilde{q}_v^{\mathrm{DL}}) = -(C_1+1)V_T q_r^{\mathrm{QG}}|_{z=0}\partial_\eta\left[\exp\left\{\frac{\bar{C}_{\mathrm{ev}}}{V_T}\int_\infty^\eta(\tilde{q}_{\mathrm{vs}}^{\mathrm{DL}} - \tilde{q}_v^{\mathrm{DL}})d\eta'\right\}\right]. \tag{142}$$

Setting

$$S(t,r,\eta) := \frac{\bar{C}_{\mathrm{ev}}}{V_T}\int_\infty^\eta(\tilde{q}_{\mathrm{vs}}^{\mathrm{DL}} - \tilde{q}_v^{\mathrm{DL}})d\eta', \tag{143}$$

we can conveniently rewrite (142) in the form

$$\partial_t\partial_\eta S = -\bar{C}_{\mathrm{ev}}(C_1+1)q_r^{\mathrm{QG}}|_{z=0}\partial_\eta e^S, \tag{144}$$

which by integration in η further simplifies to

$$\partial_t S = -\bar{C}_{\mathrm{ev}}(C_1+1)q_r^{\mathrm{QG}}|_{z=0}\left(e^S - 1\right). \tag{145}$$

The solution to this equation, with initial data $S|_{t=0} = S_0(r,\eta)$, is readily obtained in the form

$$S(t,r,\eta) = -\ln\left[1 + \left(e^{-S_0(r,\eta)} - 1\right)e^{-R^{\mathrm{QG}}(t,r)}\right], \tag{146}$$

where we have set

$$R^{\mathrm{QG}}(t,r) := \bar{C}_{\mathrm{ev}}(C_1+1)\int_0^t q_r^{\mathrm{QG}}(t',r,0)dt'. \tag{147}$$

It follows by differentiating in the vertical that

$$\tilde{q}_{\mathrm{vs}}^{\mathrm{DL}} - \tilde{q}_v^{\mathrm{DL}} =: s(t,r,\eta) = s_0(r,\eta)\frac{e^{-S_0(r,\eta)}}{e^{-S_0(r,\eta)} + e^{R^{\mathrm{QG}}(t,r)} - 1}, \tag{148}$$

which shows the decrease of the saturation deficit as a function of the time-integrated rain mass entering the DL from above. Similarly, the rain mixing ratio in the DL results as

$$q_r^{\mathrm{DL}}(t,r,\eta) = \frac{q_r^{\mathrm{QG}}(t,r,0)}{1 + \left(e^{-S_0(r,\eta)} - 1\right)e^{-R^{\mathrm{QG}}(t,r)}}. \tag{149}$$

(iii) Expressions for potential temperature, pressure and velocity: Denoting the constant-in-time equivalent potential temperature by $E_0^{\mathrm{tot}}(r,\eta)$ and further isolating the unbounded background

contributions by introducing

$$E_0 := E_0^{\mathrm{tot}} - (\bar{\theta}'(0) + L\bar{q}'_{\mathrm{vs}}(0))\eta, \tag{150}$$

we obtain

$$\tilde{\theta}^{\mathrm{DL}} = \frac{1}{C_1+1}\left[E_0(r,\eta) + Ls(t,r,\eta)\right] + \bar{\theta}'(0)\eta. \tag{151}$$

By (104), we get

$$\tilde{\phi}^{\mathrm{DL}} = \int_\infty^\eta \tilde{\theta}^{\mathrm{DL}} - \bar{\theta}'(0)\eta' d\eta' + \tilde{p}^{\mathrm{QG}}|_{z=0} + \bar{\theta}'(0)\frac{\eta^2}{2}, \tag{152}$$

which also yields the formula

$$\tilde{p}^{\mathrm{DL}}|_{\eta=0} = -\frac{1}{C_1+1}\int_0^\infty E_0(r,\eta') + Ls(t,r,\eta')d\eta' + \tilde{p}^{\mathrm{QG}}|_{z=0} \tag{153}$$

for the pressure perturbation at the bottom of the DL.

Evaluating $\nabla_{\|}^{\perp}\tilde{p}^{\mathrm{DL}}$ in polar coordinates, we obtain

$$\mathbf{u}^{\mathrm{DL}}(t,r,\eta) = \left\{\frac{1}{f_0(C_1+1)}\left[\int_\infty^\eta L\partial_r s(t,r,\eta') + \partial_r E_0(r,\eta')d\eta'\right] + \frac{1}{f_0}\partial_r\tilde{p}^{\mathrm{QG}}|_{z=0}(t,r)\right\}\mathbf{e}_\phi, \tag{154}$$

and, by (135), the Ekman pumping velocity $w^{\mathrm{QG}}|_{z=0}(t,r)$ results as

$$w^{\mathrm{QG}}|_{z=0}(t,r) = \frac{\sqrt{\mathrm{Ek}}}{2}\frac{1}{f_0}\left\{\Delta_{\|}\tilde{\phi}^{\mathrm{QG}}|_{z=0}(t,r) - \frac{1}{C_1+1}\left[\int_0^\infty L\Delta_{\|}s(t,r,\eta') + \Delta_{\|}E_0(r,\eta')d\eta'\right]\right\}. \tag{155}$$

Here, $\Delta_{\|} = \partial_{rr} + \frac{1}{r}\partial_r$, owing to axisymmetry.

7. Numerical solution of the axisymmetric PQG-DL-Ekman system

Even with all the simplifications that axisymmetry entails, the $\mathrm{PQG}_{\mathrm{DL}}$ system retains considerable complexity: neglecting diffusion and assuming no external diabatic heating, the dimensional

Eqs. (12) reduce to

$$\partial_t \mathrm{PV}_e = 0 \tag{156a}$$

$$\partial_t \tilde{M} = B(z)\left[S_{\mathrm{ev}} - S_{\mathrm{cd}}\right] \tag{156b}$$

$$\partial_t q_c^{\mathrm{QG}} = S_{\mathrm{cd}} - S_{\mathrm{ac}} - S_{\mathrm{cr}} \tag{156c}$$

$$-\frac{1}{\bar{\rho}}\partial_z\left(\bar{\rho} V_r q_r^{\mathrm{QG}}\right) = S_{\mathrm{ac}} + S_{\mathrm{cr}} - S_{\mathrm{ev}} \tag{156d}$$

$$\begin{aligned}\frac{1}{f}\Delta_{\parallel}\tilde{\phi}^{\mathrm{QG}} + \frac{f}{\bar{\rho}}\partial_z\left(\frac{\bar{\rho}}{d\bar{\theta}_e/dz}\frac{B(z)}{L_{\mathrm{ref}}/c_{\mathrm{pd}} + B(z)}\partial_z\tilde{\phi}^{\mathrm{QG}}\right) &= \mathrm{PV}_e - \beta y \\ &\quad - \frac{f}{\bar{\rho}}\partial_z\left(\frac{\bar{\rho}}{d\bar{\theta}_e/dz}\frac{L_{\mathrm{ref}}/c_{\mathrm{pd}}}{L_{\mathrm{ref}}/c_{\mathrm{pd}} + B(z)}\tilde{M}\right),\end{aligned} \tag{156e}$$

plus hydrostatic and geostrophic relations.

Solving these equations on a cylindrical domain with $z_{\max} = 10$ km and $r_{\max} = 1000$ km, other than initial conditions for $\tilde{M}$ and q_c^{QG}, as well as the top boundary condition for q_r^{QG}, we need to specify boundary conditions for the adjusted pressure perturbation $\tilde{\phi}^{\mathrm{QG}}$ in order to obtain a unique solution of (156e):

- At the bottom of the domain, it is asymptotic matching to the diabatic and Ekman layers that determines the appropriate (time-dependent) boundary condition: by axisymmetry, (135) reduces to

$$\begin{aligned}\partial_t\left(\partial_z\tilde{\phi}^{\mathrm{QG}}|_{z=0}\right) = &- g\frac{L_{\mathrm{ref}}/c_{\mathrm{pd}}}{B(0)}\partial_t\tilde{M}|_{z=0} \\ &- \frac{L_{\mathrm{ref}}/c_{\mathrm{pd}} + B(0)}{B(0)}\frac{d_{\mathrm{Ek}}}{2}\frac{1}{f}\tilde{w}^{\mathrm{QG}}|_{z=0}\frac{d\bar{\theta}_e}{dz}(0),\end{aligned} \tag{157}$$

  where d_{Ek} denotes the height of the Ekman layer and $\tilde{w}^{\mathrm{QG}}|_{z=0}$ is given by the dimensional equivalent of (155). Clearly, an initial condition for $\partial_z\tilde{\phi}^{\mathrm{QG}}|_{z=0}$ also needs to be prescribed.

- At the top, we impose the rigid lid condition $\tilde{w}^{\mathrm{QG}}|_{z=z_{\max}} = 0$, which by evaluation of the thermodynamic equation translates to

$$\partial_z\tilde{\phi}^{\mathrm{QG}}|_{z=z_{\max}} = -g\frac{L_{\mathrm{ref}}/c_{\mathrm{pd}}}{B(z_{\max})}\tilde{M}|_{z=z_{\max}}. \tag{158}$$

- At lateral boundaries, we assume homogeneous Neumann boundary conditions for simplicity.

Thus, we need to solve a Neumann problem at every time step, which demands that a compatibility condition be satisfied. Here, this will always be the case, as long as the PDL solution is initialized appropriately. Of course, the solution is determined only up to an additive constant, which can be fixed at the initial time.

To showcase how variations in available moisture can shape the flow in this idealized setting, we consider a tropospheric background state exactly at saturation and the following initial perturbation, constructed as a simple harmonic profile:

A cloudless free troposphere at rest and a strongly undersaturated DL around the center of the domain, up to a height $h_{\mathrm{ev}} \approx 2.5$ km,

$$s_{\mathrm{DL}}|_{t=0} = 0.3 q_{\mathrm{vs}_{\mathrm{ref}}} \frac{1+\cos(\pi r / r_{\max})}{2} H(h_{\mathrm{ev}} - z), \tag{159}$$

where H denotes the Heaviside step function. The constant-in-time equivalent potential temperature perturbation in the DL was set to zero for simplicity. As a further simplification, we assumed zero-PV$_e$ flow.

As far as the numerical solution method is concerned, the linear elliptic equation (156e) was solved with standard finite differences on a vertically stretched grid. The evolution Eqs. (156b) and (156c) were discretized with the standard 4th-order Runge-Kutta method, while the diagnostic rainfall Eq. (156d) was solved by numerically evaluating its integral solution representation at the end of each time step, *after* updated values of $\tilde{M}$, q_c^{QG} and $\tilde{\phi}^{\mathrm{QG}}$ had been obtained. The a priori undetermined rate constants $\bar{C}_\star$ were pragmatically chosen to fit the order-of-magnitude assumptions underlying our scaling, while the autoconversion threshold q_{ac} was set to a value reflecting liquid water contents typically observed in stratiform clouds, see Table 4:

$\bar{C}_{\text{ev}}\frac{\bar{p}}{\bar{\rho}}$	0.1	s^{-1}	Evaporation rate, multiplied by constant factor $\bar{p}/\bar{\rho}$
$\bar{C}_{\text{cd}}$	0.01	s^{-1}	Condensation rate
$\bar{C}_{\text{cn}}q_{\text{cn}}$	0.1	s^{-1}	Nucleation rate, multiplied by density of condensation kernels q_{cn} (assumed constant)
$\bar{C}_{\text{ac}}$	10^{-5}	s^{-1}	Autoconversion rate
q_{ac}	4×10^{-4}	1	Autoconversion threshold

TABLE 4. Rate constants in the bulk microphysics closures. Notice that $\bar{C}_{\text{cn}}q_{\text{cn}}$ was set to a value that keeps supersaturation one order of magnitude smaller than subsaturation, consistent with observational data.

The code used to generate the figures in this section was written in MATLAB; the corresponding author will be happy to provide it upon personal request.

Tropospheric dynamics generated by a low-level moisture trough

In this scenario, with (159) as the only nonzero initial condition, the tropospheric flow is wholly driven by updrafts produced in the Ekman layer, which in turn are effected by the horizontal moisture differential in the DL. The latter sets up a cyclonic flow in the dry sublayer that is brought to rest at the bottom by surface friction, as shown in Figs. 2 and 3. Over time, a corresponding *anticyclonic* flow develops in the middle and upper troposphere (Fig. 4). This flow gradually intensifies and weakens the low-level cyclonic motion.

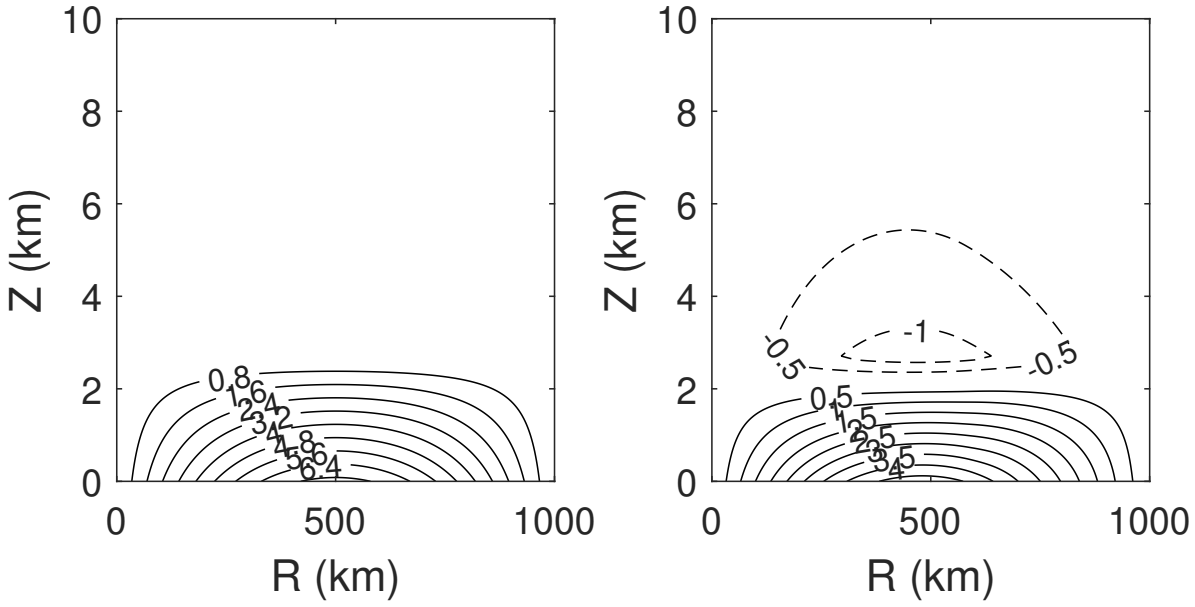

FIG. 2. Left to right: composite PQG-DL profile of the azimuthal velocity at the initial time and at t = 12 h.

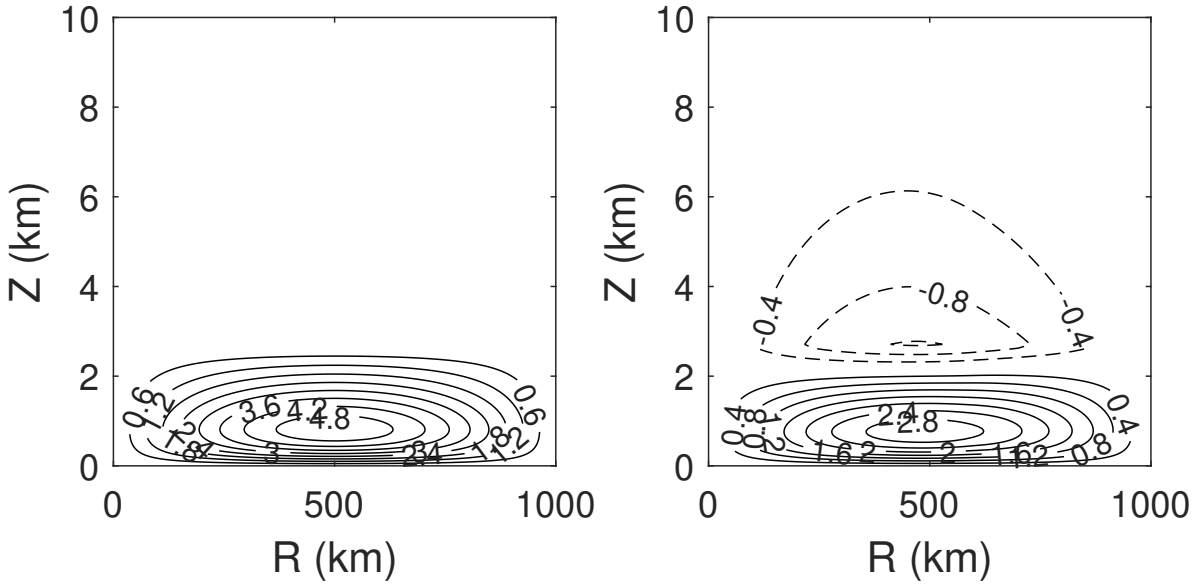

FIG. 3. Left to right: composite PQG-DL-Ekman azimuthal velocity at the initial time and at t = 12 h.

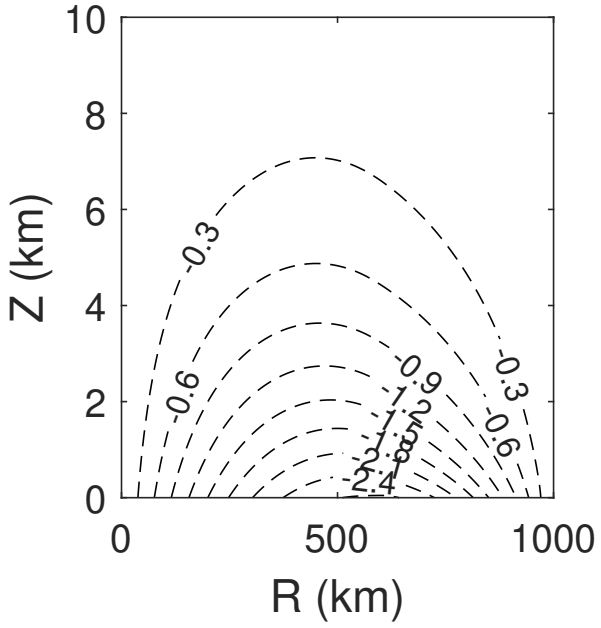

FIG. 4. Incipient anticyclonic $\mathrm{PQG_{DL}}$ flow at $t = 12$ h.

This behavior is largely analogous to that observed in the simulation of a heat low in (Klein et al. 2022) - in this application of the *dry* QG-DL-Ekman theory, however, an external heat source (parameterizing small-scale convection) was responsible for said development, which here arises directly from the synoptic-scale moisture distribution. The conspicuous edges in Figs. 2 and 3 arise from the cutoff in (159) at $z = h_{\mathrm{ev}}$.

As far as moisture in the free troposphere is concerned, an immediate subdivision into a saturated inner and an undersaturated outer region can be observed in Fig. 5. Air in the outer region progressively dries out over time, while it stays close to the saturation threshold in the inner region, where a cloud layer forms, as shown in Fig. 6. In this part of the domain, updrafts due to DL-Ekman pumping are significant, while no discernible vertical motion is generated in the outer region (Fig. 7).

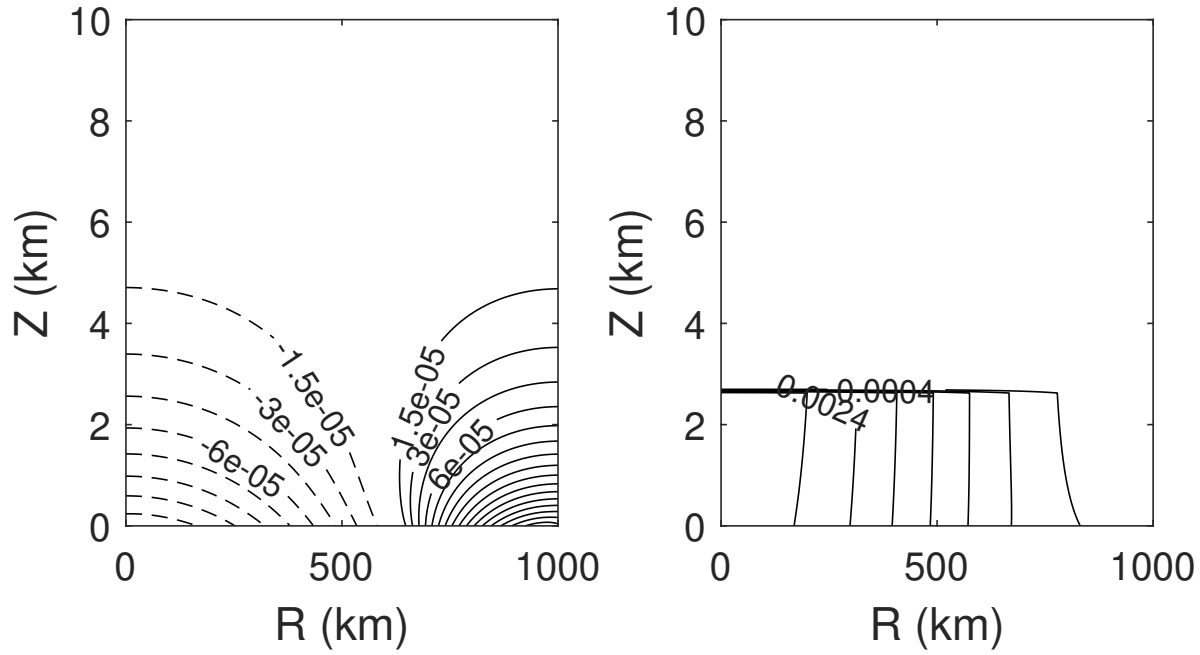

929 FIG. 5. Left to right: absolute subsaturation $\tilde{q}_{\mathrm{vs}} - \tilde{q}_v$ in the free troposphere and in the PQG-DL composite
930 solution at $t = 6$ h. On the right, only the lowest and the highest value are displayed for readability; here, contours
931 coalesce at $z = h_{\mathrm{ev}}$ due to the cutoff prescribed in (159).

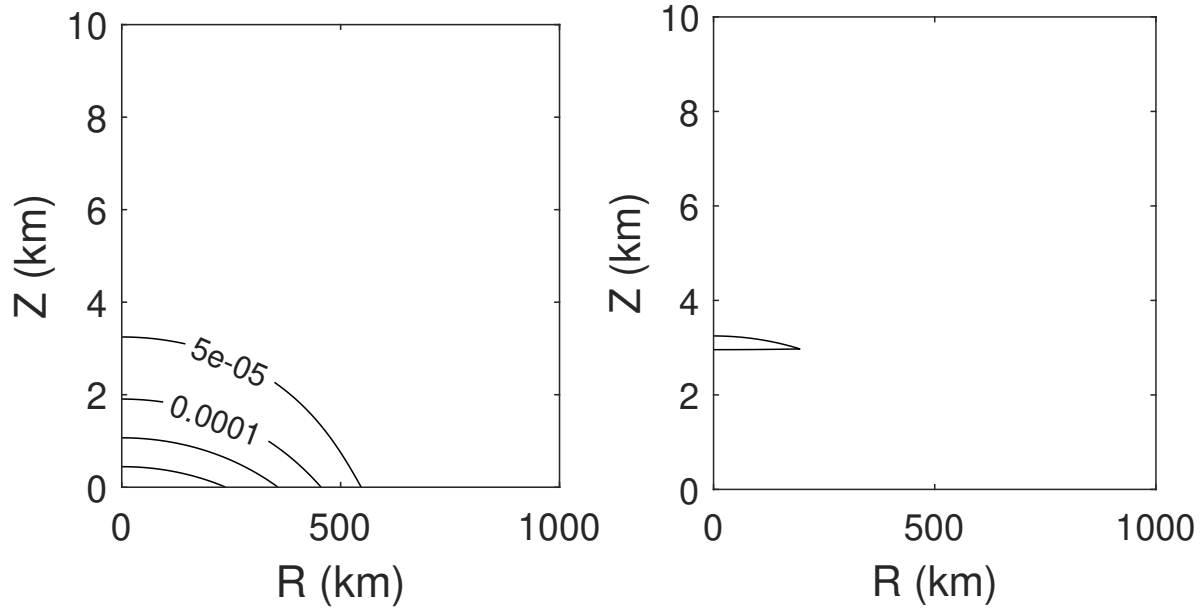

938 FIG. 6. Left to right: cloud water mixing ratio in the free troposphere and in the PQG-DL composite solution
939 at $t = 6$ h. In the latter, the cloud layer is still very thin.

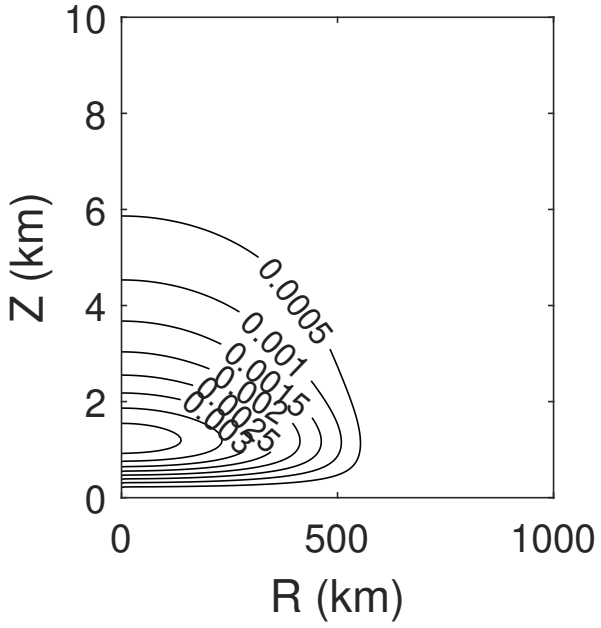

FIG. 7. Composite PQG(-DL)-Ekman vertical velocity at $t = 6$ h.

Here and in the following, the composite profile of the cloud water mixing ratio only represents a qualitatively accurate approximation: as discussed in section 6, the manner in which q_c tends to zero as we approach the dry subregion of the DL is not fully specified by the model output. Still, one can prescribe a two-component partition of unity $\chi_i = \chi_i(z)$ $(i = 1, 2)$ in the vertical and write

$$q_c^{\mathrm{DL}} = \chi_1 \cdot 0 + \chi_2 q_c^{\mathrm{QG}}, \tag{160}$$

where $\chi_2 = 1$ in the QG layer and $\chi_1 = 1$ below h_{ev}. This method of representing a solution that is undetermined in some transition region has been used in the context of formal asymptotic analysis, e.g., by Tordeux et al. (2006). As already mentioned, a model variant of the PDL equations that does not exhibit such an information loss is in preparation. The composite subsaturation profile also constitutes a rougher approximation than the other solution components, since the PDL solution does not incorporate the $O(\epsilon^3)$ perturbations of $q_{\mathrm{vs}}^{\mathrm{DL}} - q_v^{\mathrm{DL}}$ that would formally match the corresponding quantities in the QG layer. - At later times, the initial trend continues, as can be seen in Figs. 8 and 9. Here, q_c has already crossed the autoconversion threshold, which was set at $q_{\mathrm{ac}} = 0.4$ g/kg. Updrafts, conversely, have already weakened (Fig. 10).

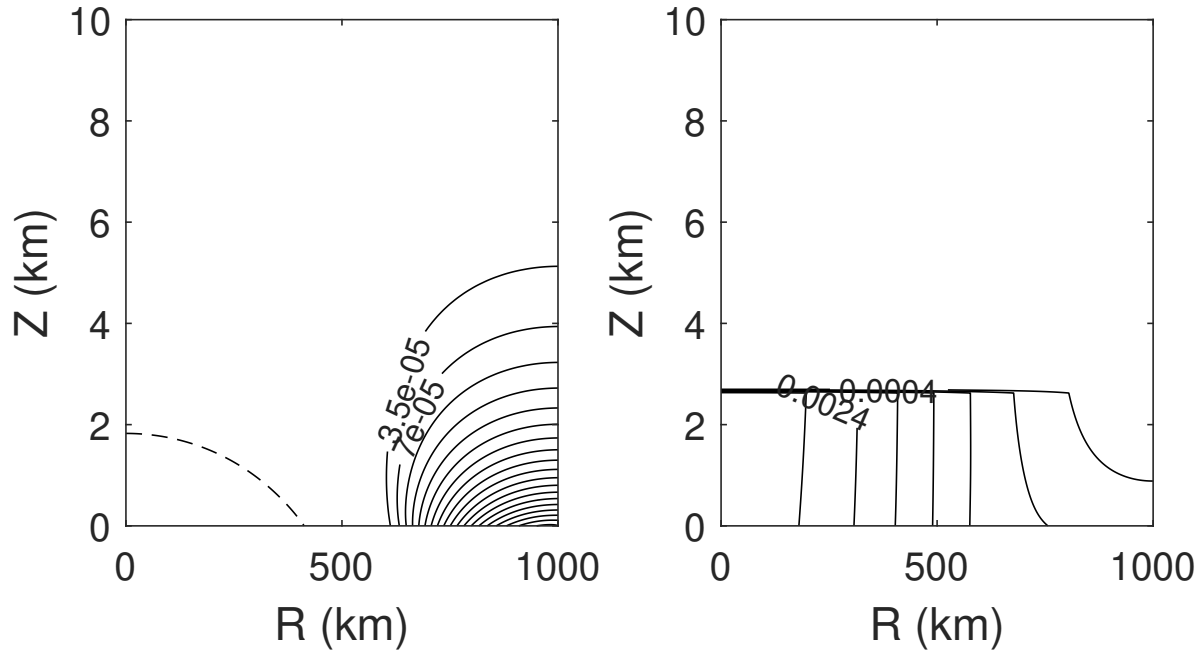

944 FIG. 8. Left to right: free tropospheric and composite subsaturation at $t = 24$ h. In the composite profile, the
945 PQG_{DL} contribution has altered the surface moisture distribution close to the lateral boundary.

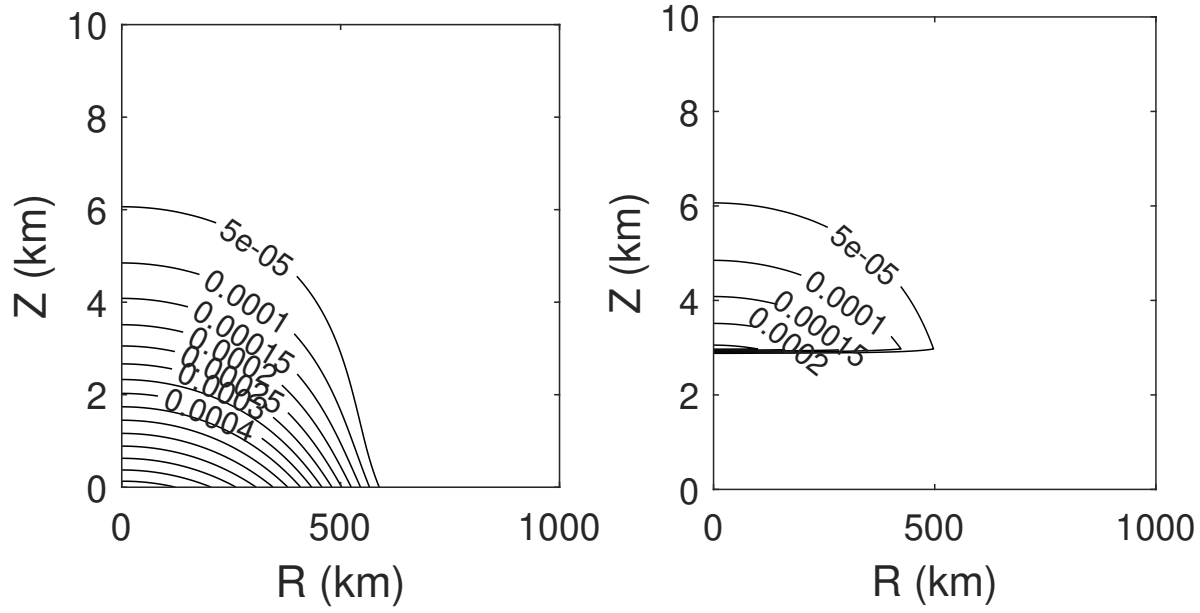

955 FIG. 9. Left to right: free tropospheric and composite cloud water at $t = 24$ h. In the composite profile,
956 contours bunch up close to h_{ev} because the cloud dissolves in a very thin sublayer.

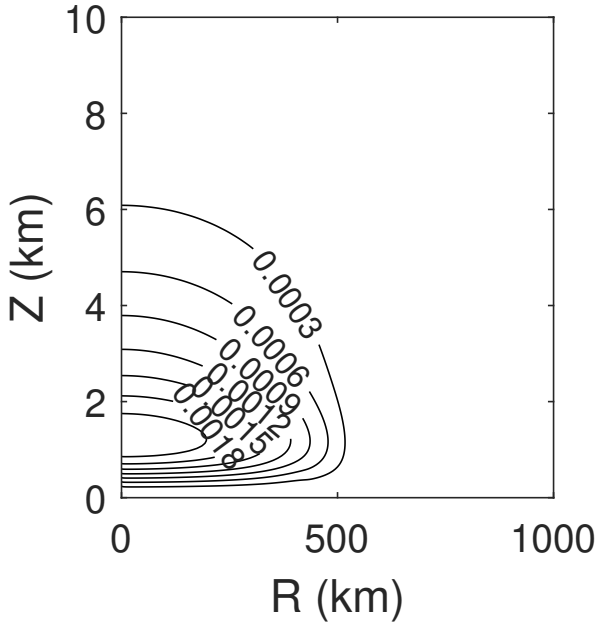

FIG. 10. Composite vertical velocity at $t = 24$ h. Still, only updrafts are seen, but they have decreased in strength.

Remarkably, while the rain mixing ratio q_r is almost negligibly small (and therefore not shown), its impact can already be seen in the composite azimuthal velocity at $t = 24$ h: since DL subsaturation is weakened by rain entering the layer from above, according to (148), and the velocity field in the diabatic layer is shaped by the horizontal moisture distribution as expressed in (154), new structures - albeit still subtle - start to emerge at low levels in Figs. 11 and 12.

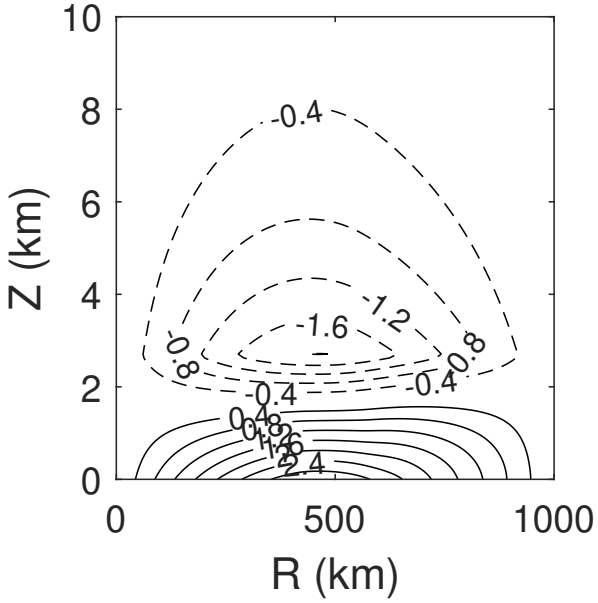

957 FIG. 11. PQG-DL composite azimuthal velocity at $t = 24$ h. The isolines of the low-level cyclonic flow have
958 started to bend slightly downward below the saturated region.

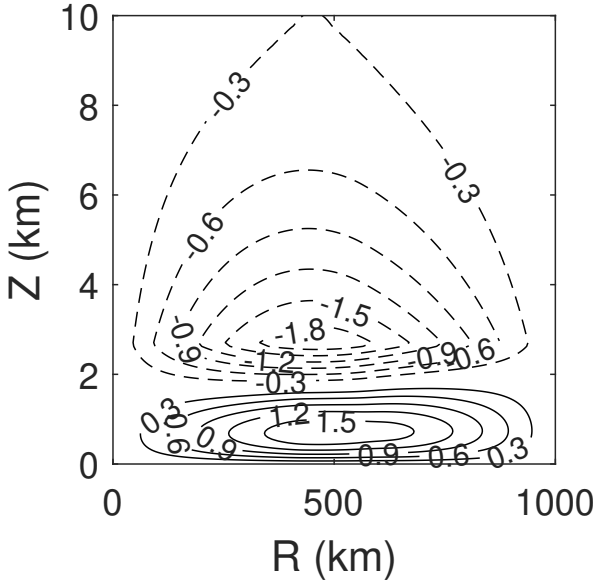

964 FIG. 12. PQG-DL-Ekman composite azimuthal velocity at $t = 24$ h. Apart from the weakening of the cyclonic
965 flow, the same trend as in Fig. 11 can be observed.

968 At the final time, $t = 48$ h, no significant changes in the evolution of the tropospheric moisture
969 distribution can be observed, other than the dampening of cloud growth beyond the autoconversion
970 threshold due to continuous conversion of cloud droplets into raindrops. The time-integrated rain

mass entering the DL from above, however, has reshaped the low-level flow almost completely, as Figs. 13 and 14 make clear.

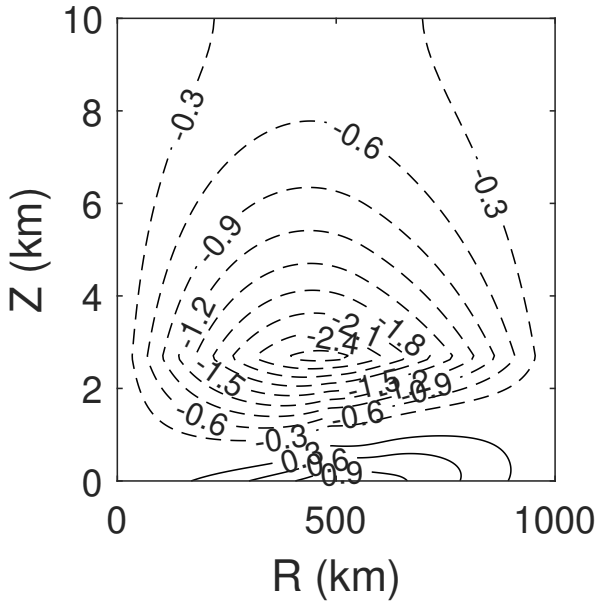

FIG. 13. PQG-DL composite azimuthal velocity at the final time. Continuous evaporation of drizzle generated in the free troposphere has accelerated the dissolution of the surface cyclone below the cloudy region.

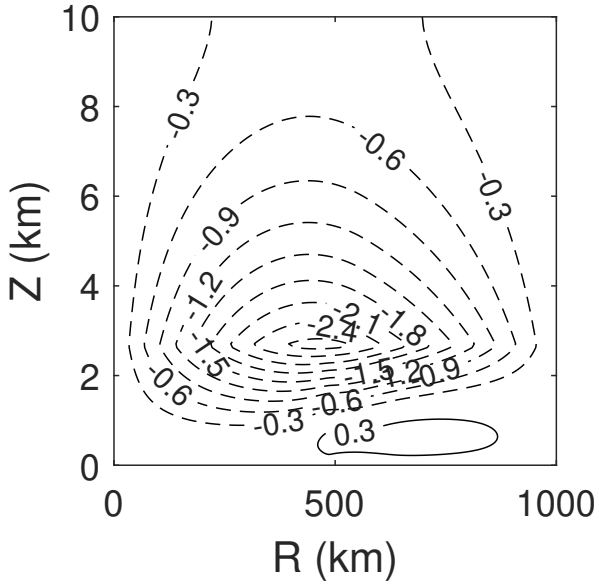

FIG. 14. PQG-DL-Ekman composite azimuthal velocity at the final time. Here, the tendency of evaporative cooling to dissolve the surface cyclone is even more apparent.

In summary, the numerical sample solution illustrates how

(i) a moisture anomaly in the diabatic layer can generate long-lasting dynamical disturbances across the whole troposphere from a stationary state and

(ii) rain generation in the bulk troposphere affects the flow closer to the surface.

8. Conclusions

A new reduced model describing moist synoptic-scale dynamics in the midlatitudes was derived. The derivation of said model, the PQG-DL-Ekman theory, builds on foundations established in a fair number of earlier asymptotic modeling studies: first, the general framework of Klein (2010) for model hierarchies in atmospheric flows; then, the studies of Klein and Majda (2006) and Hittmeir and Klein (2018) on moist convection, which systematically incorporated the Clausius-Clapeyron relation and investigated possible extensions of the dry air distinguished limit of Klein (2010) to include the thermodynamics of moist air; the PQG model family of Smith and Stechmann (2017), which was later shown by Bäumer et al. (2023) to be derivable from the Klein (2010) distinguished limit and finally the QG-DL-Ekman theory of Klein et al. (2022).

Beyond the formal derivation and the description of the resulting triple-deck boundary layer theory, a simplified axisymmetric version of the model was studied in more detail to elucidate its core features: in the precipitating DL, this simplification enabled the explicit representation of the system's solution in terms of the required data. With those explicit solutions in hand, numerical solutions of the coupled (axisymmetric) PQG-DL-Ekman system could also be computed by standard methods. The initial state was chosen to illustrate the impact of nonuniform moisture distributions at low tropospheric levels, in particular the potential of a dry DL sublayer to shape the whole tropospheric flow.

Concerning directions for future research, the various modeling alternatives mentioned throughout the article constitute an obvious starting point. Beyond those, we have already started to investigate the formation of surface fronts in the precipitating DL; rigorous PDE studies of the DL equations are also in the works. We further plan to explore in more depth the relationship between models utilizing bulk microphysics closures - like the present one - and those that model phase changes by switching functions, such as Smith and Stechmann (2017) and most subsequent studies of the PQG equations. Such work should prove to be helpful in improving our understanding of the link between cloud microphysics and large-scale atmospheric dynamics. Finally, we want to

point to the long-term goal of our asymptotic modeling endeavors, which is a unified multiscale description of cloud formation and precipitation in the earth's atmosphere, from the convective cloud towers of Hittmeir and Klein (2018) to the synoptic-scale description of moist dynamics of Smith and Stechmann (2017); Bäumer et al. (2023) and the present article.

Acknowledgments. This research was funded in part by the Austrian Science Fund (FWF) 10.55776/F65, 10.55776/I5149, 10.55776/P32788, as well as by the OeAD-WTZ project CZ 09/2023. For open-access purposes, the authors have applied a CC BY public copyright license to any author-accepted manuscript version arising from this submission. R.K. acknowledges support by Deutsche Forschungsgemeinschaft through Grant CRC 1114 "Scaling Cascades in Complex Systems", Project Number 235221301, Project C06 "Multi-scale structure of atmospheric vortices" and Grant FOR 5528 "Mathematical Study of Geophysical Flow Models: Analysis and Computation", Project No. 500072446, Project 2 "Scale Analysis and Asymptotic Reduced Models for the Atmosphere". Both authors thank the Wolfgang Pauli Institute Vienna for all kinds of support, e.g., the Pauli fellowship for R.K.
Further we acknowledge continous scientific discussions with N.J. Mauser, and valuable help with the numerical implementation by H.P. Stimming.

Data availability statement. The paper presents theoretical work and all derivations should be described in sufficient detail. No further data are required to reproduce the findings.

References

Austin, P., and R. Houze, 1972: Analysis of the structure of precipitation patterns in new england. *J. Appl. Meteor. Climatol.*, **11**, 926–935, https://doi.org/10.1175/1520-0450(1972)011⟨0926:AOTSOP⟩2.0.CO;2.

Bäumer, D., S. Hittmeir, and R. Klein, 2023: Scaling approaches to quasigeostrophic theory for moist, precipitating air. *J. Atmos. Sci.*, **80**, 1771–1786, https://doi.org/10.1175/JAS-D-22-0225.1.

Cotton, W., G. Bryan., and S. van den Heever, 2011: *Storm and Cloud Dynamics*. 2nd ed., Elsevier Science, 820 pp.

Doppler, S., R. Klein, X. Liu, and E. Titi, 2024: Local well-posedness of a system coupling compressible atmospheric dynamics and a micro-physics model of moisture in air. URL https://arxiv.org/abs/2408.15749, 2408.15749.

Grabowski, W., and P. Smolarkiewicz, 1996: Two-time-level semi lagrangian model for precipitating clouds. *Mon. Wea. Rev.*, **124**, 487–497, https://doi.org/10.1175/1520-0493(1996)124⟨0487:TTLSLM⟩2.0.CO;2.

Hernandez-Duenas, G., A. Majda, L. Smith, and S. Stechmann, 2013: Minimal models for precipitating turbulent convection. *J. Fluid Mech.*, **717**, 576–611, https://doi.org/10.1017/jfm.2012.597.

Hittmeir, S., and R. Klein, 2018: Asymptotics for moist deep convection I: refined scalings and self-sustaining updrafts. *Theor. Comput. Fluid Dyn.*, **32**, 137–164, https://doi.org/10.1007/s00162-017-0443-z.

Hittmeir, S., R. Klein, J. Li, and E. Titi, 2017: Global well-posedness for passively transported nonlinear moisture dynamics with phase changes. *Nonlinearity*, **30**, 3676–3718, https://doi.org/10.1088/1361-6544/aa82f1.

Hittmeir, S., R. Klein, J. Li, and E. Titi, 2020: Global well-posedness for the primitive equations coupled to nonlinear moisture dynamics with phase changes. *Nonlinearity*, **33**, 3206–3236, https://doi.org/10.1088/1361-6544/ab834f.

Hittmeir, S., R. Klein, J. Li, and E. Titi, 2023: Global well-posedness for the thermodynamically refined passively transported nonlinear moisture dynamics with phase changes. *Journal of nonlinear science*, **33**, https://doi.org/10.1007/s00332-023-09915-z.

Houze, R., 2014: *Cloud Dynamics*. 2nd ed., Elsevier Science, 496 pp.

Kessler, E., 1995: On the continuity and distribution of water substance in atmospheric circulations. *Atmos. Res.*, **38**, 109–145, https://doi.org/10.1016/0169-8095(94)00090-Z.

Kevorkian, J., and J. Cole, 1996: *Multiple Scale and Singular Perturbation Methods*. Springer-Verlag, 634 pp.

Klein, R., 2010: Scale-dependent models for atmospheric flows. *Annu. Rev. Fluid Mech.*, **42**, 249–274, https://doi.org/10.1146/annurev-fluid-121108-145537.

Klein, R., and A. Majda, 2006: Systematic multiscale models for deep convection on mesoscales. *Theor. Comput. Fluid Dyn.*, **20**, 525–551, https://doi.org/10.1007/s00162-006-0027-9.

Klein, R., L. Schielicke, S. Pfahl, and B. Khouider, 2022: QG-DL-Ekman: Dynamics of a diabatic layer in the quasi-geostrophic framework. *J. Atmos. Sci.*, **79**, 887–905, https://doi.org/10.1175/JAS-D-21-0110.1.

Niu, S., X. Jia, J. Sang, X. Liu, C. Lu, and Y. Liu, 2010: Distributions of raindrop sizes and fall velocities in a semiarid plateau climate: Convective versus stratiform rains. *Journal of Applied Meteorology and Climatology*, **49 (4)**, 632 – 645, https://doi.org/10.1175/2009JAMC2208.1, URL https://journals.ametsoc.org/view/journals/apme/49/4/2009jamc2208.1.xml.

Parkins, C. J., P. A. Blythe, and D. G. Crighton, 2000: Hot spot ignition: the newtonian limit. *Proc. Roy. Soc. Physical and Engineering Science*, **456**, 2857–2882.

Pedlosky, J., 1987: *Geophysical Fluid Dynamics*. 2nd ed., Springer-Verlag, 710 pp.

Razafimaharo, C., S. Krähenmann, S. Höpp, M. Rauthe, and T. Deutschländer, 2020: New high-resolution gridded dataset of daily mean, minimum, and maximum temperature and relative humidity for central europe (hyras). *Theoretical and applied climatology*, **142 (3-4)**, 1531–1553.

Remond-Tiedrez, A., L. M. Smith, and S. N. Stechmann, 2024: A nonlinear elliptic pde from atmospheric science: Well-posedness and regularity at cloud edge. *Journal of mathematical fluid mechanics*, **26 (2)**.

Smith, L., and S. Stechmann, 2017: Precipitating quasigeostrophic equations and potential vorticity inversion with phase changes. *J. Atmos. Sci.*, **74**, 3285–3303, https://doi.org/10.1175/JAS-D-17-0023.1.

Tordeux, S., G. Vial, and M. Dauge, 2006: Matching and multiscale expansions for a model singular perturbation problem. *Comptes rendus. Mathématique*, **343 (10)**, 637–642.

Vallis, G., 2017: *Atmospheric and Oceanic Fluid Dynamics*. 2nd ed., Cambridge University Press, 946 pp.

Wetzel, A., L. Smith, S. Stechmann, and J. Martin, 2019: Balanced and unbalanced components of moist atmospheric flows with phase changes. *Chinese Annals of Mathematics, Series B*, **40**, 1005–1038, https://doi.org/10.1007/s11401-019-0170-4.

Xu, J., D. Liu, Z. Wang, D. Wu, S. Yu, and Y. Wang, 2019: A study of the characteristics of vertical cloud base height distribution over eastern china. *Atmosphere*, **10 (6)**, 307.

Yang, D., W. Zhou, and S. D. Seidel, 2022: Substantial influence of vapour buoyancy on tropospheric air temperature and subtropical cloud. *Nature geoscience*, **15 (10)**, 781–788.

Zhang, W., G. Xu, B. Xi, J. Ren, X. Wan, L. Zhou, C. Cui, and D. Wu, 2020: Comparative study of cloud liquid water and rain liquid water obtained from microwave radiometer and micro rain radar observations over central china during the monsoon. *J. Geophys. Res.: Atmospheres*, **125 (20)**, https://doi.org/10.1029/2020JD032456.

Zhao, Z., and H. Lei, 2014: Observed microphysical structure of nimbostratus in northeast cold vortex over china. *Atmos. Res.*, **142**, 91–99, https://doi.org/10.1016/j.atmosres.2013.09.008.

The diabatic layer equations: well-posedness of a new boundary layer theory for quasi-geostrophic flow

Daniel Bäumer

Abstract

In this paper, we initiate the mathematically rigorous study of the so-called diabatic layer (DL) equations. These were introduced by Klein et al. in 2022 as part of a new triple-deck boundary layer theory, based on the classical quasi-geostrophic model for large-scale atmospheric flows. We briefly explain how the DL equations are related to other models characterized by geostrophic balance; then, we point to the difficulties arising in their analysis and proceed to establish the global well-posedness of a diffusive regularization, employing Bernstein's method to obtain a uniform bound on the gradient of the solution. We further mention possible refinements of the proof and directions for future research.

1 Introduction

Quasi-geostrophic (QG) theory has long been a staple of theoretical meteorology. Its textbook treatment includes a coupling to the planetary boundary layer via Ekman theory [Pedlosky, 1987, Vallis, 2017]. As Klein et al. [2022] remark, empirical data indicates that QG-Ekman theory fails to capture the increased strength of diabatic processes at lower levels in the earth's troposphere, which motivated the extension of said theory to a *triple-deck* theory, with the aptly named *diabatic layer* (DL) as a new intermediate layer. The governing equations of the DL are centered around a potential temperature perturbation that is systematically stronger than the scaling assumptions of QG theory would permit, while both geostrophic and hydrostatic balances remain valid within the layer. In scaled form, these equations read

$$\partial_t \theta + \mathbf{u} \cdot \nabla_\parallel \theta = Q \tag{1a}$$

$$f\mathbf{u} = \nabla_\parallel^\perp \phi \tag{1b}$$

$$\theta = \partial_z \phi, \tag{1c}$$

where $\theta, \phi, \mathbf{u} = (u, v)^{\mathrm{T}}$ denote the dynamical potential temperature perturbation, the (rescaled) pressure perturbation and the geostrophic horizontal velocity field, respectively. The spatial domain takes the form $\Omega = \{(\mathbf{x}, z) : \mathbf{x} \in D, z \in [0, \infty)\}$, with some

horizontal domain $D \subset \mathbb{R}^2$. We remark that it is consistent with the formal asymptotic derivation to choose $D = \mathbb{R}^2$ and assume decay at infinity, but the alternative $\mathbb{T} \times \mathbb{R}$ also has physical merit, since flow in the zonal (east-to-west) direction has an approximately periodic character. In this work, we will pick the former for convenience. The horizontal gradient is indicated by $\nabla_\parallel$, while $\nabla_\parallel^\perp$ is given by $\nabla_\parallel^\perp = (-\partial_y, \partial_x)^{\mathrm{T}}$ in Cartesian coordinates. The parameter f (which can be taken *constant* in this instance) stems from a leading-order approximation to the Coriolis force, while the source term Q represents diabatic heating, e.g., by small-scale turbulence or latent heat release in cloud formation. The DL interacts with the bulk troposphere, governed by QG, in two ways: firstly, systematic matching dictates that

$$\phi(t, \mathbf{x}, z) \to \phi^{\mathrm{QG}}(t, \mathbf{x}, 0) \text{ as } z \to \infty, \tag{2}$$

that is, the pressure at the top of the DL is given by the QG pressure at the *bottom* of the bulk layer. On the other hand, the pressure perturbation at the bottom of the DL is imprinted onto the Ekman layer below, where a vertical velocity is generated that in turn affects the QG dynamics above. It is important to note that this vertical velocity remains *unchanged* throughout the DL, and there is no vertical transport in the thermodynamic equation (1a). We refer to Klein et al. [2022] for details.

The system (1) shares certain features with well-known geophysical flow models other than QG: in its mathematical structure, it most closely resembles the planetary geostrophic (PG) equations, which have been analyzed thoroughly only in their viscous form [Cao and Titi, 2003, Cao et al., 2004]; however, the Coriolis parameter f is a function of latitude on the planetary scale, and PG incorporates vertical transport in the analogue of (1a). Therefore, results obtained for DL do not necessarily carry over to the PG system. Conversely, geostrophic balance (1b) is essential in the DL equations, which means there is no physically meaningful "viscous DL system".

It is further illuminating to compare the DL system to the the surface quasi-geostrophic (SQG) equations [Constantin et al., 1994], which have been studied extensively by the mathematical fluid dynamics community over the past 30 years. These can be written as *one* active scalar equation for the potential temperature perturbation, with a nonlocal relationship between θ and the transporting velocity field. An analogous formulation can straightforwardly be derived for the DL equations, by combining (1b) and (1c) to yield the relationship

$$\mathbf{u} = \frac{1}{f} \int_\infty^z \nabla_\parallel^\perp \theta \, dz' + \mathbf{u}_\infty, \tag{3}$$

where $\mathbf{u}_\infty = \mathbf{u}_\infty(t, \mathbf{x})$ denotes the velocity in the vertical farfield, which corresponds to the velocity at the bottom of the bulk layer (cf. (2)). Therefore, (1) reduces to the transport equation

$$\partial_t \theta + \mathbf{u} \cdot \nabla_\parallel \theta = Q, \tag{4}$$

with $\mathbf{u}$ given by (3). In the inviscid SQG model, the transport equation takes the same form, but the spatial domain is *two-dimensional,* and $\mathbf{u}$ and θ are related to one another

by the Riesz transforms. Thus, the velocity field in the DL equation, which loses one horizontal derivative relative to θ, is more singular in the direction of transport than that in SQG. Therefore, even local well-posedness of DL in finite regularity spaces is doubtful, and the only positive result one can expect is local well-posedness in the space of *analytic* functions. For that reason, we have decided to first investigate a diffusive regularization of the model, where the smoothing properties of the Laplacian counteract the singular nature of the advecting velocity.

Remark 1. *Of course, it is our long-term goal to conduct a rigorous analysis of the coupled QG-DL-Ekman dynamics, but this will only be possible once the isolated DL dynamics are properly understood; therefore, we treat the QG flow as externally given from here on.*

2 Global well-posedness of the diffusive model

We now study a streamlined version of (3)-(4), supplied with a standard closure for turbulent mixing and diffusion in the horizontal. We assume there are no external heat sources and choose the Coriolis parameter $f = 1$ for convenience. Since we do not take the coupling to QG via the Ekman layer into account at this stage, we also set $\mathbf{u}_\infty \equiv 0$ for simplicity. Thus, our object of scrutiny is the initial value problem (IVP)

$$\partial_t \theta + \mathbf{u} \cdot \nabla_\parallel \theta = \kappa \Delta_\parallel \theta, \quad \theta|_{t=0} = \theta_I(\mathbf{x}, z) \tag{5}$$

on the domain $[0, T] \times \Omega$, where $\Omega = \mathbb{R}^2 \times [0, \infty)$, $\kappa > 0$ is fixed, and the horizontal velocity field is given in terms of the scalar θ by the thermal wind relation

$$\mathbf{u} = \int_\infty^z \nabla_\parallel^\perp \theta dz'. \tag{6}$$

We remark that this relation guarantees that the velocity field $\mathbf{u}$ is divergence-free, $\mathrm{div}_\parallel \mathbf{u} = 0$. Clearly, this problem is highly anisotropic, with the direction of transport being purely horizontal and the z-dependence only coming into play via (6). Therefore, the first order of business is to introduce a corresponding anisotropic function space: in the horizontal, it is convenient to use the standard L^2-Sobolev spaces $H^k(\mathbb{R}^2)$, while we need integrability in the vertical at a minimum; it is, however, physically sensible to also assume boundedness in z. This motivates the following

Definition 1. *Let $f : \Omega \mapsto \mathbb{R}$ be a measurable function. We introduce the Banach space X^k of all such f that possess weak derivatives in $L^2(\mathbb{R}^2)$ up to order k in the horizontal variables and fulfill*

$$\|f\|_{X^k} := \int_0^\infty \|f\|_{H^k(\mathbb{R}^2)} \, dz + \operatorname*{ess\,sup}_z \|f\|_{H^k(\mathbb{R}^2)} < \infty. \tag{7}$$

Save for the nonlocal dependence on z, (5) can be viewed as a semilinear parabolic equation. Therefore, local well-posedness can be proven by textbook methods, but global existence of smooth solutions cannot be taken for granted. In the following, we will show that the local-in-time solution can be extended to a global one by applying the classical Bernstein's method [Ladyzhenskaya et al., 1967]. This yields a simple proof, but it requires strong assumptions on the smoothness of the solution. These can very likely be weakened drastically when employing more technically sophisticated methods - see the concluding discussion for ideas in that vein.

Remark 2. *In the following, we liberally use the short-hand notation $L_t^p L_x^q$ for the space $L^p\left((0,T), L^q(\mathbb{R}^2)\right)$ and analogous abbreviations for other spaces. In the energy estimates, C as usual denotes a generic constant that can change from line to line; wherever C depends on the initial data, we will highlight this dependence for clarity.*

2.1 Local well-posedness

We start by proving that (5)-(6) has a unique local solution that depends continuously on the initial data, employing the strategy described in [Taylor, 2011] for semilinear parabolic equations. To be precise, we show

Proposition 1. *For any $\theta_I \in X^k$, where $k \geq 3$, there exists a time $T^\star = T^\star(\|\theta_I\|_{X^k}) > 0$ such that the IVP (5)-(6) has a unique solution $\theta \in C\left([0,T^\star], X^k\right)$.*

Proof. Recall that the space $H^s(\mathbb{R}^2)$ is a Banach algebra for $s > 1$ [Adams and Fournier, 2003]; therefore, the operator $\Phi : X^k \mapsto X^{k-1}$,

$$\Phi(f) := \int_\infty^z \nabla_\parallel^\perp f \, dz \cdot \nabla_\parallel f, \tag{8}$$

is well-defined. Next, utilize Duhamel's formula and the heat semigroup to convert (5) to an integral equation:

$$\theta(t) = e^{t\kappa\Delta_\parallel}\theta_I + \int_0^t e^{(t-s)\kappa\Delta_\parallel}\Phi\left(\theta(s)\right) \, ds \equiv \Psi\theta(t). \tag{9}$$

The goal is to prove that Ψ has a unique fixed point in a suitable subset of $C\left([0,T^\star], X^k\right)$. For this, we will need the following properties:

(i) The one-parameter family $e^{t\kappa\Delta_\parallel} : X^k \mapsto X^k$ is a semigroup of bounded linear operators for all $t \geq 0$, locally bounded in t.

(ii) For $t > 0$, we have $e^{t\kappa\Delta_\parallel} : X^{k-1} \mapsto X^k$.

(iii) For $0 < t \leq 1$, it holds $\left\|e^{t\kappa\Delta_\parallel}\right\|_{\mathcal{L}(X^{k-1},X^k)} \leq Ct^{-1/2}$, for some constant C.

(iv) The operator $\Phi : X^k \mapsto X^{k-1}$ is uniformly Lipschitz on bounded sets.

Properties (i)-(iii) are immediate consequences of the corresponding properties of $e^{t\kappa\Delta_\parallel}$ in the spaces H^k_x, which are classical [Taylor, 2011]; regarding (iv), observe that, for $f, g \in X^k$ with $\|f\|_{X^k}, \|g\|_{X^k} \leq M$,

$$\begin{aligned}
\|\Phi(f) - \Phi(g)\|_{X^{k-1}} = &\int_0^\infty \left\| \int_\infty^z \nabla_\parallel^\perp f \, dz' \cdot \nabla_\parallel f - \int_\infty^z \nabla_\parallel^\perp g \, dz' \cdot \nabla_\parallel g \right\|_{H^{k-1}_x} dz \\
&+ \operatorname*{ess\,sup}_z \left\| \int_\infty^z \nabla_\parallel^\perp f \, dz' \cdot \nabla_\parallel f - \int_\infty^z \nabla_\parallel^\perp g \, dz' \cdot \nabla_\parallel g \right\|_{H^{k-1}_x} \\
&\leq \int_0^\infty \left[C \left\| \int_\infty^z \nabla_\parallel^\perp f \, dz' \right\|_{H^{k-1}_x} \left\| \nabla_\parallel (f-g) \right\|_{H^{k-1}_x} \right. \\
&\left. + C \left\| \int_\infty^z \nabla_\parallel^\perp (f-g) \, dz' \right\|_{H^{k-1}_x} \left\| \nabla_\parallel g \right\|_{H^{k-1}_x} \right] dz \\
&+ \operatorname*{ess\,sup}_z \left[C \left\| \int_\infty^z \nabla_\parallel^\perp f \, dz' \right\|_{H^{k-1}_x} \left\| \nabla_\parallel (f-g) \right\|_{H^{k-1}_x} \right. \\
&\left. + C \left\| \int_\infty^z \nabla_\parallel^\perp (f-g) \, dz' \right\|_{H^{k-1}_x} \left\| \nabla_\parallel g \right\|_{H^{k-1}_x} \right] \\
&\leq C \left[\|f\|_{X^k} \|f-g\|_{X^k} + \|f-g\|_{X^k} \|g\|_{X^k} \right] \leq CM \|f-g\|_{X^k},
\end{aligned} \tag{10}$$

where we used the Banach algebra property of H^{k-1}_x and Minkowski's inequality for integrals [Adams and Fournier, 2003] in the last step. Next, for an $\alpha > 0$ to be chosen later, we define

$$Z := \left\{ f \in C\left([0,T], X^k\right) : f|_{t=0} = \theta_I, \|f(t) - \theta_I\|_{X^k} \leq \alpha \right\}. \tag{11}$$

We aim to apply the Banach fixed point theorem on the set Z, utilizing the properties stated above. By (i), we know that

$$\sup_{t \in [0,1]} \left\| e^{t\kappa\Delta_\parallel} \right\|_{\mathcal{L}(X^k)} < \infty, \tag{12}$$

and we can thus choose $\alpha = \alpha(\|\theta_I\|_{X^k})$ such that

$$\left\| e^{t\kappa\Delta_\parallel} \theta_I - \theta_I \right\|_{X^k} \leq \alpha/2 \text{ for } t \in [0,1]. \tag{13}$$

For $f \in Z$, (iv) implies

$$\|\Phi(f(s))\|_{X^{k-1}} \leq C \left(\|\theta_I\|_{X^k} + \alpha \right)^2, \tag{14}$$

for every $s \in [0,1]$. Hence, by (iii),

$$\left\| \int_0^t e^{(t-s)\kappa\Delta_\parallel} \Phi(f(s)) \, ds \right\|_{X^k} \leq C t^{1/2} (\|\theta_I\|_{X^k} + \alpha)^2; \tag{15}$$

choosing $T_1 \leq 1$ such that the right-hand side is bounded from above by $\alpha/2$ for $t \in [0, T_1]$, Ψ thus maps Z into Z for such t. Now, estimate

$$\begin{aligned}\|\Psi f(t) - \Psi g(t)\|_{X^k} &= \left\| \int_0^t e^{t\kappa\Delta_\parallel} \left[\Phi(f(s)) - \Phi(g(s))\right] ds \right\|_{X^k} \\ &\leq Ct^{1/2}(\|\theta_I\|_{X^k} + \alpha) \sup_s \|f(s) - g(s)\|_{X^k} . \end{aligned} \tag{16}$$

Since both α and T_1 depend on $\|\theta_I\|_{X^k}$ alone, we can find a time $T^\star = T^\star(\|\theta_I\|_{X^k}) \leq T_1$ such that Ψ is a contraction in Z. We conclude that Ψ has a unique fixed point in Z, which yields a unique solution to (9) in the space $C\left([0, T^\star], X^k\right)$. □

2.2 Boundedness of the gradient by Bernstein's method

In 1938, the Soviet mathematician Sergei Bernstein proposed a simple method by which estimates on the gradient (and higher-order derivatives) of the solutions of second-order elliptic and parabolic equations can be obtained. Since its application, based on the maximum principle, requires the solution to be classical with an additional spatial derivative, it is not suited for the derivation of sharp results. Here, as already mentioned, we content ourselves with a result for initial data that is sufficiently smooth in the horizontal. To be specific, we have

Lemma 1. *Let $[0, T]$ be an interval of existence of the solution to* (5)-(6) *guaranteed by Proposition 1, with $\theta_I \in X^k$ and the additional condition $k \geq 5$. Then it holds*

$$\operatorname*{ess\,sup}_{t\in[0,T],(\mathbf{x},z)\in\Omega} \left|\nabla_\parallel \theta\right| = \operatorname*{ess\,sup}_{(\mathbf{x},z)\in\Omega} \left|\nabla_\parallel \theta_I\right|, \tag{17}$$

$$\int_0^\infty \max_{t,\mathbf{x}} \left|\nabla_\parallel \theta\right| \, dz = \int_0^\infty \max_{\mathbf{x}} \left|\nabla_\parallel \theta_I\right| \, dz. \tag{18}$$

Proof. Under the conditions stated here, the solution θ is in the space $C\left([0, T], X^k\right)$, for some $k \geq 5$, which by Sobolev embedding implies that it has continuous horizontal derivatives up to third order, for a.e. z. This will allow us to apply the classical maximum principle [Friedman, 2008] to an auxiliary function composed of θ itself and its horizontal gradient: consider

$$\sigma := \left|\nabla_\parallel \theta\right|^2 + \lambda \left|\theta\right|^2, \tag{19}$$

with $\lambda > 0$ to be determined later. We now apply the operator $L := \partial_t + \mathbf{u} \cdot \nabla_\parallel - \kappa\Delta_\parallel$ to σ and note that the coefficients of this operator are bounded and continuous on the given time interval (for a.e. z). We calculate

$$\begin{aligned} L\lambda \left|\theta\right|^2 =& \lambda \left[2\theta\partial_t\theta + 2\theta\mathbf{u} \cdot \nabla_\parallel \theta - \kappa \left(2\theta\Delta_\parallel\theta + 2\left|\nabla_\parallel \theta\right|^2\right)\right] \\ =& -2\lambda\kappa \left|\nabla_\parallel \theta\right|^2, \end{aligned} \tag{20}$$

$$
\begin{aligned}
L\left|\nabla_{\|}\theta\right|^2 =& 2\nabla_{\|}\theta\cdot\partial_t\nabla_{\|}\theta + 2\nabla_{\|}\theta\cdot\left[(\mathbf{u}\cdot\nabla_{\|})\nabla_{\|}\theta\right] \\
&- 2\kappa\sum_i\left[\theta_{x_i}\Delta_{\|}\theta_{x_i} + \left|\nabla_{\|}\theta_{x_i}\right|^2\right] \\
=& 2\nabla_{\|}\theta\cdot\left[\partial_t\nabla_{\|}\theta + (\mathbf{u}\cdot\nabla_{\|})\nabla_{\|}\theta - \kappa\Delta_{\|}\nabla_{\|}\theta\right] - 2\kappa\left|\nabla_{\|}^2\theta\right|^2 \\
=& -2\nabla_{\|}\theta\cdot\left[\left(\nabla_{\|}\mathbf{u}\right)^{\mathrm{T}}\nabla_{\|}\theta\right] - 2\kappa\left|\nabla_{\|}^2\theta\right|^2, \qquad (21)
\end{aligned}
$$

where the last equality follows by calculating the horizontal gradient of (5). In total, we obtain

$$
\begin{aligned}
L\sigma =& 2\left[\nabla_{\|}\theta^{\mathrm{T}}(-\nabla_{\|}\mathbf{u})^{\mathrm{T}}\nabla_{\|}\theta - \lambda\kappa\left|\nabla_{\|}\theta\right|^2 - \kappa\left|\nabla_{\|}^2\theta\right|^2\right] \\
\leq& C\left[\sup_{t\in[0,T],\mathbf{x}\in\mathbb{R}^2}\left|\nabla_{\|}\mathbf{u}\right|\right]\left|\nabla_{\|}\theta\right|^2 - 2\lambda\kappa\left|\nabla_{\|}\theta\right|^2. \qquad (22)
\end{aligned}
$$

Therefore, choosing

$$
\lambda = \frac{C}{2\kappa}\operatorname*{ess\,sup}_{t\in[0,T],(\mathbf{x},z)\in\Omega}\left|\nabla_{\|}\mathbf{u}\right|, \qquad (23)
$$

which is guaranteed to be finite on the given time interval, we can conclude that, for a.e. z, $L\sigma \leq 0$ in $[0,T]\times\mathbb{R}^2$, which implies

$$
\max_{t,\mathbf{x}}\sigma = \max_{\mathbf{x}}\sigma|_{t=0} = \max_{\mathbf{x}}\left|\nabla_{\|}\theta_I\right|^2 + \lambda\max_{\mathbf{x}}\left|\theta_I\right|^2 \qquad (24)
$$

by the classical maximum principle. Since θ itself also obeys the maximum principle, we have

$$
\max_{t,\mathbf{x}}\sigma = \max_{t,\mathbf{x}}\left|\nabla_{\|}\theta\right|^2 + \lambda\max_{t,\mathbf{x}}\left|\theta\right|^2 = \max_{t,\mathbf{x}}\left|\nabla_{\|}\theta\right|^2 + \lambda\max_{\mathbf{x}}\left|\theta_I\right|^2. \qquad (25)
$$

The claimed bounds (17) and (18) now follow after taking ess sup in z and integrating in z, respectively. □

2.3 A priori estimates

We now proceed to show that boundedness of $\sup|\nabla_{\|}\theta|$ suffices to control the growth of all H^k norms in the horizontal, and therefore the growth of all X^k norms. Essentially, we rely on standard energy estimates for second-order parabolic equations, but the presence of the integral in z in the relationship between $\mathbf{u}$ and θ does demand additional care, since we also need to integrate the horizontal relationships in the vertical: $\mathbf{u}$ is a priori bounded, but not necessarily integrable in z, thus, terms involving $\mathbf{u}$ always need to contain an integrable factor. Still, we will only highlight the z-dependence when necessary. We start with the basic energy inequality:

X^0**:** Testing Eq. (5) with θ and recalling that $\mathrm{div}_\parallel \mathbf{u} = 0$, we immediately get

$$\frac{1}{2}\frac{d}{dt}\left\|\theta\right\|_{L_x^2}^2 + \kappa \left\|\nabla_\parallel \theta\right\|_{L_x^2}^2 = 0, \tag{26}$$

which yields

$$\left\|\theta\right\|_{L_x^2}^2(t) + 2\kappa \int_0^t \left\|\nabla_\parallel \theta\right\|_{L_x^2}^2 = \left\|\theta_I\right\|_{L_x^2}^2. \tag{27}$$

In particular, this implies $\left\|\theta\right\|_{L_x^2}(t) \leq \left\|\theta_I\right\|_{L_x^2}$, for a.e. z. Adding the integral and the essential supremum over all z thus yields

$$\left\|\theta\right\|_{X^0}(t) \leq \left\|\theta_I\right\|_{X^0}. \tag{28}$$

On the other hand, we have

$$\left\|\nabla_\parallel \theta\right\|_{L_t^2 L_x^2} \leq C \left\|\theta_I\right\|_{L_x^2}, \tag{29}$$

which after integration in z and application of Minkowski's inequality for integrals leads to

$$\operatorname*{ess\,sup}_z \left\|\mathbf{u}\right\|_{L_t^2 L_x^2} \leq \int_0^\infty \left\|\nabla_\parallel \theta\right\|_{L_t^2 L_x^2} dz \leq C \left\|\theta_I\right\|_{X^0}. \tag{30}$$

X^1**:** Testing (5) with $-\Delta_\parallel \theta$, we obtain

$$\begin{aligned}
\frac{1}{2}\frac{d}{dt}\left\|\nabla_\parallel \theta\right\|_{L_x^2}^2 + \kappa \left\|\Delta_\parallel \theta\right\|_{L_x^2}^2 &= \int_{\mathbb{R}^2} \mathbf{u}\cdot\nabla_\parallel\theta\Delta_\parallel\theta\, dx \\
&\leq \left\|\mathbf{u}\right\|_{L_x^\infty} \int_{\mathbb{R}^2} |\nabla_\parallel\theta||\Delta_\parallel\theta|\, dx \\
&\leq \int_0^\infty \left\|\nabla_\parallel\theta_I\right\|_{L_x^\infty} \int_{\mathbb{R}^2} |\nabla_\parallel\theta||\Delta_\parallel\theta|\, dx,
\end{aligned} \tag{31}$$

by Lemma 1. Absorbing $\Delta_\parallel\theta$ into the left-hand side in standard fashion, this further implies

$$\frac{d}{dt}\left\|\nabla_\parallel \theta\right\|_{L_x^2}^2 + \kappa \left\|\Delta_\parallel \theta\right\|_{L_x^2}^2 \leq C(\nabla_\parallel\theta_I)\left\|\nabla_\parallel \theta\right\|_{L_x^2}^2. \tag{32}$$

We thus get

$$\left\|\nabla_\parallel \theta\right\|_{X^0}(t) \leq \exp\left[C(\nabla_\parallel\theta_I)t\right]\left\|\nabla_\parallel\theta_I\right\|_{X^0}, \tag{33}$$

which, combined with (28), yields a global-in-time bound on $\left\|\theta\right\|_{X^1}$. Furthermore, it holds

$$\kappa \left\|\Delta_\parallel \theta\right\|_{L_t^2 L_x^2}^2 \leq \left\|\nabla_\parallel\theta_I\right\|_{L_x^2}^2 + C(\nabla_\parallel\theta_I)\left\|\nabla_\parallel \theta\right\|_{L_t^2 L_x^2}^2, \tag{34}$$

from which, using $\sqrt{A^2+B^2} \leq A+B$ for $A, B \geq 0$ and integrating, we can derive the estimate

$$\int_0^\infty \left\|\Delta_\parallel \theta\right\|_{L_t^2 L_x^2} dz \leq C(\nabla_\parallel \theta_I) \left[\int_0^\infty \left\|\nabla_\parallel \theta_I\right\|_{L_x^2} dz + \int_0^\infty \left\|\nabla_\parallel \theta\right\|_{L_t^2 L_x^2} dz\right]. \tag{35}$$

By (30), we have an a priori estimate on the right-hand side, which implies that the quantity on the left is bounded for all times, as well as

$$\operatorname*{ess\,sup}_z \|\mathbf{u}\|_{L_t^2 H_x^1}. \tag{36}$$

X^2: Testing with $\Delta_\parallel^2 \theta$ yields

$$\frac{1}{2}\frac{d}{dt}\left\|\Delta_\parallel \theta\right\|_{L_x^2}^2 + \kappa \left\|\nabla_\parallel \Delta_\parallel \theta\right\|_{L_x^2}^2 = -\int_{\mathbb{R}^2} \mathbf{u} \cdot \nabla_\parallel \theta \Delta_\parallel^2 \theta. \tag{37}$$

Integrating by parts to shift one derivative on the right to either $\mathbf{u}$ or $\nabla_\parallel \theta$, we get

$$\left|\int_{\mathbb{R}^2} \mathbf{u}_{x_i} \cdot \nabla_\parallel \theta \nabla_\parallel \Delta_\parallel \theta \, dx\right| \leq \left\|\nabla_\parallel \theta_I\right\|_{L_x^\infty}(z) \left\|\nabla_\parallel \mathbf{u}\right\|_{L_x^2} \left\|\nabla_\parallel \Delta_\parallel \theta\right\|_{L_x^2} \tag{38}$$

for a.e. z, as well as

$$\left|\int_{\mathbb{R}^2} \mathbf{u} \cdot \nabla_\parallel \theta_{x_i} \nabla_\parallel \Delta_\parallel \theta \, dx\right| \leq \int_0^\infty \left\|\nabla_\parallel \theta_I\right\|_{L_x^\infty} dz \left\|\nabla_\parallel^2 \theta\right\|_{L_x^2} \left\|\nabla_\parallel \Delta_\parallel \theta\right\|_{L_x^2}. \tag{39}$$

Absorbing the highest-order derivatives, we arrive at

$$\frac{d}{dt}\left\|\Delta_\parallel \theta\right\|_{L_x^2}^2 + \kappa \left\|\nabla_\parallel \Delta_\parallel \theta\right\|_{L_x^2}^2 \leq C\left[\left\|\nabla_\parallel \theta_I\right\|_{L_x^\infty}(z) \left\|\nabla_\parallel \mathbf{u}\right\|_{L_x^2}^2 + \left\|\nabla_\parallel \theta_I\right\|_{L_z^1 L_x^\infty}^2 \left\|\nabla_\parallel^2 \theta\right\|_{L_x^2}^2\right]. \tag{40}$$

By Gronwall's inequality, this further implies

$$\begin{aligned}
\left\|\nabla_\parallel^2 \theta\right\|_{L_x^2}^2(t) \leq & \exp\left(C(\nabla_\parallel \theta_I) t\right) \left\|\nabla_\parallel^2 \theta_I\right\|_{L_x^2}^2 \\
& + C\left\|\nabla_\parallel \theta_I\right\|_{L_x^\infty}^2(z) \int_0^t \left\|\nabla_\parallel \mathbf{u}\right\|_{L_x^2}^2(s) \exp\left[C(\nabla_\parallel \theta_I)(t-s)\right] ds \\
\leq & \exp\left(C(\nabla_\parallel \theta_I) t\right) \left[\left\|\nabla_\parallel \theta_I\right\|_{L_x^2}^2 + \left\|\nabla_\parallel \theta_I\right\|_{L_x^\infty}^2(z) \left\|\nabla_\parallel \mathbf{u}\right\|_{L_t^2 L_x^2}^2\right],
\end{aligned} \tag{41}$$

from which we get

$$\begin{aligned}
\int_0^\infty \left\|\nabla_\parallel^2 \theta\right\|_{L_x^2} dz\,(t) \leq & \exp\left(C(\nabla_\parallel \theta_I) t\right) \\
& \times \left[\int_0^\infty \left\|\nabla_\parallel^2 \theta_I\right\|_{L_x^2} dz + \int_0^\infty \left\|\nabla_\parallel \theta_I\right\|_{L_x^\infty} dz \operatorname*{ess\,sup}_z \left\|\nabla_\parallel \mathbf{u}\right\|_{L_t^2 L_x^2}\right].
\end{aligned} \tag{42}$$

Recalling (35) and (36), the rightmost term is globally bounded in time; therefore, after applying the analogous estimate for the essential supremum in z, we can conclude that $\|\theta\|_{X^2}$ is bounded for all times. It is straightforward to now deduct from (40) and the previous estimates that

$$\int_0^\infty \left\|\nabla_\parallel \theta\right\|_{L_t^2 H_x^2} dz \quad \text{and} \quad \operatorname*{ess\,sup}_z \|\mathbf{u}\|_{L_t^2 H_x^2} \tag{43}$$

are also bounded.

X^k, $k \geq 3$: Going further, we only sketch how the desired estimates can be obtained inductively: we need to estimate

$$\left| \int_{\mathbb{R}^2} \mathbf{u} \cdot \nabla_\parallel \theta \Delta_\parallel^k \theta \, dx \right|. \tag{44}$$

Integrating by parts to shift $(k-1)$ derivatives away from $\Delta_\parallel^k \theta$, we observe that terms where all these derivatives fall on either $\mathbf{u}$ or $\nabla_\parallel \theta$ can be estimated in the same fashion as the corresponding terms in the case $k = 2$. It therefore remains to investigate terms of the form

$$\int_{\mathbb{R}^2} \mathbf{u}_\alpha \cdot \nabla_\parallel \theta_\beta \nabla_\parallel^{\delta(k)} \Delta_\parallel^{\frac{k+1}{2} - \delta(k)} \theta \, dx, \tag{45}$$

where α, β denote multi-indices, $\delta(k) = 1$ for even k and $\delta(k) = 0$ otherwise, and $1 \leq |\alpha|, |\beta| \leq k-2$. We first apply a Hölder inequality to obtain the bound

$$\|\mathbf{u}_\alpha\|_{L_x^4} \left\|\nabla_\parallel \theta_\beta\right\|_{L_x^4} \left\|\nabla_\parallel^{\delta(k)} \Delta_\parallel^{\frac{k+1}{2} - \delta(k)} \theta\right\|_{L_x^2}. \tag{46}$$

Absorbing $\nabla_\parallel^{\delta(k)} \Delta_\parallel^{\frac{k+1}{2} - \delta(k)} \theta$ into the left-hand side with Young's inequality, but retaining the remainder on the right as a product, we get terms of the form

$$C \|\mathbf{u}_\alpha\|_{L_x^4}^2 \left\|\nabla_\parallel \theta_\beta\right\|_{L_x^4}^2. \tag{47}$$

Now, it suffices to apply the Sobolev embedding $H^1 \hookrightarrow L^4$ [Adams and Fournier, 2003]: we need to deal with terms of the form

$$C \|\mathbf{u}_\alpha\|_{H_x^1}^2 \left\|\nabla_\parallel \theta_\beta\right\|_{H_x^1}^2, \tag{48}$$

and, since we know from the previous step that both $\|\theta\|_{X^{k-1}}$ and $\operatorname{ess\,sup}_z \|\mathbf{u}\|_{L_t^2 H_x^{k-1}}$ are bounded, we only need to pay closer attention to the case $|\beta| = k-2, |\alpha| = 1$. Here, application of Gronwall's inequality yields a contribution to the exponent from (48) that is bounded by $\operatorname{ess\,sup}_z \|\mathbf{u}\|_{L_t^2 H_x^2}^2$, which by (43) is already known to be globally bounded. Thus, we again arrive at a global bound for $\|\theta\|_{X^k}$ and $\operatorname{ess\,sup}_z \|\mathbf{u}\|_{L_t^2 H_x^k}$.

We can concisely summarize the calculations outlined above in

Lemma 2. *As long as* (5)-(6) *has a solution in X^k, for any $k \geq 5$, we have*

$$\|\theta\|_{X^k}(t) \leq K(t, \|\theta_I\|_{X^k}), \tag{49}$$

for a function K that is finite for all $t \geq 0$. □

2.4 Global existence

We are now in a position to prove

Theorem 1. *Let $T > 0$ be arbitrarily large and let $\theta_I \in X^k$, for some $k \geq 5$. Then the solution obtained in Proposition 1 can be extended to the time interval $[0, T]$ and thus is a global solution.*

Proof. Let us recall that Proposition 1 yields a time of existence $T^\star$ that can be bounded from below by the norm of the initial data. If $T \leq T^\star$, there is nothing to prove. Otherwise, restart at $T^\star$ with $\theta|_{t=T^\star}$ as initial data and observe that, by Lemma 2,

$$\|\theta|_{t=T^\star}\|_{X^k} \leq K(T, \|\theta_I\|_{X^k}); \tag{50}$$

applying Proposition 1, we can extend the lifespan of the solution by a time $T^{\star\star}$ *that only depends on the upper bound on the right-hand side.* Now, if $T^\star + T^{\star\star} < T$, we can repeat this procedure, since the upper bound remains valid. After finitely many steps, we get $T^\star + nT^{\star\star} \geq T$, and the claim is proven. □

Remark 3. *Regularity of the solution in the vertical, if present in the initial data, can be established immediately by the following observation: differentiating* (5) *with respect to z and noticing that $\partial_z \mathbf{u} \cdot \nabla_\parallel \theta = 0$, we see that $\partial_z \theta$ obeys* the same equation as θ itself. *Hence, regularity in z is preserved for all times.*

3 Conclusions and outlook

We have made a first contribution to the rigorous analysis of the diabatic layer (DL), the central component of a new triple-deck boundary layer theory in the atmospheric sciences. Specifically, we have established the global well-posedness of a diffusive version of the model for sufficiently regular initial data. This result might very well be strengthened considerably: looking at the work of Friedlander and Vicol [2011, 2012] on the magneto-geostrophic equations, it seems plausible that the De Giorgi method, which was employed in the cited works, can be adapted to the DL equation to yield global smooth solutions *even for L^2 initial data.* This is the subject of ongoing work. Regarding the non-diffusive limit, it would be of the utmost importance to determine in what sense the existence of a (weak) solution can be established. Finally, we reiterate that it is our ultimate goal to achieve an understanding of the coupled QG-DL-Ekman system. To this end, we *will* need results on the non-diffusive equation, since the introduction of a closure as in (5) is asymptotically inconsistent with the QG system.

References

R. A. Adams and J. Fournier. *Sobolev spaces.* Academic Press, 2nd ed. edition, 2003.

C. Cao and E. S. Titi. Global well-posedness and finite-dimensional global attractor for a 3-d planetary geostrophic viscous model. *Communications on pure and applied mathematics*, 56(2):198–233, 2003.

C. Cao, E. S. Titi, and M. Ziane. A 'horizontal' hyper-diffusion three-dimensional thermocline planetary geostrophic model: well-posedness and long-time behaviour. *Nonlinearity*, 17(5):1749–1776, 2004.

P. Constantin, A. Majda, and E. Tabak. Formation of strong fronts in the 2-d quasi-geostrophic thermal active scalar. *Nonlinearity*, 7(6):1495–1533, 1994.

S. Friedlander and V. Vicol. Global well-posedness for an advection–diffusion equation arising in magneto-geostrophic dynamics. *Annales de l'Institut Henri Poincaré. Analyse non linéaire*, 28(2):283–301, 2011.

S. Friedlander and V. Vicol. Higher regularity of hölder continuous solutions of parabolic equations with singular drift velocities. *Journal of mathematical fluid mechanics*, 14(2):255–266, 2012.

A. Friedman. *Partial differential equations of parabolic type*. Dover Publications, dover ed., unabridged republ. of the work orig. publ. in 1964 by prentice-hall edition, 2008.

R. Klein, L. Schielicke, S. Pfahl, and B. Khouider. QG-DL-Ekman: Dynamics of a diabatic layer in the quasi-geostrophic framework. *J. Atmos. Sci.*, 79:887–905, 2022. doi: 10.1175/JAS-D-21-0110.1.

O. A. Ladyzhenskaya, N. Ural'tseva, and V. Solonnikov. *Linear and quasi-linear equations of parabolic type*. American Mathematical Society, 1967.

J. Pedlosky. *Geophysical Fluid Dynamics*. Springer-Verlag, 2nd edition, 1987.

M. E. Taylor. *Partial differential equations. 3, Nonlinear equations*. Springer, 2nd ed. edition, 2011.

G. Vallis. *Atmospheric and Oceanic Fluid Dynamics*. Cambridge University Press, 2nd edition, 2017.

CV Daniel Bäumer

Date and place of birth: 10.11.1987, Salzburg, Austria;
Nationality: Austrian;
Languages: **German** (native), **English** (fluent), **Polish** (elementary), **French** (elementary), **Italian** (elementary)

Academic qualifications

- **2021-2025** *PhD in mathematics,* University of Vienna
  PhD thesis *Asymptotic PDE models of intermediate complexity for large-scale dynamics of a moist atmosphere* (Supervision: Norbert J. Mauser, Co-supervision: Sabine Doppler)
- **2019-2021** *MSc in mathematics,* University of Vienna
  Master thesis *Multiscale modeling and analysis for near-equatorial flows* (Supervision: Norbert J. Mauser, Co-supervision: Sabine Doppler)
- **2005-2008** *BSc in mathematics,* University of Salzburg
- **2005** *Abitur,* Musisches Gymnasium Salzburg

Talks

- **2025** "Scaling regimes for moist atmospheric flows and the Clausius-Clapeyron relation", *Workshop "Mathematical Advances in Geophysical Fluid Dynamics",* Oberwolfach
- **2024** "Reduced models for large-scale atmospheric flow in the midlatitudes with moist process closures", *Applied Dynamics Seminar,* University of Hamburg
- **2023** "Clouds and precipitation in midlatitude cyclones: new asymptotic models", *Colloquium of the Institute of Meteorology and Geophysics,* University of Vienna

Research fields

- Mathematical modeling in geophysical fluid dynamics, with a focus on asymptotic models with moist process closures
- Analysis of partial differential equations in (geophysical) fluid dynamics
- Analysis of singular perturbations in the physical sciences

Publications

- D. Bäumer: The diabatic layer equations: well-posedness of a new boundary layer theory for quasi-geostrophic flow. *Manuscript,* 2025
- D. Bäumer, R. Klein and N.J. Mauser: A general framework for the asymptotic analysis of moist atmospheric flows. *Journal of Asymptotic Analysis,* accepted, 2025.
- D. Bäumer and R. Klein: PQG-DL-Ekman: a triple-deck boundary layer theory for large-scale atmospheric flow with moist process closures. *Submitted,* 2025
- D. Bäumer, S. Hittmeir and R. Klein: Scaling approaches to quasigeostrophic theory for moist, precipitating air. *Journal of the Atmospheric Sciences,* **80,** 1771–1786, 2023.

Teaching experience

- **2024/2025** *Applied Analysis,* Co-lecturer, Master of mathematics, U. Vienna
- **2023-2025** *Mathematical Modeling,* Co-lecturer, Bachelor of Mathematics, U. Vienna
- **2021-2022** *Mathematical Modeling,* Exercise class, Bachelor of Mathematics